"STUDY OF WEAR BEHAVIOUR OF CHROME-NITRIDE COATING USING PHYSICAL VAPOR DEPOSITION"

Submitted to Delhi Technological University in Partial Fulfilment of the Requirement for the Award of the Degree of

Master of Technology

In

Mechanical Engineering

With specialization in Production Engineering

By

SHAILESH KUMAR SINGH
(2K13/PIE/20)

Under the guidance of

DR. QASIM MURTAZA (Associate Professor)

MR. SHAILESH MANI PANDEY (Assistant Professor)

Department of Mechanical Engineering

DELHI TECHNOLOGICAL UNIVERSITY

Shahabad Daulatpur

Bawana Road, Delhi-110042, INDIA

SESSION 2013-15

"STUDY OF WEAR BEHAVIOUR OF CHROME-NITRIDE COATING USING PHYSICAL VAPOR DEPOSITION"

Submitted to Delhi Technological University in Partial Fulfilment of the Requirement for the Award of the Degree of

Master of Technology

In

Mechanical Engineering

With specialization in Production Engineering

By

SHAILESH KUMAR SINGH
(2K13/PIE/20)

Under the guidance of

DR. QASIM MURTAZA
(Associate Professor)

MR. SHAILESH MANI PANDEY
(Assistant Professor)

Department of Mechanical Engineering

DELHI TECHNOLOGICAL UNIVERSITY

Shahabad Daulatpur

Bawana Road, Delhi-110042, INDIA

SESSION 2013-15

CERTIFICATE

This is to certify that the project entitled "Study of Wear Behaviour of Chrome-Nitride Coating using Physical Vapor Deposition" being submitted by me, is a bonafide record of my own work carried by me under the guidance and supervision of Dr. Qasim Murtaza (Associate Professor) & Mr. Shailesh Mani Pandey (Assistant Professor) in partial fulfilment of requirements for the award of the Degree of Master of Technology in Production Engineering from Department of Mechanical Engineering, Delhi Technological University, Delhi.

The matter embodied in this project either full or in part have not been submitted to any other institution or University for the award of any other Diploma or Degree or any other purpose what so ever.

Shailesh Kumar Singh
Registration Number: DTU/13/M-Tech/261
University Roll Number: 2K13/PIE/20

This is to certify that the above statement made by the candidate is correct to the best of our knowledge.

DR. QASIM MURTAZA
(Associate Professor)

MR. SHAILESH MANI PANDEY
(Assistant Professor)

DEPARTMENT OF MECHANICAL AND PRODUCTION ENGINEERING
DELHI TECHNOLOGICAL UNIVERSITY
Shahabad Daulatpur, Bawana Road, Delhi-110042, India

ACKNOWLEDGMENT

I have a great pleasure in expressing my deep sense of gratitude and indebtedness to Dr. Qasim Murtaza & Mr. Shailesh Mani Pandey of Mechanical Engineering Department, Delhi Technological University for their continuous guidance, invaluable suggestion and exquisite time at all stages from conceptualization to experimental and final completion of this project work. I also wish to place on record the patience and understanding showed by them at critical situations. Along with academics, I learnt from them the resilience to undertake challenges that the research world would be putting my way.

I am also grateful to Prof. (Dr.) R. S. Mishra, Head, Department of Mechanical Engineering, Delhi Technological University for providing the experimental facilities. His constant support, co-operation and encouragement for successful completion of this work is indebt-able.

My special thanks to Dr. R. C. Singh, Dr. R. S. Walia, and Dr. Mohit Tyagi for their valuable time and very useful critical comments from their experience has helped me to do the project work on time. They have guided me for fundamentals and provided many technical papers on the subject matter and thus inculcated the interest and quest for knowledge of this work.

I also have great respect and obligation for Mr. Rajesh Bora and Mr. Sandeep Kumar (Technician SEM & XRD), for their assistance and facilities provided for experiments, required for the completion of this special subject.

This research work would not have become possible without strong cooperation, immense support and keen involvement of my friends and colleagues specially Mr. Parvesh, Santosh, Ashish, Pawan, Rashid, Vasu, Nishant, Siddhartha, Jaspreet and Gopal. I also extend my heartfelt thanks to an undergraduate Dhruv Gupta for the thesis editing, presentation and development of results.

All my academic pursuits become a perceptible reality just because of my parents, my sister, brother Vivek, Atul and special thanks to Bhawna Singh who played a pivotal role at each step providing encouragement and support in every possible way. My sincere thanks to entire dear and near ones who contributed directly or indirectly for accomplishing this arduous task.

Shailesh Kumar Singh

University Roll Number: 2K13/PIE/20

ABSTRACT

In the present investigation, Wear behaviour of chrome coating was examined using PVD (Ion Plating) in dry and flooded condition. The PVD having 93.7% Cr and 6.3% Nitrogen is used. The cast iron substrate of same composition as of piston rings was used to get the similar result as in the engine cylinder piston combination. After preparation of the coating, the plate (90×90×2 mm) was prepared with the help of a surface grinder and further wear test were performed on a pin-on disc configuration. The load and velocity range varies from (50, 60, 70, 80, 90 & 100 N), and Speed (319, 764, & 1433 rpm) keeping the sliding distance 2500 m. The wear rate was calculated using mass loss methods on an electronic balance having least count of 0.0001g. The morphology of worn surface was analysed with SEM & EDS which allow to elucidating the mechanism of wear and chemical composition of the tribo-film formed during the pin and disc sliding contact. The main wear mechanisms observed by SEM were adhesion, deformation, microcutting and erosion. There was a significant decrease in the specific wear rate of coated sample compared to uncoated and large reduction of coated sample in flooded condition compare to dry condition of test. The wear rate of the coating was found to be increased with increase in load as well as sliding speed for the Ion Plating with the counter body that is material of Cylinder liner which is alloy of cast iron. However, The Coefficient of friction was found to be decreased with the increase of load of 50 to 70 N and sliding speed from 1 m/s to 3 m/s. In these conditions chrome coating shows the better tribological behaviour.

INDEX

LIST OF FIGURES

LIST OF TABLES

ABBREVIATIONS

PVD	Physical Vapour Deposition
CVD	Chemical Vapour Deposition
IBAD	Ion Beam Assisted Deposition
PE	Plasma enhanced
HVOF	High Velocity Oxy-Fuel
PIII	Plasma Immersion Ion Implantation
µm	Micrometre
N_2	Nitrogen
EPA	Environment Protection Agency
HF	Hydro-Fluoric Acid
IR	Infra-Red
DLC	Diamond Like Carbon Coating
mm	Millimetre
Pa	Pascal
°C	Degree Celsius
Ag	Silver
HSS	High Speed Steel
PM	Powder Metallurgy
SEM	Scanning Electron Microscopy
OM	Optical Microscopy
EDS	Energy Dispersive spectroscopy
MEMS	Micro-Electro-Mechanical Systems
CrN	Chromium Nitride
EHC	Electrolytic Hard Chrome
UBM	Unbalanced Magnetron Sputtering
TEM	Transmission Electron Microscopy
XRD	X-Ray Diffraction
FCC	Face-Centered Cubic

HV	Hardness Value
SiC-Nw	Silicon-Carbide Nano-wires
Mo	Molybdenum
A˚	Armstrong
Kg	kilogram
N	load in Newton
Rpm	Revolution per minute
μ	co-efficient of friction
g	grams
d	Intermolecular distance
3D	Three dimensional
θ	Angle of incidence
D_1, D_2	Diagonals of indente

CHAPTER 1

INTRODUCTION

1.0 SURFACE ENGINEERING

Surface engineering involves changing the properties of the surface and near-surface region in a desirable way. Surface engineering can involve an overlay process or a surface modification process. In overlay processes a material is added to the surface and the underlying material (substrate) is covered and not detectable on the surface. A surface modification process changes the properties of the surface but the substrate material is still present on the surface. For example, in aluminium anodization, oxygen reacts with the anodic aluminium electrode of an electrolysis cell to produce a thick oxide layer on the aluminium surface. Table 1.1 shows a number of overlay and surface modification processes that can be used for surface engineering.

Each process has its advantages, disadvantages, and applications. In some cases surface modification processes can be used to modify the substrate surface prior to depositing a film or coating. For example, a steel surface can be hardened by plasma nitriding prior to the deposition of a hard coating by a physical vapor deposition (PVD) process. In other cases, a surface modification process can be used to change the properties of an overlay coating. For example, a sputter-deposited coating on an aircraft turbine blade can be shot peened to densify the coating and place it into compressive stress. An atomistic deposition process is one in which the overlay material is deposited atom-by atom. The resulting film can range from single crystal to amorphous, fully dense to less than fully

dense, pure to impure, and thin to thick. Generally the term "thin film" is applied to layers which have thicknesses on the order of a micron or less (1 micron = 10^{-6} meters) and may be as thin as a few atomic layers. Thicker deposits are called coatings. The term "thick film" is usually not used for thick atomistically deposited vacuum deposits as that term is used for "paint-on, fire-on" types of deposition. Often the properties of thin films are affected by the properties of the underlying material (substrate) and can vary through the thickness of the film. Thicker layers are generally called coatings. An atomistic deposition process can be done in a vacuum, gaseous, or electrolytic environment [1].

Table 1.1: Some Processes for Surface Engineering [1].

Atomistic/Molecular Deposition	**Bulk Coatings**
Electrolytic Environment Electroplating Electroless platings Displacement plating Electrophoretic deposition *Vacuum Environment* Vacuum evaporation Ion beam sputter deposition Ion beam assisted deposition (IBAD) Laser vaporization Hot-wire and low pressure CVD Jet vapor deposition *Plasma Environment* Sputter deposition Arc vaporization Ion plating Plasma enhanced (PE) CVD Plasma polymerization	*Wetting Processes* Dip coating Spin coating Painting *Fusion Coatings* Thick films Enameling Sol-gel coatings Powder coating *Solid Coating* Cladding Weld overlay Gilding ***Surface Modification*** *Chemical Conversion* Wet chemical solution (dispersion & layered) Gaseous (thermal) plasma

Chemical Vapor Environment Chemical vapor deposition (CVD) Pack cementation *Chemical Solution* Spray pyrolysis Chemical reduction ***Particulate Deposition*** *Thermal Spray* Flame spray Arc-wire spray Plasma spraying D-gun High-velocity-oxygen-fuel (HVOF) *Impact Plating* Mechanical plating	*Electrolytic Environment* Anodizing Ion substitution Plasma electrolysis *Mechanical* Shot peening Work hardening *Thermal Treatment* Thermal stressing *Ion Implantation* Ion beam Plasma immersion ion implantation (PIII) *Roughening and Smoothing* Chemical Mechanical Chemical–mechanical polishing Sputter texturing *Enrichment and Depletion* Thermal Chemical

1.1 COATINGS

Materials are the rare resources of the earth and it is very important to protect them for efficient and proper use. There are various surface treating phenomena to improve the tribo-mechanical properties of materials. Surface coating is also a phenomenon to form a protective layer on the top of material or a brittle, wear resistant material can be improved by the support of a more ductile bulk material. It is also possible to combine several material properties within coating like a hard phase with a lubricious phase.

The hard phase is usually a carbide or nitride and the lubricious phase is often amorphous carbon (a-C) that can reduce adhesion and sticking to the counter surface. There are several deposition techniques low-friction wear resistant properties frequently used in various machine elements to reduce energy losses and some specific properties which are needed can be attained by surface coating phenomenon.

Physical vapour deposition (PVD) is a common technique for thin coatings in range of 1-10 μm and also offered high quality of coating at relatively low substrate temperature with variable composition. PVD can be achieved by either evaporation or sputtering of a solid source in vacuum. In both cases, the vapour can form a coating either with the same composition as the evaporated material or in an altered form after reaction with a gas introduced into the deposition chamber (such as TiN formed from sputtered Ti reacted with N_2 gas).

The superior coating properties are achieved due to a multi-layer microstructure and a special coating composition that contains carbon, deposited in diamond-like form, as well as hydrogen and tungsten. The unique structure can be produced for a coating thickness of 10 microns, more than three times that of the industry's latest DLC coating. A specialized advanced process based on the combination of physical vapour deposition and plasma-assisted chemical vapour deposition, specifically developed for piston ring application, is used in applying Carbo-Glide. The coating's multi-layer architecture, together with the company's surface machining and finishing expertise, ensure the integrity of the coating structure, optimal adhesion of the coating and high coating stability on both steel and cast iron rings [2].

1.1.1 Chromium Electroplating

Hard chromium coatings are used in several fields. Due to the low friction of hard chromium coatings they are used in applications like cylinders, engine vales, shafts and bearings. Chrome coating has been used since 1940's is a very hard and common coating. In starting chromium coating was very popular hard and common coating due to cheap, wear and corrosion resistance. Further it moves towards electroplating of chromium which is replaced by chromium nitride coating due to environmental issues concerned with hexavalent chromium(Cr^{+6}). This was very hazardous so it has to be removed from environment and waste water after plating. Thickness is a critical parameter in CrN coating by PVD it affects by the supply pressure of nitrogen and other parameters also. Various Tribo-mechanical properties like wear friction and hardness affects by the coating thickness [2]. Chrome plating was declared unfriendly to the environment the U.S. *Environmental Protection Agency* (EPA) same year the European Union directive *Restriction of Hazardous Substances* (RoHS) decided to ban hexavalent chrome [3].

1.2 SAFETY AND ENVIRONMENTAL CONCERNS

Safety and environmental concerns are areas where there is a great deal of difference between the development and manufacturing environments. This may be due to the types or amounts of materials used. For example, a common drying agent is anhydrous alcohol, which can be used safely in a well-ventilated open area by careful people. However, in manufacturing, fire regulations do not allow alcohol to be used in the open environment because of its low flash point and large volume. Instead, the alcohol vapor must be contained and condensed or some other drying technique must be used.

By US law, every worker must be informed about the potential dangers of the chemicals that they encounter in the workplace (OSHA – Hazard Communication Standard 29 CFR 1910.1200). This includes common chemicals, such as household dishwasher soaps. It is the responsibility of managers to keep workers informed about the chemicals being used and their potential hazards. Chemical manufacturers must provide users with MSDSs on all their chemicals. These MSDSs must be made available to all workers. There are MSDSs on all kinds of chemical, ranging from the toner used in copiers, to common household detergents, to really hazardous chemicals such as hydrofluoric acid (HF). Information on environmental aspects of processing can be obtained from the Center for Environmental Research Information [1].

1.3 COATING MATERIAL

Coating material is chosen to meet the demands of application and it should be resistant to damage in emergency conditions. For Ex-In piston rings according to running condition at various load and sliding velocity for a long run. Elasticity and corrosion resistance of the ring material is required. The ring coating, if applied, needs to work well together with both the ring and the liner materials, as well as with the lubricant. As one task of the rings is to conduct heat to the liner wall, good thermal conductivity is required. Grey cast iron is used as the main material for piston rings. From a tribological point of view, the grey cast iron is beneficial, as a dry lubrication effect of the graphite phase of the material can occur under conditions of oil starvation. Furthermore, the graphite phase can act as an oil reservoir that supplies oil at dry starts or similar conditions of oil starvation. Reduced width piston rings in gasoline engines to match reductions in the overall height of pistons, and increasing combustion pressures in diesel

engines call for materials with increased strength characteristics. These challenges are met by the use of high-chromium alloyed steels and spring steels. The greater durability under increased stresses is demonstrated by the improved fatigue strength manifested as form stability.

Some materials deposited by PVD processes are as follows: [4]

- Gold – electrical conductor, anticorrosion surface, infrared (IR) reflectance
- Silver – electrical conductor, heat reflector, optical mirrors, low shear film lubricant
- Aluminium – electrical conductor, optical reflectance, corrosion resistance
- Copper – electrical conductor, solderability
- Cadmium – corrosion resistance (being phased out)
- Zinc – corrosion resistance
- Titanium – "glue layer" to oxides
- Chromium – "glue layer" to oxides, corrosion resistance, hard coating
- Palladium – galvanic corrosion layer between Ti and Au
- Molybdenum – "glue layer" to oxides
- Tantalum – corrosion and erosion resistance
- Beryllium – freestanding X-ray windows
- Carbon (DLC) – hard coat, chemically resistant, low friction
- Nickel – "glue layer" to metals, basecoat on brass
- Silicon – semiconductor devices
- Selenium – photosensitive material

Some mixtures (physical mixtures or above solubility limits):

- Silicon + dopants – semiconductor devices
- Nanophase composites – hard coatings

Some glasses:

- Amorphous silicon (a–Si) – semiconductor, photovoltaic
- Phosphorus + silicon oxides (PSGs) – encapsulant

Some alloys:

- Zinc + aluminium – corrosion protection
- Aluminium + copper + silicon – semiconductor metallization
- Indium + tin/oxide – transparent electrical conductor, IR reflection
- Nickel + chromium – "glue layer" to oxides, electrical resistance
- Tungsten + titanium – semiconductor metallization, diffusion barrier (W:Ti [90:10 wt%; 70:30 at %])

Some compounds:

- Titanium nitride – diffusion barrier coating, tool coating, decorative coating
- Titanium/Carbon nitride – tool coating, decorative coating
- Titanium/Aluminium nitride – wear coating
- Chromium nitride – hard coating, low friction
- Aluminium oxide – permeation barrier, diffusion barrier
- Titanium oxide – high index optical coating
- Silicon dioxide – low index optical coating
- Magnesium fluoride – low index optical coating
- Molybdenum di-sulphide – solid film lubricant
- Molybdenum di-selenide – solid film lubricant (electrical conductor)
- Tantalum oxide – high index optical coating
- Zinc sulphide – high index optical coating

Some layered systems:

- Ti/Au, Ti/Pd/Cu/Au, Ti/Ag, Ti/Pd/Ag – electrical conductor electrodes on oxides
- Cr/Au, Cr/Pd/Au – oxide metallization
- Mo/Au – oxide metallization
- TiN/Al – silicon metallization
- Ni/Cr – basecoat on brass
- Nanolayered composites – hard/wear coatings
- ZnO_x : Ag : Zn (thin): ZnO_x : TiO_x – low-e (low emission) glass coating
- SnO_x : Ag : NiCr (thin) : SnO_x – low-e glass coating on glass

1.4 WEAR RESISTANT COATINGS & ITS CLASSIFICATION

Tribo – mechanical properties of uncoated material can be improved by the coating of hard material to protect against wear. Abrasive wear, fretting wear and adhesive wear are often reduced by hard coating. Wear and friction is a critical problem in most of the application another benefit of hard chrome plating is that a cheap substrate material wear performance can be improved by coating of an exotic, high-performance material. Applications of wear resistant coatings are found in every industry, and for example, include mining excavator shovels and crushers [5-7]. There are various methods for improving the wear properties of metal substrate some of them which are newly developed are very efficient to deposit a wear resistant coating [6-8]. Localized heat treatment like thermal hardening and alloying some element like nitriding and carburizing are used to improve the wear resistance. Many of these methods have been in use for many years but unfortunately suffer from the disadvantage that the substrate needs to be heated to a high temperature. Carburizing, nitriding and carbonitriding in particular suffer from this problem. Most engineering items are made of steel and it is often found that some material other than steel is needed to fulfil the wear and friction requirements. Many wear resistant materials are brittle or expensive and can only be used as a coating, so improved coating technology has extended the control of wear to many previously unprotected engineering components. Various coating techniques available with their principal merits and demerits are listed in Table 1.2.

Table 1.2: Available techniques to improve its tribological Characteristics

Techniques	Principal Merits And Demerits
PVD & CVD	Thin discrete coating; no limitations on materials
Thermal spraying	Very thick coatings possible but control of coating purity is difficult
Ion implantation	Thin diffuse coating; mixing with substrate inevitable
Laser glazing	Thick coatings; coating material must be able to melt
Friction surfacing	Simple technology but limited to planar surfaces; produces thick metal coating
Electroplating	Wide range of coating thicknesses, but adhesion to substrate is poor and only certain materials can be coated by this technique
Surface welding	Suitable for very thick coatings only; limited to materials stable at high temperatures; coated surfaces may need further preparation
Explosive cladding	Rapid coating of large areas possible and bonding to substrate is good. Can give a tougher and thicker coating than many other method

A detailed classification of coating is given in given by a flow chart to give us clear understanding of various type of coating.

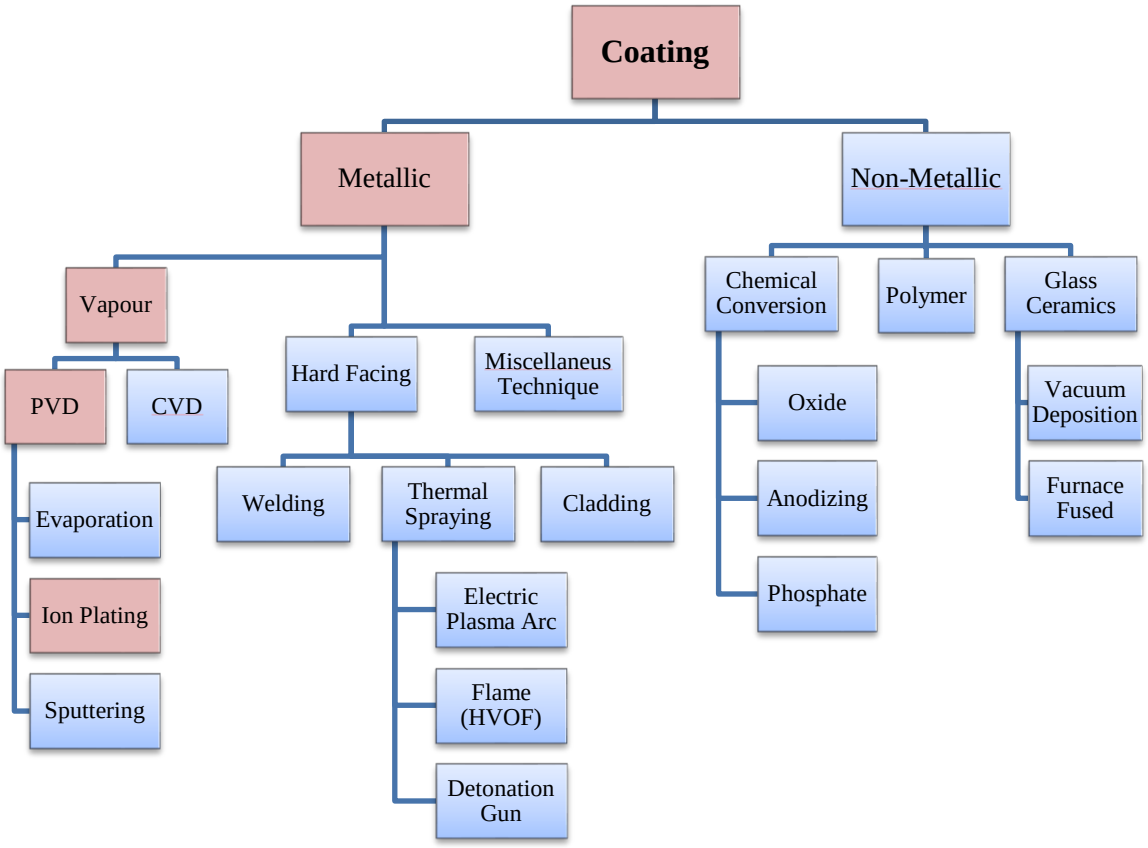

Figure 1.1: Coating Deposition Techniques

Figure 1.1 depicts the flow chart of various coating techniques. In which physical vapour deposition (PVD) and its types are discussed latter broadly. Thermal spray coating is also very popular according to industrial application among researchers. Cold spraying which is also a type of thermal spray is currently in trend due to its advantages. Some Non-metallic and nano-composite coating is also developed as per need in medical surgery equipment. Plasma assisted diffusion technologies are able to modify metallic surface by incorporation of light element like nitrogen, boron, and oxygen, such engineering techniques are widely used in automotive industry like piston rings coating.

1.5 VACUUM DEPENDENT COATING TECHNIQUES

Basic type of coating technique physical vapour deposition (PVD), chemical vapour deposition (CVD) and ion implantation are in current use. These are also suitable for precision components and thin coating of the range from 0.1-10 μm. Process requires enclosure in a vacuum from which atmospheric oxygen and water have been removed. Removing of air from enclosure has some advantage over coating in air. The exclusion of contaminants results in strong adhesion between the applied coating and substrate and greatly improves the durability of the coating. Some high quality coating is also produced by plasma based process without any limitation on the coating or substrate material. Some of the most utilized applications of thin film deposition processes include:

- Single and multilayer films and coatings
- Nano-layered & Nano-composite materials
- Optical films for transmission and reflection
- Decorative films
- Decorative and wear-resistant (decorative/functional) coatings
- Corrosion-resistant films
- Electrically insulating layers for microelectronics
- Coating of engine turbine blades
- Coating of high strength steels to avoid hydrogen embrittlement
- Diffusion barrier layers for semiconductor metallization
- Magnetic films for recording media
- Transparent electrical conductors and antistatic coatings
- Wear and erosion-resistant (hard) coatings (tool coatings)
- Dry film lubricants
- Composite and phase-dispersed films and coatings
- Thin-walled freestanding structures and foils

1.5.1 Physical Vapour Deposition (PVD)

In physical vapour deposition coating is done by condensation in vacuum vacuum and glow discharge result a perfect adhesion between the atoms of coating material and the atoms of the substrate. Concerned to the materials metallic, intermetallic, ceramics or many other compound cam be deposited onto the substrate by PVD. Porosity is also suppressed by the absence of dirt inclusions. In recent years, a number of specialized PVD techniques have been developed has its own advantages and range of preferred applications. Some applications of PVD range from the decorative to microelectronics, over a significant segment of the engineering, chemical, nuclear and related industries. Physical vapour deposition consists of three major techniques.

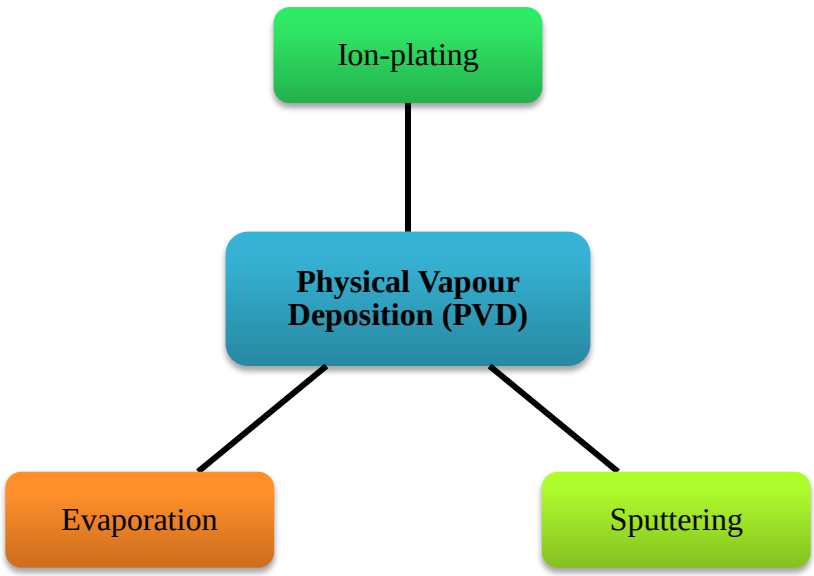

Figure 1.2: Classification of PVD

1.5.1.1 Evaporation

It is also one of the relatively simple and cheap vacuum deposition processes for thickness of 1 mm. Operating pressure and temperature range of evaporating coating material 10 – 6 Pa and 1000 – 2000°C. At this pressure and temperature atoms travel in straight line towards substrate and condensation take place. For the proper bonding between the base plate and coated material kinetic energy of the source material atoms and the ambient gas atoms. To minimize these collisions the source to substrate distance is adjusted so that it is less than the free path of gas atoms. Because of the low kinetic energy of the vapour the coatings produced during the evaporation exhibit low adhesion and therefore are less desirable for tribological applications compared to other vacuum based deposition processes. Furthermore, because the atoms of vapour travel in straight lines to the substrate, this results in a 'shadowing effect' for surfaces which do not directly face the coating source and common engineering components such as spheres, gears, moulds and valve bodies are difficult to coat uniformly. The source material can be heated by electrical resistance, eddy currents, electron beam, laser beam or arc discharge. Electric resistance heating usually applies to metallic materials having a low melting point while materials with a high melting point, e.g. refractory materials, need higher power density methods, e.g. electron beam heating. Since the coating material is in the electrically neutral state it is expelled from the surface of the source. The substrate is also pre-heated to a temperature of about 200 – 1600°C [7]. The evaporation process is schematically illustrated in Figure 1.3.

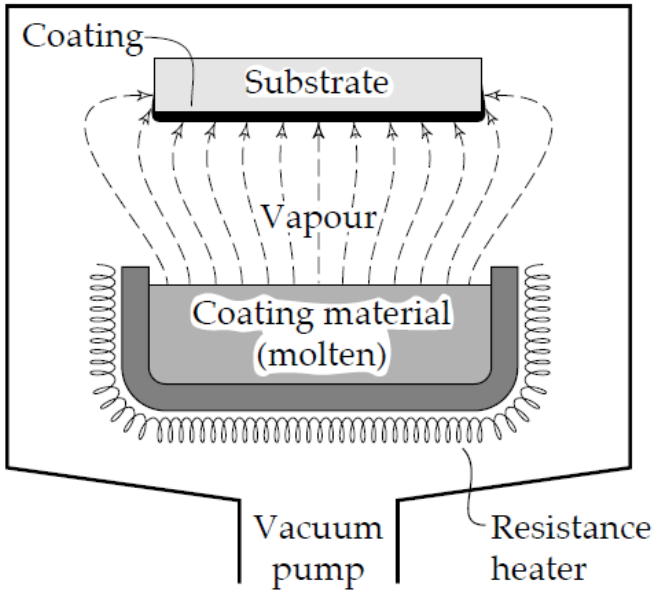

Figure 1.3: Schematic diagram of the evaporation process [2]

1.5.1.2 Ion-plating

The process of ion-plating therefore involves thermal evaporation of the coating material in a manner similar to that used in the evaporation process and ionization of the vapour due to the presence of a strong electric field and previously ionized low pressure gas, usually argon. The argon and metal vapour ions are rapidly accelerated towards the substrate surface, impacting it with a considerable energy. Glow discharge utilized in these phenomena by applying electric potential applied between two electrodes immersed in gas at reduced pressure, a stable passage of current is possible. At a voltage coating material can be transferred from the 'source' electrode to the 'target' electrode which contains the substrate. Before to ion-plating, surface impurities of the base material need to be removed by high energy inert gas for better bonding. Ion plating processes can be classified into two general categories: glow discharge (plasma) ion plating conducted in a

low vacuum of 0.5 to 10 Pa and ion beam ion plating (using an external ionization source) performed in a high vacuum of 10^{-5} to 10^{-2} Pa [7]. The most important aspect of ion-plating which distinguishes this process from the others is the modification of the microstructure and composition of the deposit caused by ion bombardment [8]. The ion-plating process is schematically illustrated in Figure 1.4.

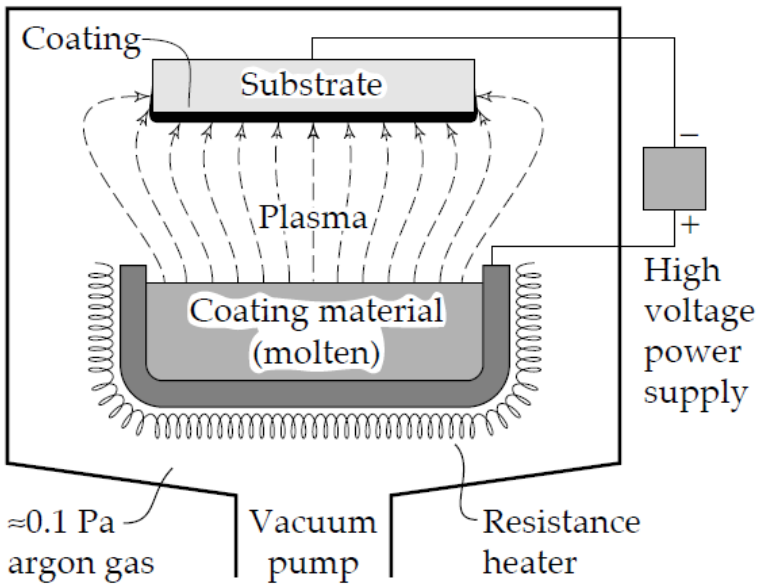

Figure 1.4: Schematic diagram of the ion-plating process [2]

1.5.1.3 Sputtering

It based on dislodging and ejecting the atoms from the coating material by bombardment of high-energy ions of heavy inert or reactive gases, usually argon. Coating material is not evaporated and instead, ionized argon gas is used to dislodge individual atoms of the coating substance. For example, in glow-discharge sputtering a coating material is placed in a vacuum chamber which is evacuated to 10^{-5} to 10^{-3} Pa and then back-filled with a working gas, e.g. argon, to a pressure of 0.5 to 10 Pa [7].The substrate is positioned in front of the target so that it intercepts the flux of dislodged atoms. Therefore the coating

material arrives at the substrate with far less energy than in ion-plating so that a distinct boundary between film and substrate is formed. When atoms reach the substrate, a process of very rapid condensation occurs. The condensation process is critical to coating quality and unless optimized by the appropriate selection of coating rate, argon gas pressure and bias voltage, it may result in a porous crystal structure with poor wear resistance. The most characteristic feature of the sputtering process is its universality. Since the coating material is transformed into the vapour phase by mechanical (momentum exchange) rather than a chemical or thermal process, virtually any material can be coated. Therefore the main advantage of sputtering is that substances which decompose at elevated temperatures can be sputtered and substrate heating during the coating process is usually negligible. Although ion-plating produces an extremely well bonded film, it is limited to metals and thus compounds such as molybdenum disulphide which dissociate at high temperatures cannot be ion-plated. The sputtering process is schematically illustrated in Figure 1.5.

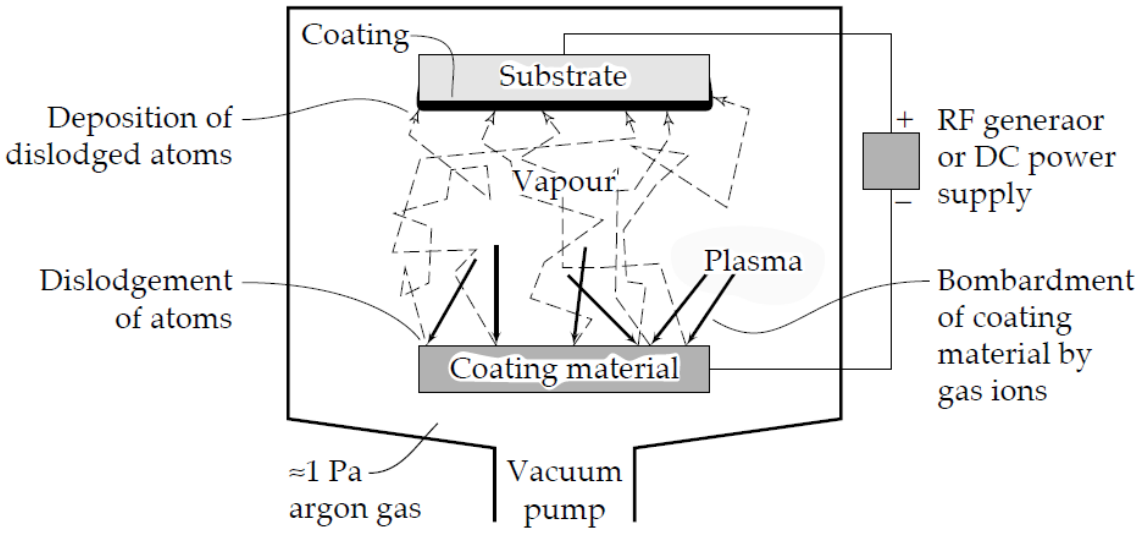

Figure 1.5: Schematic diagram of the sputtering process [2]

1.5.2 Chemical Vapour Deposition (CVD)

Coating material will be formed in vapour state by volatilization if not already in vapour state further it is forced to flow by a pressure difference or action of carrier gas towards the substrate surface. To produce a metallic coating frequently reactant gases and other required material introduced like coating of titanium nitride with the help of introducing nitrogen during titanium evaporation. Temperature and pressure range 150 – 2200°C and 50 Pa for happening of chemical reaction at atmospheric pressure [7]. Vapour will be condensing at relatively cool surface so all the parts of the system need to be hot as the vapour source. Generally, reaction portion of the system is more higher than vapour source but below the melting temperature of coating. Electric resistance and infra-red heating or inductance usually uses to heat the substrate. During the process the coating material is deposited, atom by atom, on the hot substrate. Although CVD coatings usually exhibit excellent adhesion, the requirements of high substrate temperature limit their applications to substrates which can withstand these high temperatures. The CVD process at low pressure allows the deposition of coatings with superior quality and uniformity over a large substrate area at high deposition rates [7].

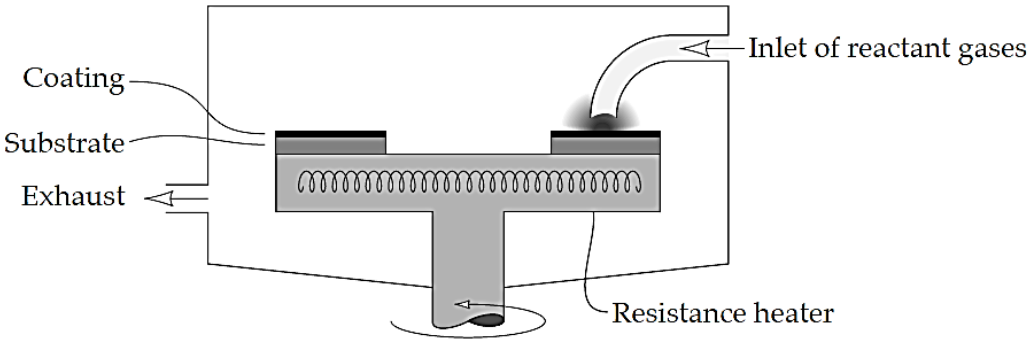

Figure 1.6: Schematic diagram of the CVD [2]

1.5.3 Ion Implantation

The energy of ions in a plasma can be raised to much higher levels than is achieved either in ion-plating or sputtering. If sufficient electrical potential is applied then the plasma can be converted to a directed beam which is aimed at the material to be coated allowing the controlled introduction of the coating material into the surface of the substrate. This process is known as ion implantation. During the process of ion implantation, ions of elements, e.g. nitrogen, carbon or boron, are propelled with high energy at the specimen surface and penetrate the surface of the substrate. It is done in a vacuum in the range of 10^{-3} to 10^{-4} Pa by means of high energy beams [2].The mass of implanted ions is limited by time, therefore compared to other surfaces, the layers of ion-implanted surfaces are very shallow, about 0.01 to 0.5 μm. The thickness limitation of the implanted layer is the major disadvantage of this method. The coatings generated by ion implantation are only useful in lightly loaded contacts. The technique allows for the implantation of metallic and non-metallic coating materials into metals, cermets, ceramics or even polymers. The ion implantation is carried out at low temperatures. Despite the thinness of the modified layer, a long lasting reduction in friction and wear can be obtained, for example, when nitrogen is implanted into steel. The main advantage of the ion implantation process is that the treatment is very clean and the deposited layers very thin, hence the tolerances are maintained and the precision of the component is not distorted. Ion implantation is an expensive process since the cost of the equipment and running costs are high [7]. The ion implantation process is schematically illustrated in Figure 1.7.

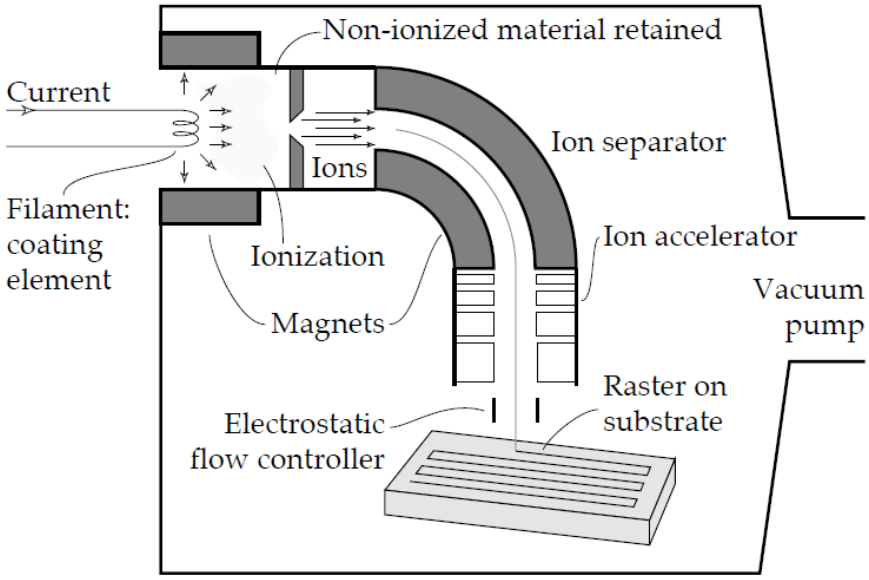

Figure 1.7: Schematic diagram of the ion implantation process [2]

1.6 TYPES OF WEAR IN THE COATING

The study of the processes of wear of coating is part of the discipline of Tribology. The complex nature of coating wear has resulted in isolated studies towards specific wear mechanisms or processes. Some wear mechanisms of coating include

1. Adhesive wear
2. Fatigue Wear
3. Fretting Wear
4. Diffusive Wear
5. Impact Wear
6. Erosive wear
7. Abrasive wear
8. Cavitation Wear

A number of different wear phenomena of coating are also commonly encountered and represented in literature. Impact wear, cavitation's wear, diffusive wear and corrosive wear are all such examples. These wear mechanisms; however, do not necessarily act independently in many applications. Wear mechanisms of the coatings are not mutually exclusive. "Industrial Wear" is the term used to describe the incidence of multiple wear mechanisms occurring in unison. Wear mechanisms and/or sub-mechanisms frequently overlap and occur in a synergistic manner, producing a greater rate of wear than the sum of the individual wear mechanisms.

1.6.1 Adhesive Wear

This type of wear can be observed in the material from one surface to another during relative motion by a process of solid-phase welding or as a result of localized bonding between contacting surfaces. Removed particle from one surface are either permanently or temporarily attached to another surface [9, 10]. This wear causes high wear and friction coefficient to overcome these problems soft metal coating is introduced for this purpose, and Au, Ag, Pb and In are representative ones [11]. One cannot observe the adhesion it two casually placed objects because of some contaminants like layer of oxygen and oil films. By increasing the hardness and surface roughness of contacting surface adhesion can be controlled. Adhesive wear of the coating can be described as plastic deformation of very small fragments within the surface layer when two surfaces slides against each other. The asperities (i.e., microscopic high points) found on the mating surfaces will penetrate the opposing surface and develop a plastic zone around the penetrating asperity [12]. By increasing the hardness and surface roughness of contacting surface adhesion can be controlled.

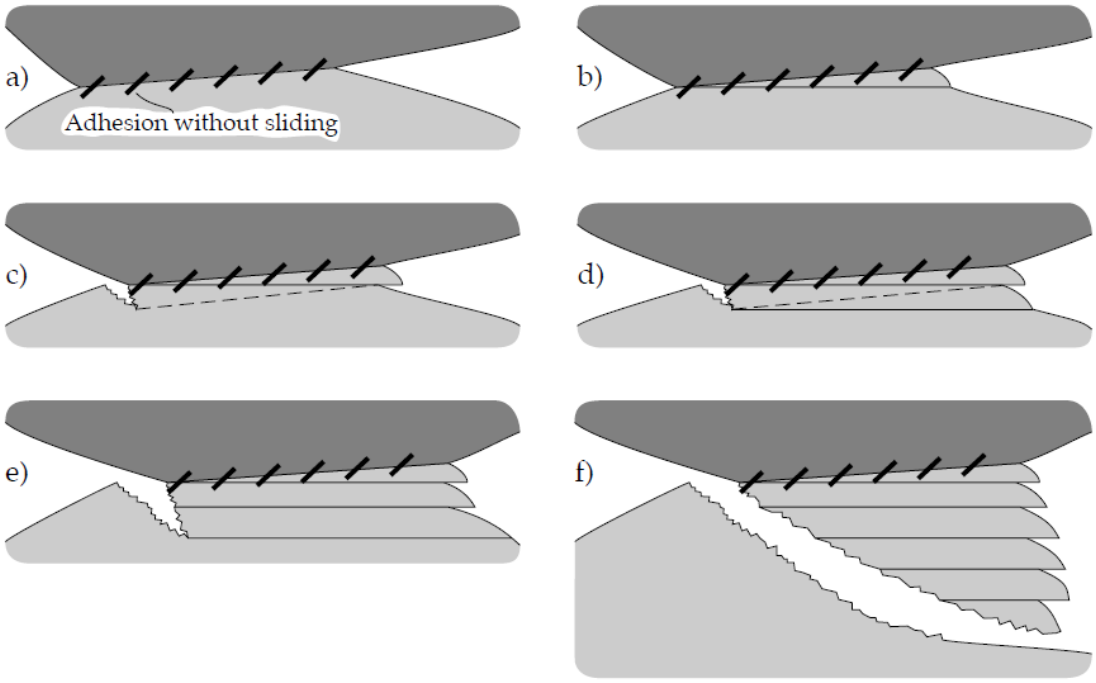

Figure 1.8: Schematic diagram of the formation of an adhesive transfer particle [2]

1.6.1.1 Metal Transfer Mechanism

It is observed that before the transfer of a wear particle from one surface to another there will be a transfer film formation which characterizes and distinguish the adhesive wear from other wear mechanism. Earlier studies of adhesive wear were observed that brass rubbed against steel leaves a transferred film of brass on steel surface which are at wear track [13]. The transferred brass was found to be highly work-hardened and probably capable of wearing the brass sample itself. This observation of inter-metallic transfer was confirmed later by tests on a variety of combinations of metals in sliding [14-15]. Formation of wear metal and its removal is explained in schematic diagram in figure 1.9; shows that phenomena of negative wear rate in the form of transfer particle can lift the pin away from the opposing surface.

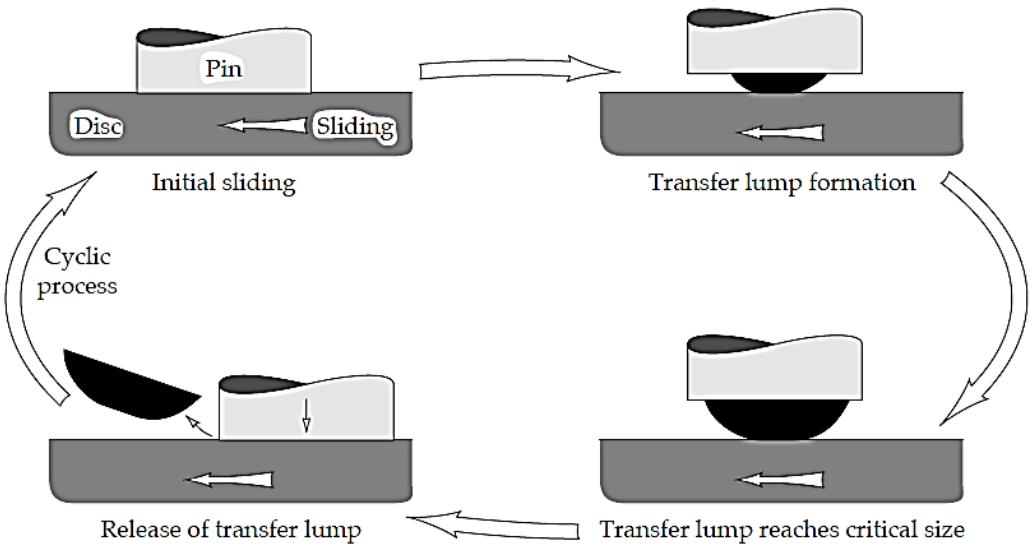

Figure 1.9: Formation and removal of a transfer particle [2]

1.6.2 Fatigue Wear

Surface fatigue wear of the coating is a process by which the surface of coating is weakened by cyclic loading, which is one type of general material fatigue. Fatigue wear in coating is produced when the wear particles are detached by cyclic crack growth of micro cracks on the surface of the coating [16]. These micro cracks are either superficial cracks or subsurface cracks. It is extremely important to improve the resistance of the material against fracture in aerospace applications and bearing failure caused by contact fatigue. In many well lubricated contacts adhesion between the two surfaces is negligible, yet there is still a significant rate of wear. This wear is caused by deformations sustained by the asperities and surface layers when the asperities of opposing surfaces make contact. Contacts between asperities accompanied by very high local stresses are repeated a large number of times in the course of sliding or rolling, & wear particles are generated

by fatigue propagated cracks, hence 'fatigue wear'. Wear under these conditions is determined by the mechanics of crack initiation, crack growth and fracture [17-18].

To solve the fatigue damage problems of high-speed steels (HSS) the powder metallurgy (PM) routes are used. As a result of the finer and more uniform microstructure that PM-HSSs exhibit, as compared to their conventionally produced counterparts, they also present enhanced cross-sectional hardness uniformity (wear resistance), fracture toughness and fatigue strength [19].

1.6.3 Fretting Wear

Fretting wear of the coating is the repeated cyclical rubbing between coating and another surface, which is known as fretting, over a period of time which will remove material from one or both surfaces in contact. It occurs typically in bearings, although most bearings have their surfaces hardened to resist the problem. Another problem occurs when cracks in either surface are created, known as fretting fatigue [20]. Fretting occurs wherever short amplitude reciprocating sliding between contacting surfaces is sustained for a large number of cycles. It results in two forms of damage: surface wear and deterioration of fatigue life. The extent of wear and surface damage is much greater than suggested by the magnitude of sliding distance. Reciprocating movements as short as 0.1 μm in amplitude can cause failure of the component when the sliding is maintained for one million cycles or more. Contacts which seem to be devoid of relative movement such as interference fits do in fact allow sliding on the scale of 1 μm when alternating and oscillating loads are carried. It is very difficult to eliminate such movements and the resultant fretting. Fretting wear and fretting fatigue are present in almost all machinery

and are the cause of total failure of some otherwise robust components. The fundamental characteristic of fretting is the very small amplitude of sliding which dictates the unique features of this wear mechanism. Under certain conditions of normal and tangential load applied to the contact a microscopic movement within the contact takes place even without gross sliding. The centre of the contact may remain stationary while the edges reciprocate with amplitude of the order of 1 μm to cause fretting damage, fretting wear can be further accelerated by corrosion, temperature and other effects.

1.6.3.1 Effect of Temperature on Fretting

Contact point temperature plays a vital role between every moving surface whereas in fretting it can be observed in two ways, oxidation and corrosion rates which usually increases with temperature and second one is mechanical properties of metal which affected by the temperature. Fretting wear rate generally decreases with increase in temperature if an oxide film forms on the surface. The formation of protective films has been observed in high temperature fretting of, for example, carbon steel [21], stainless steel [22], titanium alloys [23] and nickel alloy [24-25].

1.6.4 Diffusive Wear

When there is true contact between the atoms of opposing surfaces and a high interface temperature, significant diffusion of chemical elements from one body to another can occur. The most widespread example of such a contact is the rake face of a cutting tool close to the cutting edge in high speed machining. In this situation, there is almost the perfect contact between the tool and the metal chip due to the extreme contact stresses and very high temperatures, reaching 700°C or more [26]. The metal chip represents a

continually refreshed supply of relatively pure metal whilst the tool is a high concentration mixture of some radically different elements, e.g. tungsten and carbon. Therefore, there is a tendency for some of the elements in the tool to diffuse into the chip where solubility conditions are more favorable. When the surface material of the tool loses a vital alloying element it becomes soft and is very soon worn away by the chip.

1.6.5 Impact Wear

Impact wear is caused by repetitive collision between opposing surfaces. A classic example of this form of wear is found on the heads of hammers. This form of wear involves flat surfaces or nearly flat surfaces with a large radius of curvature compared to the size of the wear scar. This feature distinguishes impact wear from erosive wear where a sharp particle indents a flat surface. In impact wear the surface is subjected to repetitive impact by a series of pulses of high contact stress combined with some energy dissipation in each impact as shown schematically in Figure 1.10. The mechanism of impact wear involves elastic and plastic deformation when impact energy is high and/or fatigue accompanied by wear debris release due to crack formation [27-28]. If oxygen is present and the wearing material can be oxidized then a corrosive or oxidative wear mechanism can also take place. Iron and steel components are susceptible to impact wear by tribo-oxidation especially at elevated temperatures at which rapid oxidation occurs [29]. In general, impact wear is dependent on the formation of deformed layers, particularly when wear by fatigue or crack formation is predominant [30].

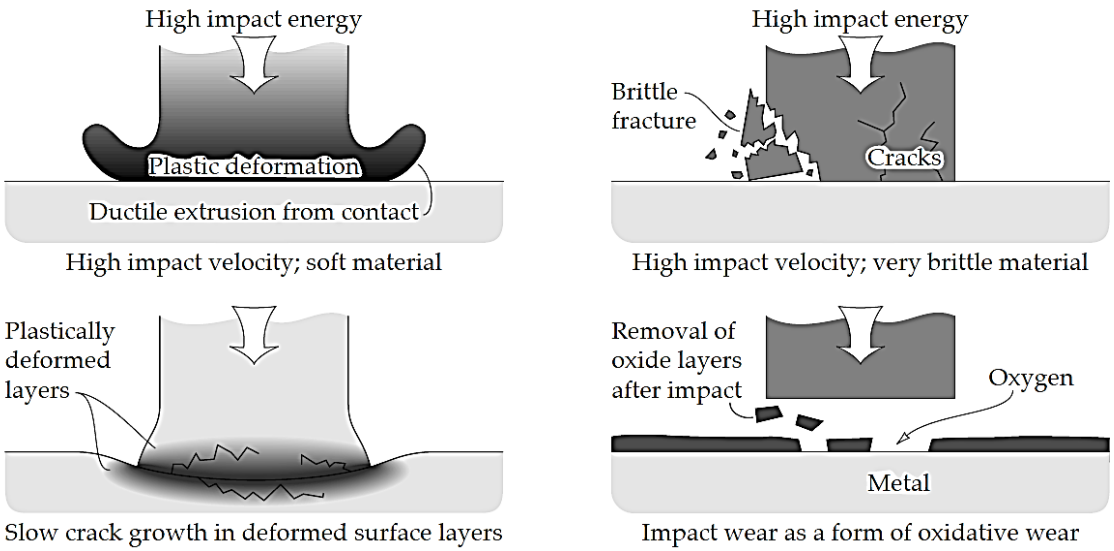

Figure 1.10: Schematic illustrations of the mechanisms of impact wear [2]

1.6.6 Cavitation Wear

Cavitation wear is known to damage equipment such as propellers or turbine blades operating in wet steam, and valve seats. Wear progresses by the formation of a series of holes or pits in the surface exposed to cavitation. The entire machine component can be destroyed by this process. Operation of equipment, e.g. propellers, is often limited by severe vibration caused by cavitation damage. Cavitation wear can be accelerated by the simultaneous occurrence of erosive wear, in other words synergistic interaction between these two wear mechanisms is possible.

1.6.7 Erosive Wear

Erosive wear is caused by the impact of particles of solid or liquid against the surface of an object. Erosive wear occurs in a wide variety of machinery and typical examples are the damage to gas turbine blades when an aircraft flies through dust clouds, and the wear

of pump impellers in mineral slurry processing systems. In common with other forms of wear, mechanical strength does not guarantee wear resistance and a detailed study of material characteristics is required for wear minimization. The properties of the eroding particle are also significant and are increasingly being recognized as a relevant parameter in the control of this type of wear. Erosive wear of the thermal spray coating is caused by the impact of particles of solid or liquid against the surface of coating [31].

1.6.7.1 Mechanism of Erosive Wear

Erosive wear mechanism controlled by various factors like angle of impingement, material, impact velocity particle size and material. The term 'erosive wear' refers to an unspecified number of wear mechanisms which occur when relatively small particles impact against mechanical components. A low angle of impingement favours wear processes similar to abrasion because the particles tend to track across the worn surface after impact. A high angle of impingement causes wear mechanisms which are typical of erosion. The speed of the erosive particle has a very strong effect on the wear process. If the speed is very low then stresses at impact are insufficient for plastic deformation to occur and wear proceeds by surface fatigue. When the speed is increased to, for example, 20 m/s, it is possible for the eroded material to deform plastically on particle impact. In this regime, which is quite common for many engineering components, wear may occur by repetitive plastic deformation. If the eroding particles are blunt or spherical then thin plates of worn material. The size of the particle is also of considerable relevance and most of the erosive wear problems involve particles between 5 -500 μm in size, although there is no fundamental reason why eroding particles should be limited to this size range [32].

1.6.8 Abrasive wear

The abrasive wear of a material is defined as the progressive loss of material due to abrasive action of hard particles present between the counter surfaces. The abrasive wear depends on various factors like abrasive size, rake angle of abrasives, applied load and shape, size, volume fraction of the dispersed phases. In addition to these factors the abrasive wear rate of a material also depends on the surface hardness and materials properties like fracture toughness [33]. A major difficulty in the prevention and control of abrasive wear is that the term 'abrasive wear' does not precisely describe the wear mechanisms involved. There are, in fact, almost always several different mechanisms of wear acting in concert, all of which have different characteristics. The mechanisms of abrasive wear are described next, followed by a mode of wear.

1.6.8.1 Mechanisms of Abrasive Wear

It was originally thought that abrasive wear by grits or hard asperities closely resembled cutting by a series of machine tools or a file. However, microscopic examination has revealed that the cutting process is only approximated by the sharpest of grits and many other more indirect mechanisms are involved. The particles or grits may remove material by micro cutting, micro fracture, pull-out of individual grains or accelerated fatigue by repeated deformations [34]. Literature denotes two basic modes of abrasive wear:

- Two-body and
- Three-body abrasive wear

Two-body abrasive wear is exemplified by the action of sand paper on a surface. Hard asperities or rigidly held grits pass over the surface like a cutting tool. In three-body

abrasive wear the grits are free to roll as well as slide over the surface, since they are not held rigidly. Two-body abrasive wear corresponds closely to the 'cutting tool' model of material removal whereas three-body abrasive wear involves slower mechanisms of material removal, though very little is known about the mechanisms involved. It appears that the worn material is not removed by a series of scratches as is the case with two-body abrasive wear. The two and three-body modes of abrasive wear are illustrated schematically in Figure 1.11.

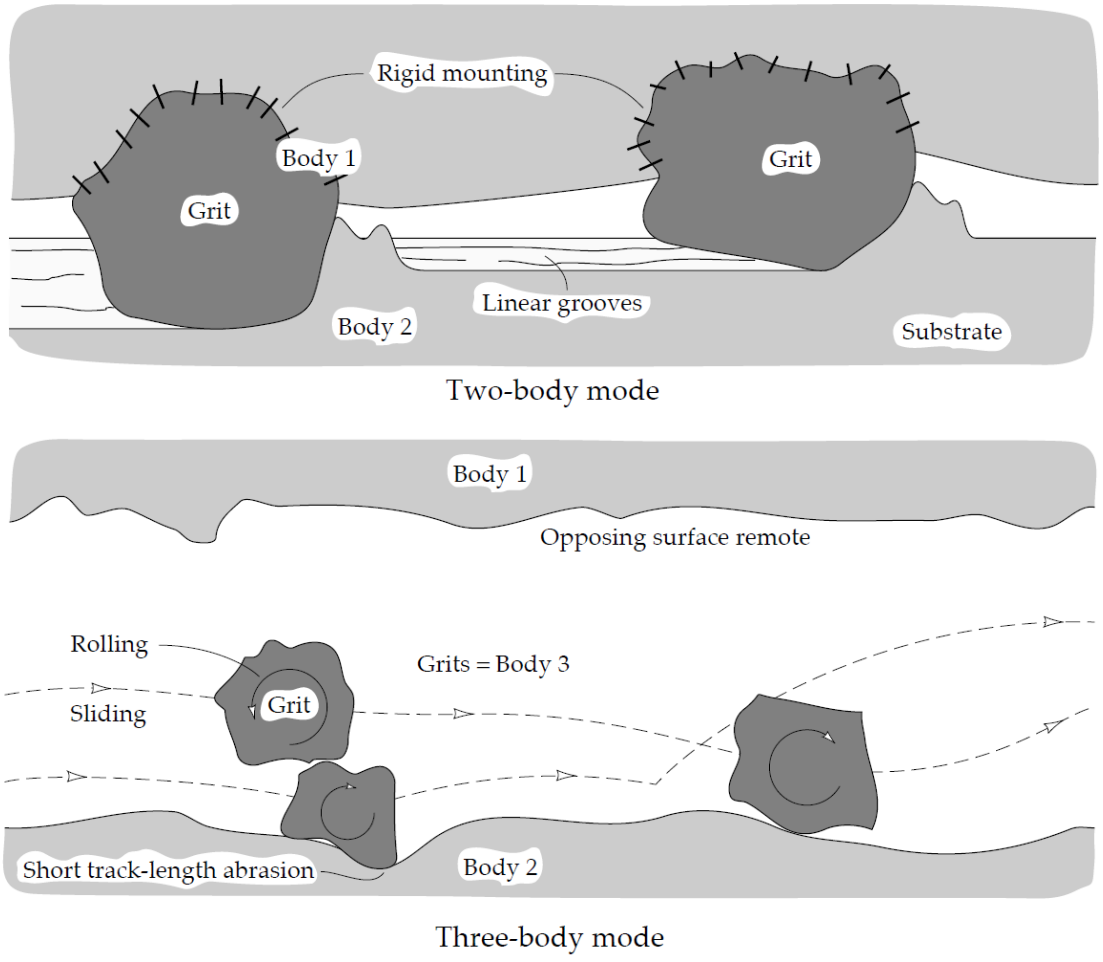

Figure 1.11: Two and three-body modes of abrasive wear [2]

1.7 PRESENT WORK

Materials are rare resources of the earth, to increase the tribological performance and life of materials, coating techniques should be adopted with help from surface engineering. Various researchers worked at different type of metallic coating which is improving the wear behaviour of uncoated material and friction force also.

This study deals with the wear behaviour of chromium nitride coating at cast iron with physical vapour deposition (PVD). After coating, the analysis for the friction and wear or weight loss of the coated materials and counter-body in dry and flooded condition at Pin-On-Disc Tribometer. For continuous lubrication, Castrol GT-20W50 engine oil is used in testing, at lubrication coated sample is showing a large mass reduction in weight loss. By varying load and sliding velocity, the progress of wear and wear mechanisms were studied by the Scanning Electron Microscopy (SEM), Microstructure by optical microscope (OM) and elemental analysis by Energy Dispersive Spectroscopy (EDS). This was performed to develop knowledge on general performance of hard coatings, wear mechanisms, and ideas of coating selection for advanced applications. By coating friction could be reduced, which is positive for engineering applications at macro level. If the adhesion force would be reduced in the dual coated system, the application at smaller scale would open up new possibilities to new technical devises like MEMS with non-sticking surfaces.

CHAPTER 2

LITERATURE REVIEW

2.0 INTRODUCTION

Several studies have been made about surface coatings deposition process, properties and performance. There are a lot of studies comparing wear properties of electroplated chromium and Titanium nitride, nickel-phosphorus coatings. Some Studies regarding hard chrome reported to large amount of mass of counter-body and minor loss of coating. Various researchers investigate the possibilities to replace hard chromium with electroless nickel coatings but the cost of the nickel coating itself was more expensive than hard chrome. Chromium coating with the nitrogen is also studied by various researchers but still many aspects are not clear by the publications. Generic studies have done about the wear behaviour chromium nitride coating at dry condition but wear mechanism is not clear properly. An effort to classify the previous findings while establishing a relation in their crude nature has been made in the following way.

2.1 EFFECT OF THICKNESS AND TEMPERATURE

Friedrich et. al (1997) Studied tribological behaviour of chromium nitride (CrN) deposited by RF magnetron sputtering. Mechanical properties like hardness, residual stress, adhesion and thickness are used for characterization. Sliding kinematics is used to understand the contact mechanics of tribological system at high loading condition at the range of 7 mm thickness. Result shows the moderate residual stress and surface adhesion

from the substrate followed by reducing wear rate comparison to uncoated material in tribological application [35].

Broszeit et. al. (1999) investigated the deposition and application of CrN coating deposited by physical vapour deposition (PVD) and discussed the problems associated with chromium (Cr) electroplating and behaviour of titanium nitride (TiN) which are not up to the mark with various process parameters. CrN is one of the answers of these problems suggested by author. Coating thickness of CrN slightly decreases by increasing the temperature while thickness of TiN increase at elevated temperature. Electroplated chromium (Cr) shows highest deposition rate but deposition rate of TiN and CrN, chromium nitride shows higher deposition rate. It replaces the TiN and electroplating of Cr with their promising corrosion resistance and several applications. Titanium (Ti) alloy against alumina-bronze 630 is reported by M.Y.P [36].

Costa et. al. (2010) High velocity oxygen fuel (HVOF) WC–10%Co–4%Cr thermal sprayed and TiN, CrN and DLC physical vapor deposition (PVD) coatings were applied to increase titanium substrate wear and friction resistance. Quantitative comparison was done at force of 5N and speed of 0.5m/s at various co0ndition.Graphite carbon structures for Ti–6Al–4V alloy DLC coated and aluminum–bronze 630 tribological pair works as a solid lubricant to prevent the wear [37].

According to the need of industrial application; **Navinsek et. al. (1997)** studied single layer, low and high temperature CrN coatings and double TiN + CrN coatings. CrN PVD coatings deposited at 450°C high temperature and 250°C lower temperature mainly in new field of application. Thickness of 5-10 mm of CrN coating shows good adhesion to

substrate more corrosion resistant than traditional coating of TiN which are thermally stable up to 700°C.Double TiN + CrN coatings were used as a highly abrasive resistant coating in the production of rotors (in the electromotor industry), and in cold forming and forging in mass manufacturing of screws [38].

2.2 CrN WITH DLC AND EFFECT OF DOPING

Simon et. al. (2003) investigated the friction and wear behaviour of chrome plated piston rings of steel and nitride stainless steel against cast iron cylinder liner segments in fully-formulated engine oils at reciprocating tribometer of high frequency. CrN was coated by thermal spray and diamond like carbon (DLC) coated by PVD. It was observed that DLC shows lower wear compare to CrN. Additives like molybdenum dithiocarbamate (MoDTC) reduces the friction and wear effectively where acidic fuels promotes the scuffing [39].

Etsion et. al. (2006) analysed the scuffing resistance of piston pin by designing a test ring to characterize the tribological performance. The test rig was used to study scuffing resistance provided by CrN and diamond-like carbon (DLC) coatings and by laser surface texturing in comparison with a base line standard pin. Treated pin performed better than untreated while laser surface texturing offers the best performance [40].

Lanigan et. al. (2015) also worked on diamond like carbon coating (DLC) to enhance the tribological properties and coating durability by doping of silicon (Si) which in turn can affect hardness and improves the adhesion of coating by lowering the internal stress. Doping also help to form a protective layer in flooded condition by composed of recognized wear reducing element like sulphur, phosphorus, calcium and zinc [41].

In recent trends to represent the wear and friction, **M.B. dos Santos et. al. (2014)** draws the wear map of track by the help of positioning sensor. Friction increases due to accumulation of wear debris at the end of wear track in dry sliding condition. Triboscopic image of DLC-CrN coating clearly indicates the spalling. By the distribution of graphite friction decreased periodically following approximately the size and spacing of the graphite inserts [42].

Rohollah Ghasemi et. al. (2014) studied the relationship between flake graphite orientations, smearing effect, and closing tendency under abrasive wear conditions microstructural observations indicated a uniform distribution of graphite flakes on unworn surfaces, whereas worn surfaces demonstrated a tendency towards a preferred orientation. Approximately 40% of the open flakes of the unworn surfaces were closed during sliding, which may result in the deterioration of the self-lubricating capability of cast iron [43].

Giovanni Bolelli et. al. (2006) studied mechanical and tribological properties of electrolytic hard chrome (EHC) and high velocity oxy-fuel (HVOF) sprayed coatings. EHC coating shows very hard nature with no crack at 10 N load in indentation test. While harder coating shows severe mass loss in dry condition but a promising quality more abrasive resistance can't be neglected. Author also concludes that HVOF sprayed coating especially cermets coating are alternative to EHC with lower friction coefficient [44].

Yamamoto et. al. (2007) studied the PVD and unbalanced magnetron sputtering (UBM) of multi-layered CrN/BCN for low friction and anti-wear applications. Transmission Electron microscopy (TEM) confirms the coating thickness of CrN coating was 20-

100nm while BCN layer was 1-5 nm. Sliding tests were conducted using a reciprocating-type tribotester against bearing steel ball under dry condition. The CrN/BCN coatings had a low friction coefficient of about 0.2, which was one-third that of standard CrN coating. The wear rate of counter body (bearing steel) was also markedly reduced [45].

Cengiz Oner et. al. (2009) analysed tribological properties of CrN coated engine cylinders by PVD Coated engine cylinder surface of cast iron were tested by normal operating conditions. Concern to the wear CrN coated cylinder shows almost no wear while on uncoated cast iron many deep groove, surface cracks and severe deformation are observed. Surface roughness of cast iron cannot prevent the failure of oil film, but CrN coating helps to achieve hydrodynamic lubrication and hence reduces wear and deformation [46].

Hetal N. Shah et. al. (2011) studied CrN and CrSiN coatings were deposited on stainless steel substrate by reactive magnetron sputtering. The coatings were characterized for phases, chemical composition, microstructure, and mechanical properties by X-ray diffraction (XRD), field emission scanning electron microscopy (FESEM)/energy dispersive spectroscopy (EDS), atomic force microscopy (AFM), and nano-indentation technique, respectively. The improved hardness in both the coatings was attributed mainly to a reduction in crystallite size, decrease in surface roughness, and dense morphology. The incorporation of Si into the CrN coatings has improved both hardness and Young's modulus [47].

2.3 EFFECT OF NITROGEN

P. Z. Shi et. al. (2013) studied the deposition of CrN under different nitrogen pressure and characterize by Vickers indentation technique which shows the crystal structure of CrN coatings varied from substoichiometric β-Cr2N (111) to fcc-CrN (200) preferential orientations with increasing deposition pressure and the better surface morphologies were achieved when nitrogen pressure was in between 2 Pa and 5 Pa. A maximum hardness of 2210 HV and deposition rate of 10.2 μm/h were obtained and the lowest wear rate of 3.3×10^{-6} mm^3/N m at 5 Pa was exhibited, and the coatings applied on piston rings exhibited a hardness exceeding 1600 HV [48].

Lorenzo-Martin et. al. (2013) studied the coating thickness and effect of micro-structure on friction and wear of CrN coating were determined under sliding conditions. The friction behaviour was observed to be strongly dependent on coating thickness at relatively low loads (5 N). At higher loads, however, the coating was 1 mm thickness quickly worn through, while the thicker ones (5 and 10 mm) remained intact. Author also concludes morphological behaviour of coating for 1μm thickness coating surface is relatively smooth and grain structure is uniaxial. At the thickness of 5μm surface morphology is coarser and grain distribution is bimodal. Cauliflower and coarsest texture is observed at 10 μm thickness of CrN with most columnar and fan shaped [49].

Chang-Ming Shi et. al. (2014) worked on double layer coating with various thickness ratios of CrN vs Cr_2O_3 by arc ion plating which shows the insertion of CrN layer between the Cr_2O_3 layer and substrate can effectively decrease the internal stress level of the coating. By increasing the thickness ratio of CrN vs Cr_2O_3 layer, the surface roughness of

double-layered coatings decreased gradually, which had a certain influence on the friction coefficient. In addition, the micro-hardness also declined gradually, the adhesive strength almost increased linearly, whereas the wear rate declined firstly and then increased slightly. As the thickness ratio was 2:1, the double-layered coating exhibited the best wear resistance [50]. Various researchers are working towards metallic coating with some rare earth material and composite coating to enhance the tribological properties of the substrate at various operating conditions.

2.4 NANO – TREATMENT OF COMPOSITE COATINGS

Hao–Jie Song et. al. (2006) reported the effect of nano-Al_2O_3 surface treatment on tribological performance of phenolic composite coating. Friction coefficient of composite coating decreases with increasing sliding speed and load by reinforcement of different fillers. Anti-wear behaviour of the coating filled with 3.0 wt. % TDI- Al_2O_3 was the best under 320 N and at a speed of 3.0 m/s [51].

Li Hejun et. al. (2013) investigated carbon/carbon composite and SiC nano-wires to improve the wear resistance of SiC coating. Two methods were used one was chemical vapour deposition (CVD) and second, pack cementation for dense silicon-carbide nano-wire reinforced (SiCNW-SiC) coating. This incorporation improves fracture toughness with the wear resistance of the coating. Wear behavior were also analyzed at elevated temperature at 8000c and result showed significantly improvement by introducing SiC nano-wires. The wear mechanisms of SiC NW-SiC coating at 800°C were abrasive wear and delamination, pullout and breakage of SiC grains resulted in failure of SiC coating without SiCNWs at tested temperature [52].

R. N. Rao et. al. (2013) reported the wear coefficient of aluminum matrix composite in boundary region between mild to severe wear, author concludes that there are four wear regimes; they are ultra-mild wear, mild wear or oxidative wear, delamination wear & severe wear. All facts are discussed on the basis of prevailing wear mechanism [53].

2.5 WEAR MAP

R. Bosman et. al. (2012) predicted a mild wear map for boundary lubricated contacts is presented and validated using model experiments. Both the transition from mild to severe wear as mild wear itself is modelled. The criterion for the transition from mild to severe wear is a thermal one. The mild wear model is based on the hypothesis that for an additive to protect the surface against severe wear a sacrificial chemical layer should be present at the surface [54].

Wear map of grey cast iron is reported by **A. R. Riahi et. al. (2003)** to summarize wear rate and its mechanism of A30 grey cast iron against AISI 52100 type steel at load of 0.3-50.0 N and sliding range of 0.2-3.0 m/s. Ultra mild wear at a rate of 8×10^{-7} and 9×10^{-7} mm^3/m at 0.3 N for 0.2 and 0.5 m/s. In mild wear regime rage of wear rate 10^{-5} mm^3/m at low loading condition, and 10^{-4} mm^3/m at high operating condition. Severe wear regime shows the rate of 10^{-1} to 3.2×10^{-1} mm^3/m compared to those of mild regime [55].

Wear maps for titanium nitride coatings deposited on copper and brass a widely used group of engineering materials in numerous applications reported by **C. Subramanian et. al. (2000)** which shows the coefficient of friction increases with the increase in the thickness of electroless nickel (EN) interlayer for both copper and brass substrates.

Scratch adhesion tests were performed and the results interpreted via a profilometer and microscopic examination. Recommendations have been made as to appropriate nickel interlayer thicknesses for a given degree of wear resistance as reflected in the coating failure mechanism, by way of the so-called wear map [56].

2.6 EFFECTS OF LUBRICATION

Some other hard coatings are also investigated by various researchers. **Zhiqiang Liu et. al. (1999)** studied wear mechanism and transition of molybdenum (Mo) coating against bearing steel and boron cast iron in lubricated condition. Wear resistance of Mo coating was superior to that of uncoated and wear rates of the coating against a steel slider were lower compared with those worn against a cast iron slider. Mo coating were showing 2 to 18 times better than that of uncoated hardened steel [57].

Al-Mo-Ni on AISI 440ºC test steel, piston ring material and testing were carried out by **M. B. Karamis et. al. (2004**) at various loads and constant sliding velocity of 1 m/s in both dry and lubricated condition with grey cast iron as counter-face material. Under lubricated conditions, the roughness decreased under the loads of 100 N and then increased. Roughness is also affected by the temperature also; Frictional forces were generally lower at a higher test temperature than those at a lower test temperature. Surprisingly, the test temperature of 200ºC was a critical point for frictional forces and surface roughness [58].

There are various methods to form a layer at the substrate or coat the material at uncoated material. Thermal spray coating is also one of the coating methods, Wear behaviour of Plasma spray Al_2O_3 coating against steel AISI D2 at different load and various speed

reported by **J.E. Fernadez et. al. (1995).** Wear rate is lower in conformal contact in steady-wear state and there exists a maximum-wear load both in dry sliding and lubricated sliding, sliding velocity range is from 1 m/s to 5 m/s. author explain the wear rise of plasma-sprayed at the velocity range of 1-3 m/s finally the failure types of plasma-sprayed Al_2O_3 coating when sliding against steel AISI D2 in conformal contact are: plastic deformation, adhesive wear and brittle fracture and in flooded condition wear of plasma sprayed Al_2O_3 remains small at low siding velocity and further increases proportionally to the kinetic energy of moving specimen from 1 m/s to 2.8 m/s [59].

S. Johanssona et. al. (2011) optimized the mechanical friction of automotive engines piston rings. Various thermally coated cylinder liners are used to optimize the frictional impact of the contact between the cylinder liner and piston rings. CrC-NiCr and MMC are two liner material showed lower frictions than the other material. In compare to base materials thermally sprayed liner shows less wear and friction [60].

2.7 RESEARCH GAP

In starting chromium coating was very popular hard and common coating due to cheap, wear and corrosion resistance. Further it moves towards electroplating of chromium which is replaced by chromium nitride coating due to environmental issues concerned with hexavalent chromium(Cr+6).This was very hazardous so it has to be removed from environment and waste water after plating. Thickness is a critical parameter in CrN coating by PVD it affects by the supply pressure of nitrogen and other parameters also. Various Tribo-mechanical properties like wear friction and hardness affects by the coating thickness. Researchers did a lot of work in CrN coating but there is some also some lack in CrN PVD coating. In entire literature researcher are not working towards optimization of coated surface and bonding mechanism of CrN still not very clear to the substrate like cast iron. Roughness of the coated surface needs to be optimized. Friction of the coating should be as low as possible by supply of engine oil and literature shows some doping of materials, there is a possibility to mix the nano-particle with the engine oil and observed the behaviour of wear and friction of CrN coating by PVD.

CHAPTER 3

EXPERIMENTAL SETUP

3.0 SAMPLE PREPARATION

Casting is a manufacturing process by which a liquid material is usually poured into a mold, which contains a hollow cavity of the desired shape, and then allowed to solidify. The solidified part is also known as a casting, which is ejected or broken out of the mold to complete the process.

Rings is always produced in circular shape for the market use and it is very hard to get a fresh piston rings to produce in our desired shaped because lots of finishing operation is already performed on the rings material. As per our machine Pin-on-Disc tribometer either a pin of circular shape or discs of desired dimension have to be produced. With prior analysis, it was decided that a disc of the well know composition will be produced for the testing and experimentation purpose.

A wooden pattern of the desired dimension based on the constrained of the plasma spray coating machine is prepared, for the easy removal of the casting a draft of ½º is provided on the pattern. A sand mould is prepared with the help of press and the cavity is ready for the pouring of metal.

3.1 COATING PREPARATION

Coating is a covering that is applied to the surface of an object, usually referred to as the substrate. In many cases coatings are applied to improve surface properties of the

substrate, such as appearance, adhesion, weldability, corrosion resistance, wear resistance, and scratch resistance. In other cases, in particular in printing processes and semiconductor device fabrication (where the substrate is a wafer), the coating forms an essential part of the finished product.

3.2 PHYSICAL VAPOR DEPOSITION

Physical vapor deposition processes (often just called thin film processes) are atomistic deposition processes in which material is vaporized from a solid or liquid source in the form of atoms or molecules and transported in the form of a vapor through a vacuum or low pressure gaseous (or plasma) environment to the substrate, where it condenses.

Typically, PVD processes are used to deposit films with thicknesses in the range of a few nano-meters to thousands of nano-meters; however, they can also be used to form multi-layer coatings, graded composition deposits, very thick deposits, and free standing structures. The substrates can range in size from very small to very large, for example the 10'×12' glass panels used for architectural glass. The substrates can range in shape from flat to complex geometries such as watchbands and tool bits. Typical PVD deposition rates are 10–100Å (1–10 nano-meters) per second. Physical vapor deposition processes can be used to deposit films of elements and alloys as well as compound susing reactive deposition processes. In reactive deposition processes, compounds are formed by the reaction of the depositing material with the ambient gas environment such as nitrogen (e.g. titanium nitride, TiN) or with a co-depositing material (e.g. titanium carbide, TiC). Quasi-reactive deposition is the deposition of films of a compound material from a compound source where loss of the more volatile species or less reactive species during

the transport and condensation process is compensated for by having a partial pressure of reactive gas in the deposition environment; for example, the quasi-reactive sputter deposition of ITO (indium–tin oxide) from an ITO sputtering target using a partial pressure of oxygen in the plasma. The main categories of PVD processing are vacuum deposition (evaporation), sputter deposition, arc vapour deposition, and ion plating, as depicted in Figure 3.1.

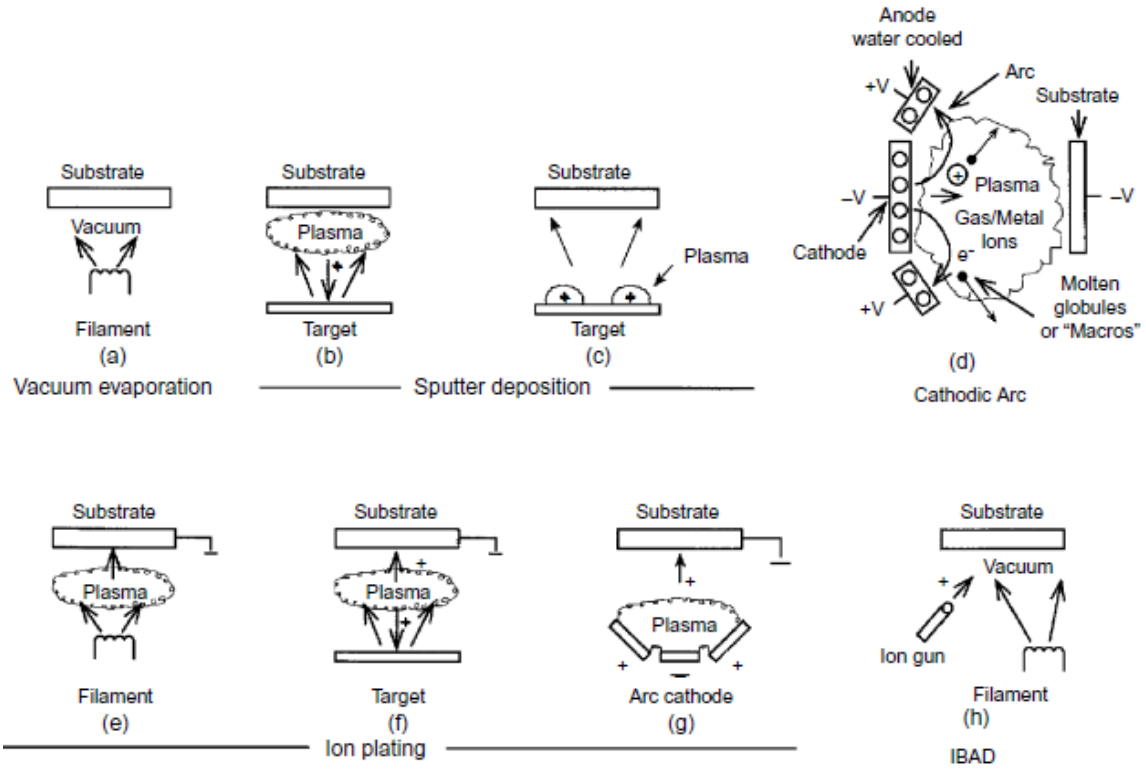

Figure 3.1: PVD Processing Technique (a) Vacuum Evaporation (b) & (c) Sputter Deposition in plasma environment (d) Sputter deposition in vacuum (e) Ion plating in plasma environment with a thermal evaporation source and (f) Ion plating with sputtering source (g) Ion plating with an arc vaporization source and (h) Ion beam assisted deposition (IBAD) with a thermal evaporation source & Ion bombardment from an ion gun.

3.2.1 Ion Plating

Ion-Plating is an atomistic deposition process that utilizes continuous or periodic bombardment of the substrate and depositing atoms of film material by atomic-size denergetic particles. The bombardment prior to deposition sputter cleans the surface. Bombardment during deposition is used to obtain good adhesion, densify the depositing material, aid in chemical reactions, modify residual stress, and otherwise modify the structure, morphology, and properties of the depositing film or coating. It is important, for best results, that the bombardment be continuous between the cleaning and the deposition portions of the process in order to maintain an atomically clean interface.

Ion-plating is also called ion-assisted deposition or ionization-assisted deposition (IAD), ion vapor deposition (IVD), ionized physical vapor deposition (IPVD) [61], and energetic condensation [62]. This definition does not specify the source of the depositing film material, the source of the bombarding particles, nor the environment in which the deposition takes place. The concept and application of ion plating was first reported in the technical literature in 1964 the technique was initially used for the improvement of adhesion and surface coverage as well as the densifying of PVD films [63]. The technique was subsequently shown to enhance chemical reactions in the reactive deposition of compound thin films. Later it was shown that the concurrent bombardment could be used where the depositing atoms were from a chemical vapor precursor. The bombardment was shown to control film properties such as density and residual film stress [64].

Often the term “ion plating” is accompanied by modifying terms – for example, “sputterion plating”, “reactive ion plating”, “chemical ion plating”, “alternating ion plating”, “arc ion plating”, “vacuum ion plating”, etc. – which indicate the source of the depositing material, the method used to bombard the film, the deposition environment, or other particular conditions of the deposition. There are two common versions of the ion plating process. In “plasma-based ion plating”, typically a negatively biased substrate is in contact with plasma and bombarding positive ions are accelerated from the plasma and arrive at the surface with a spectrum of energies. In plasma-based ion plating, the substrate can be positioned in the plasma-generation region or in a remote or downstream location outside the active plasma-generation region. The substrate can be the cathode electrode in establishing plasma in the system. Figure 3.2 (a) shows a simple plasma-based ion plating configuration using a resistively heated vaporization source. In “vacuum-based ion plating”, the film material is deposited in a vacuum and the bombardment is from an ion source (“gun”). The first reference to vacuum-based ion plating or vacuum ion plating was in 1973, [65] when it was used to deposit carbon films using a carbon ion (“film ion”) beam [66]. In a vacuum, the source of vaporization and the source of energetic ions for bombardment may be separate. This process is often called ion beam-assisted deposition (IBAD) [67]. Often, the ion beam is “neutralized” by the addition of electrons so the beam is volumetrically neutral. This prevents columbic repulsion in the beam and charge build-up on the bombarded surface. Figure 3.2 (b) shows a simple vacuum-based (IBAD) system using an e-beam evaporation source and an ion gun. In reactive ion plating, the plasma activates the reactive species, or reactive and inert ion species are produced in an ion source or plasma source.

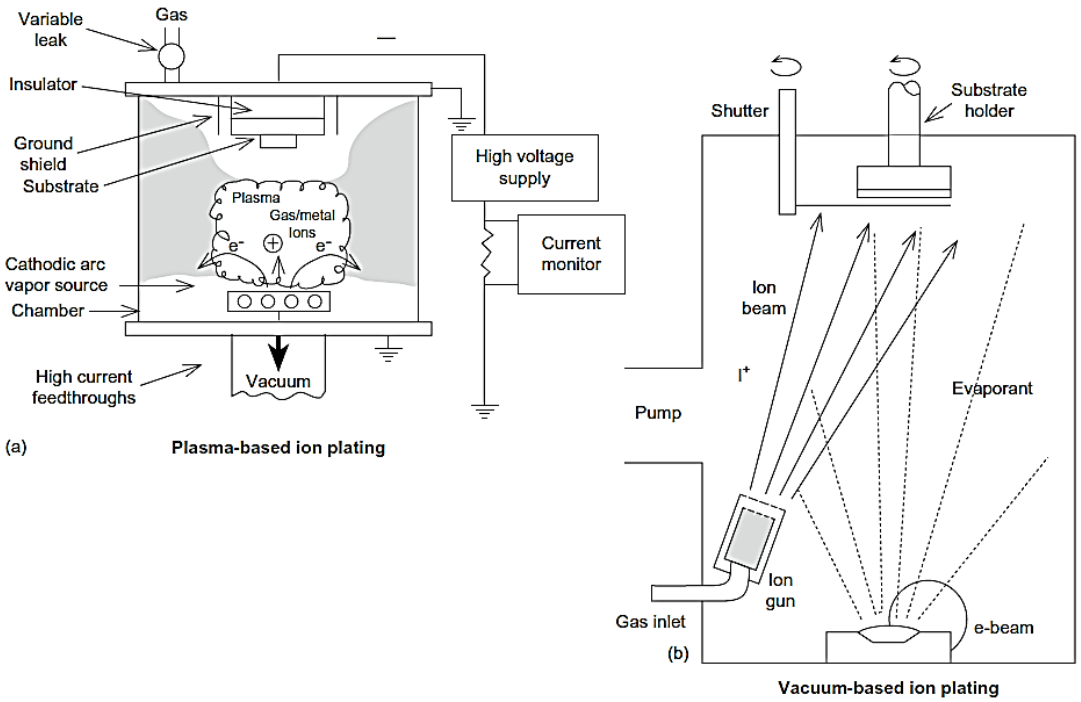

Figure 3.2: Ion Plating Configurations:

(a) Plasma Based Ion Plating (b) Vacuum Based Ion Plating.

The bombardment enhances the chemical reactions and densify's the depositing film. The bombardment-enhanced interactions on the surface are complex and poorly understood [68]. In some cases, such as when using low voltage, high current e-beam evaporation, arc vaporization, high power pulse magnetron sputtering, or post-vaporization ionization, an appreciable portion of the vaporized film atoms is ionized to create "film ions", which can also be used to bombard the substrate surface and growing film. The important parameters in non-reactive ion plating are the mass and energy distribution of the bombarding species, and the flux ratio of bombarding species to depositing atoms [69, 70]. The flux ratio (ions: atoms) may be from 1: 10 if energetic (500 eV) ions are used to greater than 10: 1 if low energy (10 eV) ions are used. Typically, it is found that above a

certain energy level the flux ratio is more important in the modification of film properties than is the bombardment energy. High energy bombardment can have differing effects from low energy bombardment.

For example, low energy (~5 eV) bombardment promotes surface mobility of the ad atoms and is used to aid in epitaxial growth [71], while high energy bombardment generally promotes the formation of a high nucleation density and a fine-grained deposit. The energy distribution of the bombarding species is dependent on the gas pressure, [72] so gas pressure control is an important process parameter in plasma-based ion plating. In reactive ion plating, the chemical reactivity of the energetic bombarding and depositing species are important process parameters.

3.2.1.1 Stages of Ion plating

The ion plating process can be divided into several stages where the bombardment affects the film formation:

1. The substrate surface can be sputter cleaned or the surface "activated" in the deposition chamber.
2. Bombardment during the nucleation stage of film deposition can increase the nucleation density and cause recoil implantation of depositing film atoms into the substrate surface.
3. Bombardment during interface formation adds thermal energy to the surface and introduces lattice defects into the surface region, which promotes diffusion and reaction.

4. Bombardment during film growth densify's the film, causes recoil displacement of near-surface atoms (atomic peening), causes sputtering and re-deposition, and adds thermal energy.
5. In reactive deposition, bombardment aids chemical reactions on the surface and the presence of plasma activates reactive species. The bombardment may also preferentially remove un-reacted species from the growing deposit. It is important that the surface preparation stage blends into the deposition stage so that there will be no recontamination of the substrate surface after in situ surface cleaning and activation. Also, the high potential & bombarding flux used for surface preparation must be decreased during the nucleation stage in order to allow a film to form & not sputter away all of the depositing film atoms.

3.3 DESIGN OF EXPERIMENT

Statistical methods are commonly used to improve the quality of a product or process. Such methods enable the user to define and study the effect of every single condition possible in an experiment where numerous factors (load and sliding speed) were involved in present work to study the wear behavior of the piston rings coatings. There was one parameter (Load) which was taken into consideration to determine the wear rate and coefficient of friction. There are several methods to design the experiment but a chosen constant sliding distance (2500 m) &variable 319, 764 and 1433 rpm with varying load of 50 N, 60 N, 70 N, 80 N, 90 N, and 100 N in two set of experiment as shown in table below. To determine the response such as wear rate, coefficient of friction, microstructure, elemental and phase analysis.

Table 3.1: Variables for wear test

Variables	Level/Track 1	Level/Track 2	Level/Track 3
Sliding speed (rpm)	319 rpm	764 rpm	1433 rpm
Load (kg)	5 kg	6 kg	7 kg
Load (kg)	8 kg	9 kg	10 kg

Table 3.2: Design of experiment for wear test

Coatings	Counter Body	Run	Load(N)	Sliding speed (rpm)
Hard Chrome	Cylinder liner pin	Base plate, Dry, Flooded	50	319
Hard Chrome	Cylinder liner pin	Base plate, Dry, Flooded	60	764
Hard Chrome	Cylinder liner pin	Base plate, Dry, Flooded	70	1433
Hard Chrome	Cylinder liner pin	Base plate, Dry, Flooded	80	319
Hard Chrome	Cylinder liner pin	Base plate, Dry, Flooded	90	764
Hard Chrome	Cylinder liner pin	Base plate, Dry, Flooded	100	1433

3.4 PIN ON DISC TEST

Pin on disc type wear monitor with data acquisition system was used to evaluate the wear behavior of chrome plating against the cylinder liner. Load was applied on pin by dead weight through pulley string arrangement. The system had maximum loading capacity of 200 N. The test was performed under dry lubricated condition and for lubrication 20W50

Engine oil being used. The wear test can be performed on any wear tester, but for thin coatings pin on disc wear test is most commonly used (figure 3.3).

Figure 3.3: Wear and friction monitor machine for pin on disc test

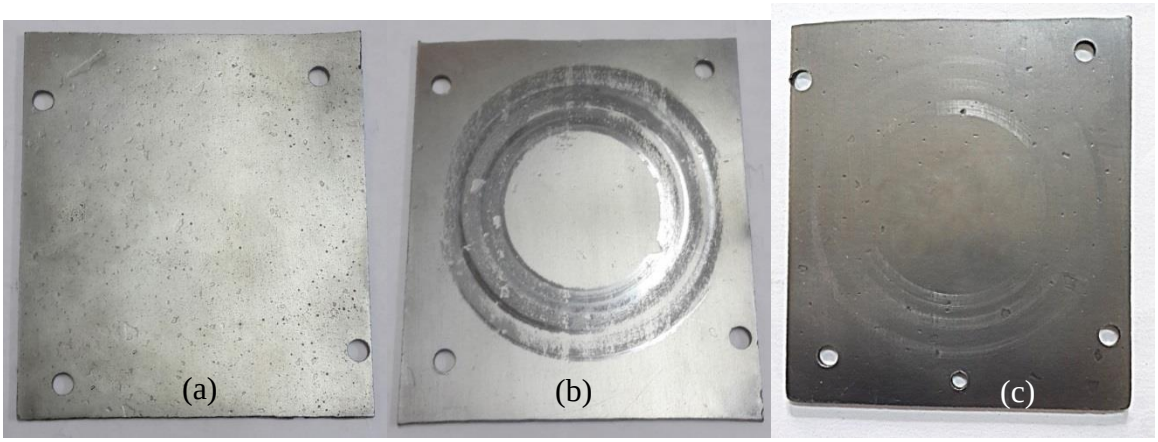

Figure 3.4: (a) Hard Chrome coating before wear test

(b) Hard Chrome coating after wear test in dry condition

(c) Hard Chrome coating after wear test in flooded condition

The machine is attached with the computer with software WINDCUM 2008. A window is open in the software and there are options to select various loads, times, pin diameter. The machine directly gives the coefficient of friction on the selected loading and sliding conditions. In this machine basically there is a rotating disc; and a pin is fixed over stainless steel pin holder. The pin can be loaded with different loads, it can be change externally. The coating pasted disc fastened on the machine with the help of screws .The load was applied on the pin through dead weight loading arrangement. The coating surface and pin was initially washed with methyl alcohol so that, moisture should not present on coating surface. Initially, cylinder liner material pin was fixed on the pin holder; the wear rate of the coatings was calculated at different loading and sliding conditions. The wear rate was calculated by weighing the disc before after the wear test in terms of grams on an electronic balance of least count 0.00001 g. The load was taken as 50, 60, and 70 N respectively and the sliding speed was taken as 319 rpm & distance was taken 2.5 km. The wear behavior against same counter pin material was analyzed. The pin of diameter 6 mm was chosen for all of experiment set. The wear test carried out at room temperature of 20˚C. During the wear test some amount of material also gets deposited on the pin in the form of a tribolayer so pin was cleaned after every test. So that there was always contact between pin and the coating surface, and the wear mechanism was between pin and coating surface, and a wear track was formed on the coating (figure 3.4 (b) & (c)).

3.5 SCANNING ELECTRON MICROSCOPE

A scanning electron microscope (SEM) is a type of electron microscope that images a sample by scanning it with a high-energy beam of electrons in a raster scan pattern (figure 3.5). The electrons interact with the atoms that make up the sample producing signals that contain information about the sample's surface topography, composition, and other properties such as electrical conductivity.

Figure 3.5: Scanning electron microscope

In a typical SEM, an electron beam is thermionically emitted from an electron gun fitted with a tungsten filament cathode. Tungsten is normally used in thermionic electron guns because it has the highest melting point and lowest vapour pressure of all metals, thereby allowing it to be heated for electron emission, and because of its low cost. For conventional imaging in the SEM, specimens must be electrically conductive, at least at the surface, and electrically grounded to prevent the accumulation of electrostatic charge

at the surface. Metal objects require little special preparation for SEM except for cleaning and mounting on a specimen stub. Nonconductive specimens tend to charge when scanned by the electron beam, and especially in secondary electron imaging mode, this causes scanning faults and other image artifacts. They are therefore usually coated with an ultrathin coating of electrically-conducting material, commonly gold, deposited on the sample either by low vacuum sputter coating or by high vacuum evaporation. Conductive materials in current use for specimen coating include gold, gold/palladium alloy, platinum, tungsten, chromium and graphite [73]. Coating prevents the accumulation of static electric charge on the specimen during electron irradiation. For SEM, a specimen is normally required to be completely dry, since the specimen chamber is at high vacuum. Hard, dry materials such as wood, dried insects or shells can be examined with little treatment, but living cells and tissues and whole, soft-bodied organisms usually require chemical fixation to preserve and stabilize their structure. Fixation is usually performed by incubation in a solution of a buffered chemical fixative, such as glutaraldehyde, sometimes in combination with formaldehyde [74 – 76].

The worn surface was examined by scanning electron microscope of S-3700 series. To see the microstructure of the wear track the coating material is coated with gold. Then it was put on job holder, the job holder was then moved inside the chamber of the scanning electron microscope. The scanning electron microscopy was used to determine the surface morphology of the wear track which gave the wear mechanism at various loading conditions and speeds. For SEM of samples following parameters were chosen that were Accelerating Voltage=15000 Volt, Deceleration Voltage = 0 Volt, Magnification=1000, Working Distance=12600 um, Emission Current=80000 nA.

3.6 X -RAY DIFFRACTOMETER

X ray diffractometer is a measuring instrument for analyzing the structure of a material from the scattering pattern produced when a beam of radiation or particles (as X rays or neutrons) interacts with it. A typical diffractometer consists of a source of radiation, a monochromator to choose the wavelength, slits to adjust the shape of the beam, a sample and a detector (figure 3.6). In a more complicated apparatus also a Gonio meter can be used for fine adjustment of the sample and the detector positions. When an area detector is used to monitor the diffracted radiation a beam stop is usually needed to stop the intense primary beam that has not been diffracted by the sample. Otherwise the detector might be damaged. Usually the beam stop can be completely impenetrable to the X-rays or it may be semi-transparent. The use of semi-transparent beam stop allows the possibility to determine how much the sample absorbs the radiation using the intensity observed through the beam stop. The specimen of the worn surfaces was placed on X-ray chamber. The scanning of the specimen was done from angle 20˚ to 90˚ and the scanning speed was chosen as 2 degree/min.

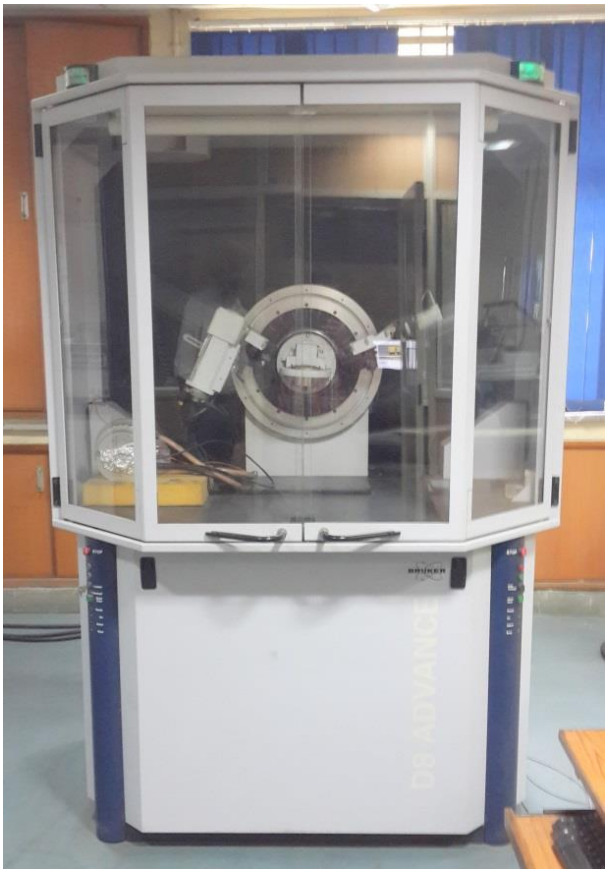

Figure 3.6: X-Ray diffractometer

3.7 VICKERS MICRO HARDNESS TESTER

Vickers Hardness Tester is a key piece of equipment that is indispensable to metallographic research, product quality control, and the development of product certification materials.

Vickers Micro hardness test procedure as per ASTM E-384, EN ISO 6507, and ASTM E-92 standard specifies making indentation with a range of loads using a diamond indenter which is then measured and converted to a hardness value. For this purpose as long as test samples are carefully and properly prepared, the Vickers Micro hardness method is considered to be very useful for testing on a wide type of materials, including metals,

composites, ceramics, or applications such as testing foils, measuring surface of a part, testing individual microstructures, or measuring the depth of case hardening by sectioning a part and making a series of indentations. Two types of indenters are generally used for the Vickers test family, a square base pyramid shaped diamond for testing in a Vickers hardness tester and a narrow rhombus shaped indenter for a Knoop hardness tester.

The Vickers hardness test method requires a pyramidal diamond with square base having an angle of 136° between the opposite faces. Upon completion of indentation, the two diagonals will be measured and the average value will be considered (figure 3.7).

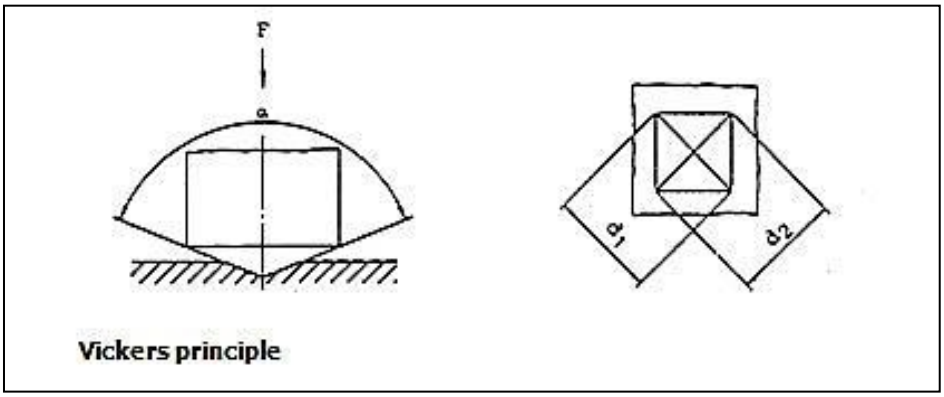

Figure 3.7: Vickers micro hardness indentation

The loads for Micro Vickers or Knoop hardness testing methods are typically very low, ranging from a few grams to 2 kg. The load range for Macro Vickers hardness test procedure can range up to 50kgs.Normally the prepared specimens; using metallographic mounting presses are mounted in a plastic medium to facilitate the preparation and testing. In order to enhance the resolution of measurement, the indentations should be as large as possible. The micro hardness was measured with the help of Vickers micro

hardness tester. It was compatible with computer; the indentations formed by indenter can be seen. The load can be takes over the micro hardness tester was upto 100 kg. And the magnification of the indentation was 200X and 400X. The load selected was 5 gm, because at high load the indenter would be large. The magnification chosen was 400 X, because at that low load indentation was very small.

3.8 OPTICAL MICROSCOPE

It is an instrument used to see objects too small for the naked eye. The science of investigating small objects using such an instrument is called microscopy. Microscopic means invisible to the eye unless aided by a microscope.

This is an optical instrument containing one or more lenses producing an enlarged image of a sample placed in the focal plane. Optical microscopes have refractive glass and occasionally of plastic or quartz, to focus light into the eye or another light detector. Mirror-based optical microscopes operate in the same manner. Typical magnification of a light microscope, assuming visible range light, is up to 1500x with a theoretical resolution limit of around 0.2 micrometres or 200 nanometers. Specialized techniques (e.g., scanning confocal microscopy, Vertico SMI) may exceed this magnification but the resolution is diffraction limited. The use of shorter wavelengths of light, such as the ultraviolet, is one way to improve the spatial resolution of the optical microscope, as are devices such as the near-field scanning optical microscope.

CHAPTER 4

RESULT AND DISCUSSION

4.0 COATING CHARACTERIZATION

The microstructures of the coating were studied with the help of scanning electron microscope. The microstructures of the coating suggest that the splat of the deposited material does not seem to form a continuous layer but at the cross section, it was observed that the coating was more homogeneous and regular (figure 4.1 (a), (b)). Literature shows the thickness of hard chrome ranging from 10µm to 40µm .Figure shows the thickness of coating is 12.3 µm illustrates deposition of an apparently uniform coating with adhesion characteristics. Interface of coating/substrate is showing in below figure 4.2 (a), (b) but bonding mechanism is not very clear yet.

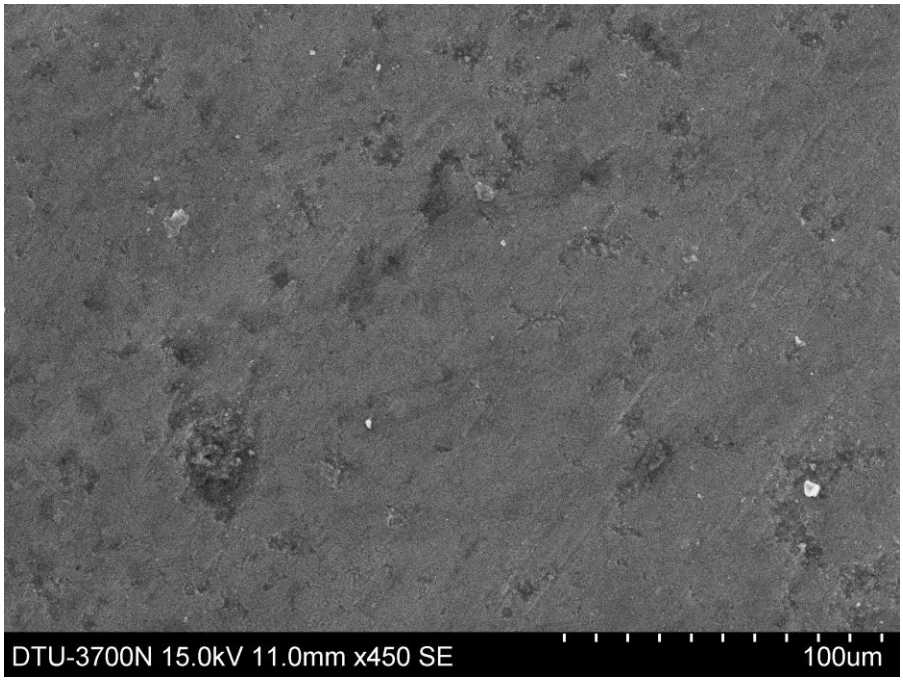

Figure 4.1: (a) Top view of Ion-Plating at 100 µm

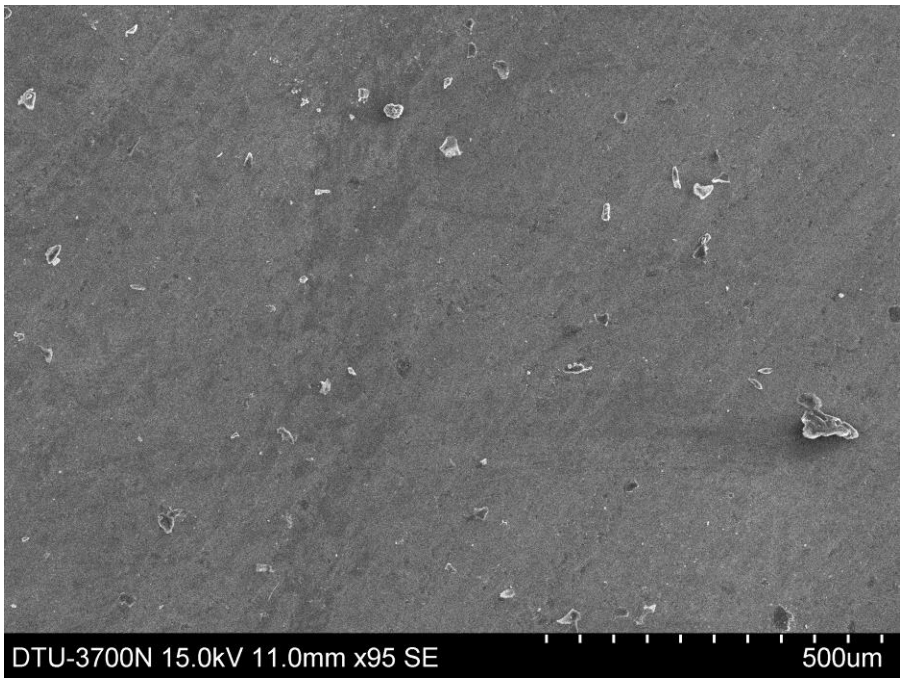

Figure 4.1: (b) Top view of Ion-Plating at 500 µm

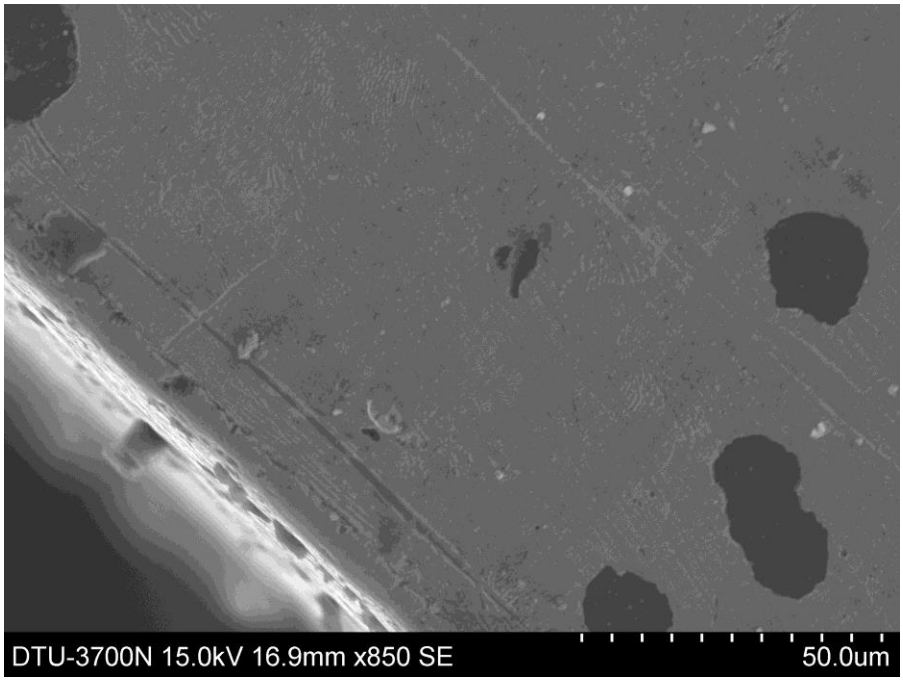

Figure 4.2: (a) Cross-sectional view of Ion-Plating at 50 µm

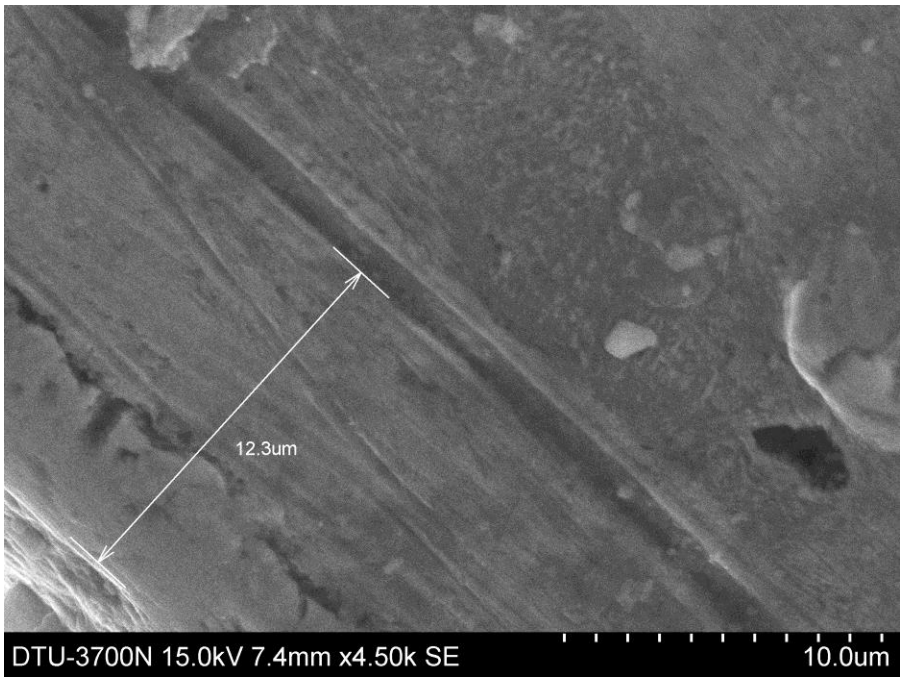

Figure 4.2: (b) Cross-sectional view of Ion-Plating at 10 µm

The Ion plating was found in the form of continuous layer with dome shape structure of its particle. The blow holes & porosity were regular having homogeneous structure with complete melted part. Elemental analysis of the coating is showing in a Figure 4.3 and table 4.1, graph is not showing the nitrogen content due to its light weight but table is confirming the presence of nitrogen 7.77% by weight and chromium is 92.33% by weight.

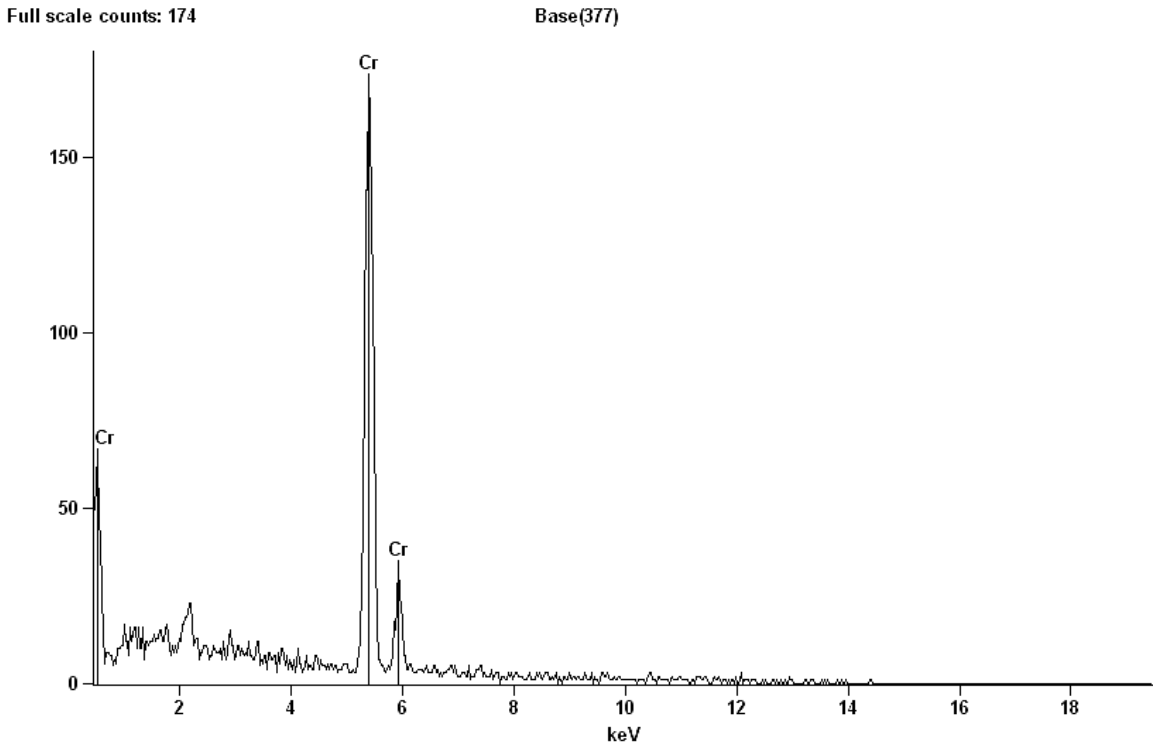

Figure 4.3: EDS analysis of Chrome Plating

Table 4.1: Elemental Analysis of Chrome Plating

Element	**Net Counts**	**Weight %**	**Weight % Error**	**Atom %**	**Atom % Error**
Nitrogen	394	7.77	± 0.89	23.83	± 2.72
Chromium	2864	92.23	± 2.64	76.17	± 2.18
Total		100.00		100.00	

4.1 SPECIFIC WEAR RATE

Simplest way of measuring wear is based on measuring the weight loss in each track or after a test. It is direct method but one should be careful in taking the measurement. Wear volume can be calculated from equation based on the wear scar shape. The wear depth is considered a reliable way to assessing weight loss. A wear coefficient is often used to categories resistance to contact wear. It is used to calculate the specific wear rate or wear coefficient (K).

$$\text{Specific Wear Rate} = \frac{\text{Wear Volume}}{\text{Load} \times \text{Sliding Diastance}}$$

$$\text{Wear Volume} = \text{Wear Depth (Average value of Wear)} \times \text{Area Of Pin}$$

Diameter of Pin in all the experiment = 6 mm

Area of the Pin = 28.2857 mm^2

Where wear volume in mm^3 and load in Newton and sliding distance in meter and wear volume can be calculated by above expression. Above wear coefficient was suggested by Holmberg and Matthews as a standard for wear test.

The comparison of specific wear rate of uncoated plate and hard chrome plating in dry and flooded condition in Figure 4.4 (a), (b), (c), (d), (e) & (f) indicates a considerable difference between specific wear rates of coated materials in dry and flooded condition followed by highest wear rate in uncoated material. Wear test was performed on tribometer of uncoated and coated in dry and flooded condition at six runs under two set of experiment as discussed in chapter – 3. Figure 4.4 (a) shows the variation of specific

wear rate of base plate hard chrome plating in dry and flooded condition at constant lad of 50 N and sliding velocity of 1 m/s for a constant run of throughout the experiment of 2500 m against the pin of cylinder liner. Specific wear rate of base plate was 0.00008 and chrome plating was 0.00004 in dry and 0.000003 in flooded condition. There is a large reduction in specific wear rate in the sample after the coating of 0.00004 and considerable decrease in flooded condition also. At the same sliding velocity in fourth run of experiment when the load of 80 N was applied as shown in Figure 4.4 (d) the specific wear rate of base plate was 0.00008 and hard chrome plated sample in dry condition was 0.000006 and in flooded condition was 0.000001.Which is showing the large reduction in specific wear rate of coating in flooded condition by increasing the load at same sliding velocity. This was also reported by A. L. Bandeira et. al. (2013) that wear and friction of CrN coated sample in engine oil lubrication had a much lower value comparable to wear and friction of coated sample in dry condition and uncoated sample also. It is due to the tribo-chemical reaction, in which chromium reacts and forms a layer of oxides [77].

Figure 4.4 (b) shows the specific wear rate of uncoated sample and coated in dry and flooded condition for the second run of the experiment at the load of 60 N and sliding velocity of 2 m/s. Specific wear rate of uncoated sample was 0.00005 and coated sample in dry and flooded condition was 0.00003, 0.000004.which is showing that with the increase in rpm there is a decrease in the hard chrome plating in dry condition while significant increase in the flooded condition with the increase in load and rpm both. Giovani et. al. (2006) also reported the decrease in the specific wear rate by increasing the rpm of hard chrome plating [78]. At the same sliding speed by applying the load of 90 N the specific wear rate shown in Figure 4.4 (e). Specific wear rate of uncoated sample

was 0.00063 while in second run at the same speed but at 60 N load, it was very less with about 0.00005. Specific wear rate of hard chrome plating by increasing the load of 90 N at the same sliding velocity was 0.00004. According to the investigation it is shown that at the same sliding velocity by increasing the load specific wear rate of coated sample in flooded and dry conditions are decreasing.

Specific wear behaviour of base plate and chrome plating in dry and flooded condition is shown in Figure 4.4 (c) at load of 70 N and sliding velocity of 3m/s. In this run of the experiment rpm was 1433 which is very high comparable to first and second run of 319 and 764. Specific wear rate if base plate was 0.00003 and chrome plating in dry and flooded was 0.00002, 0.000004. This is very less when compare to the first run of experiment in figure 4.4 (a). At the same sliding speed, when the load of 100 N is applied, the behaviour is shown in figure 4.4 (f); Specific wear rate of uncoated sample was 0.00005 and chrome plating in dry and flooded condition was 0.00003, 0.000004. Investigation shows that specific wear rate of chrome plating in dry and flooded condition in increasing with the increasing load at the same rpm.

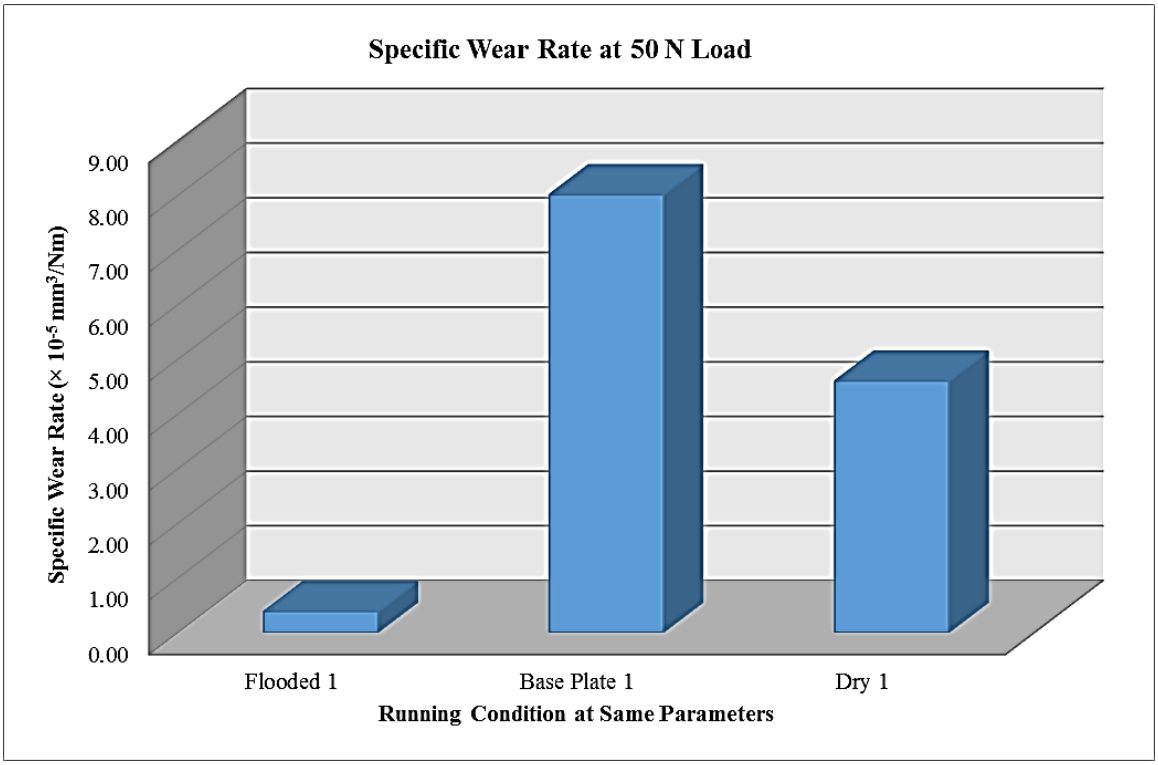

Figure 4.4 (a): Specific wear rate at 50 N Load and Sliding Velocity of 1 m/s

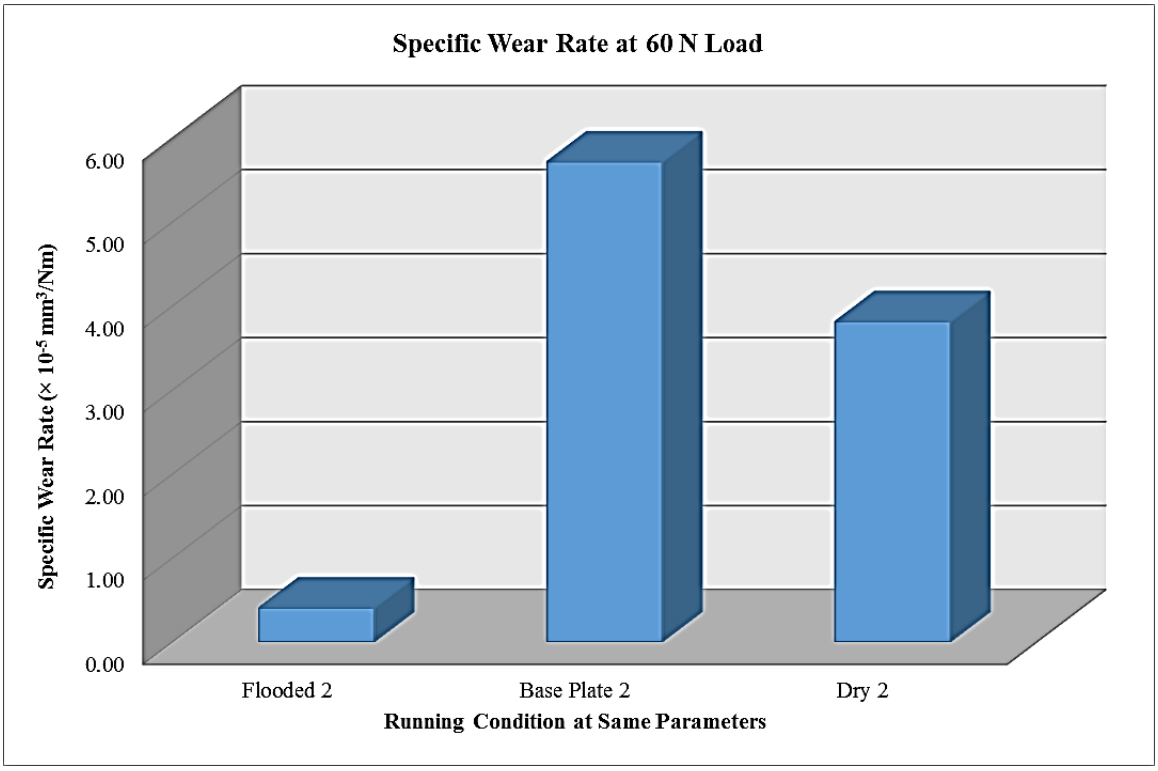

Figure 4.4 (b): Specific wear rate at 60 N Load and Sliding Velocity of 2 m/s

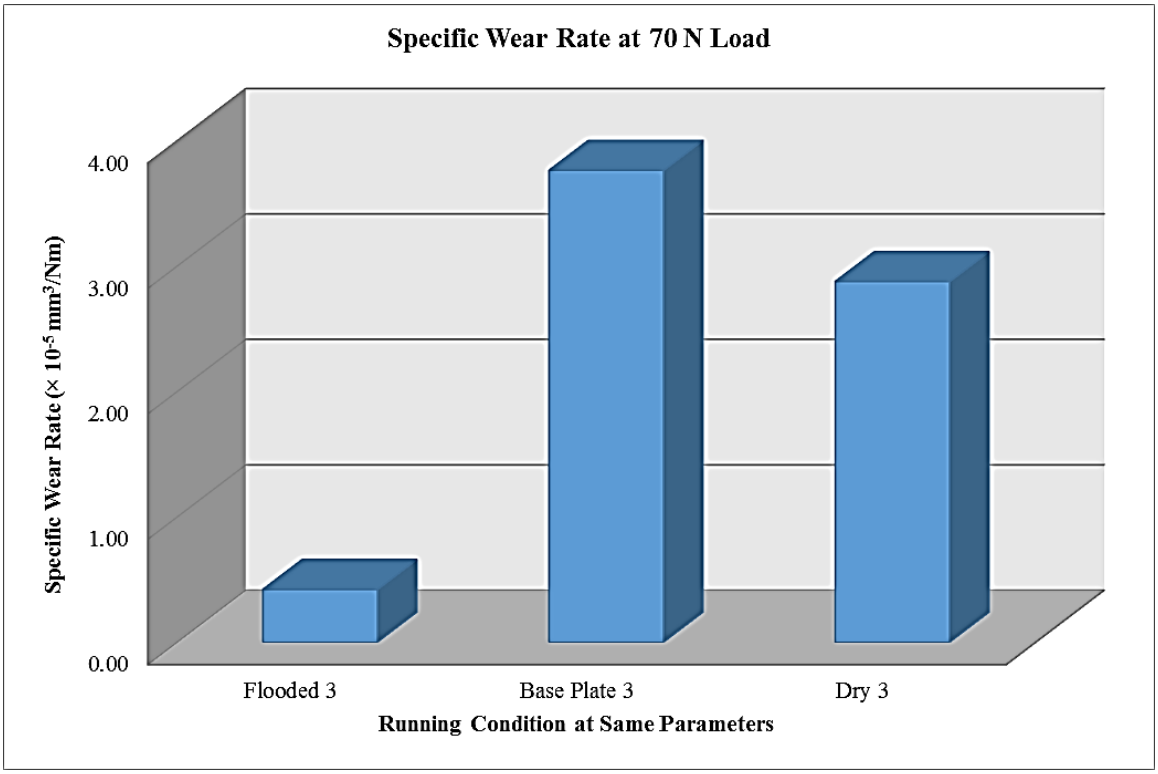

Figure 4.4 (c): Specific wear rate at 70 N Load and Sliding Velocity of 3 m/s

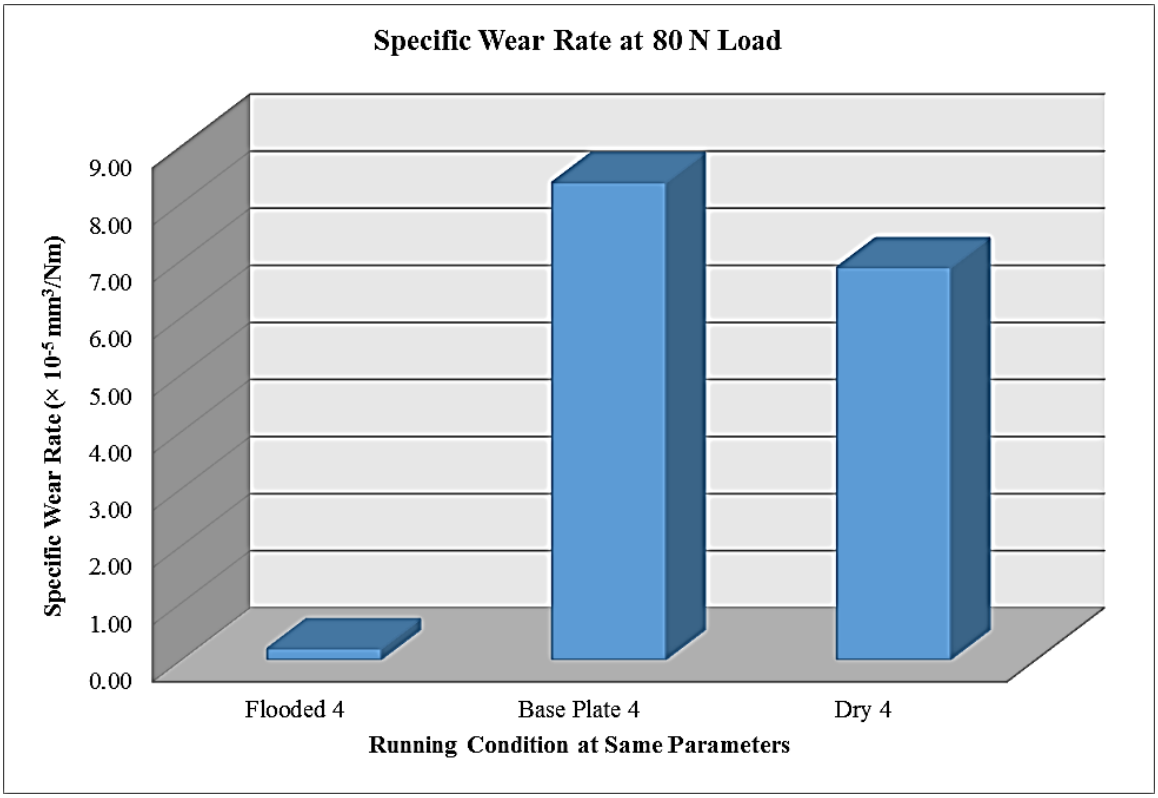

Figure 4.4 (d): Specific wear rate at 80 N Load and Sliding Velocity of 1 m/s

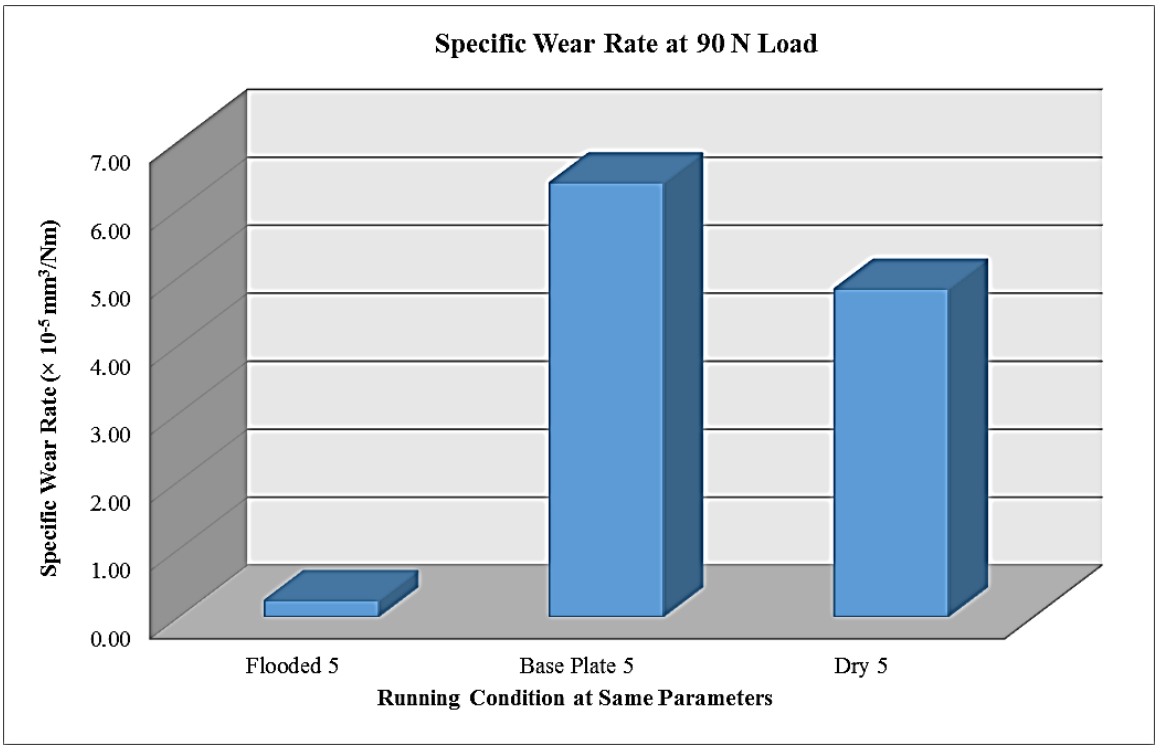

Figure 4.4 (e): Specific wear rate at 90 N Load and Sliding Velocity of 2 m/s

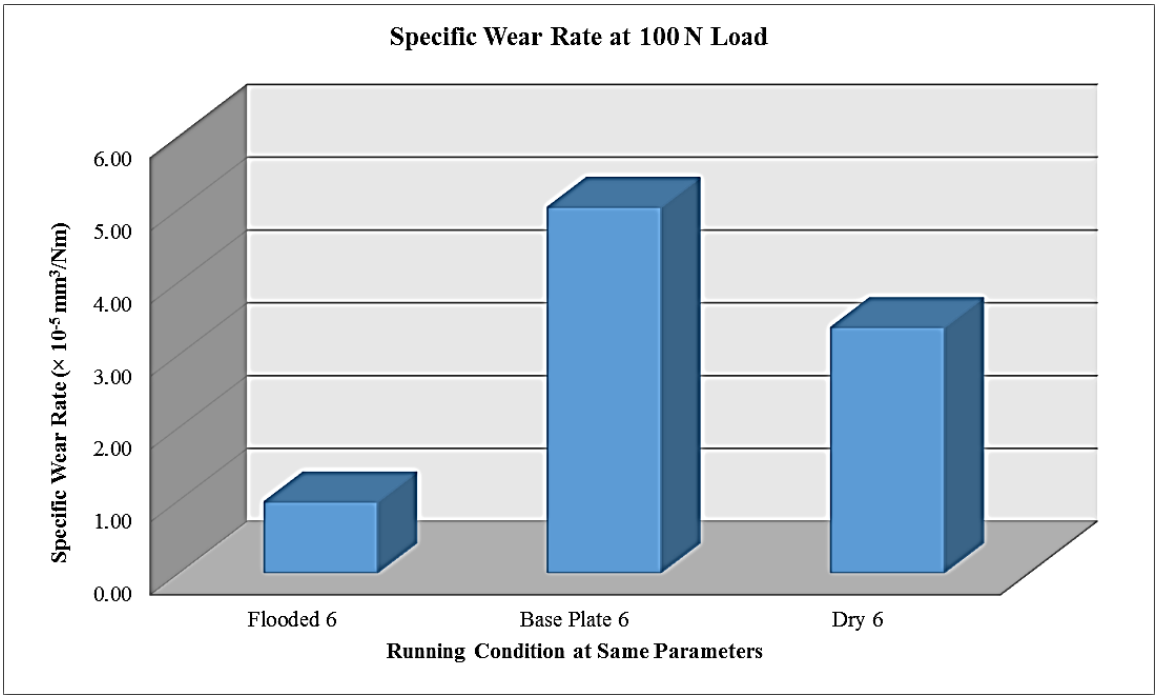

Figure 4.4 (f): Specific wear rate at 100 N Load and Sliding Velocity of 3 m/s

Specific Wear rate of chrome plating also investigated at low sliding velocity of 0.3 m/s, 0.4 m/s, 0.6 m/s and 0.8 m/s at a load of 10 N, 20 N, 30 N and 40 N for a run of 1000 m. Wear behaviour is shown in Figure 4.4 (g) in the first run at 0.3 m/s and 10 N load wear rate was 0.00011 and at 0.4 m/s and 20 N load 0.000031 and at 0.6 m/s and 30 N load 0.000037 and at 0.8 m/s and load 40 N was 0.000009. It reveals that with the increase in speed wear rate is decreasing of chrome plating. At very low velocity showing significantly large wear in the coated sample. Various researchers also reported the decrease in specific wear rate of chrome plating with the increase in sliding velocity [79].

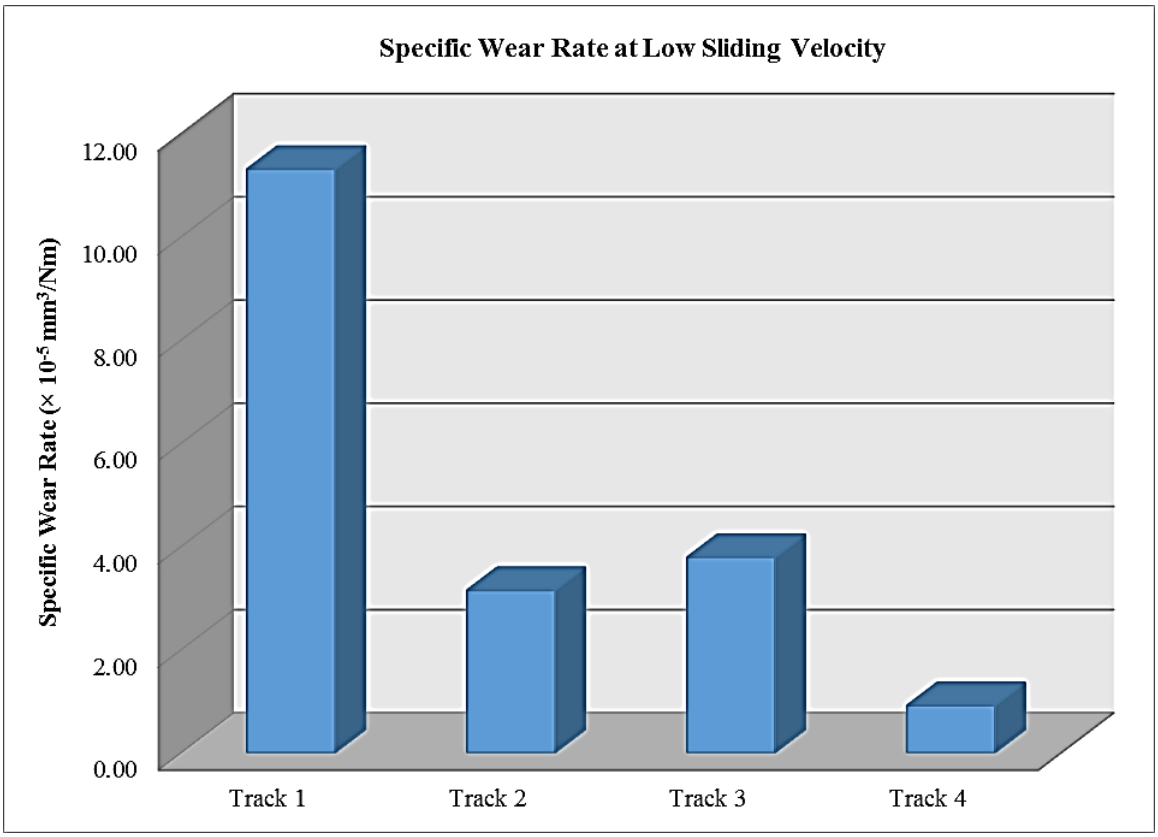

Figure 4.4 (g): Specific wear rate at low Sliding Velocity with increasing load

4.2 COEFFICIENT OF FRICTION & FRICTIONAL FORCE

Wear behavior of chrome plating is being characterized by the pin-on-disc Test on tribometer where the frictional force of uncoated or base plate and chrome plated sample is analysed in dry and flooded condition of the contact surface of pin and plate. Further, the coefficient of friction by the given equation –

$$F = \mu N$$

Where F = Frictional force in Newton, μ = Coefficient of Friction, N = Normal force that is the applied load in each track or run of the test. Figure 4.5 (a), (b), (c), (d), (e) & (f) shows the evolution of coefficient of friction for a constant sliding distance of 2500 m at various loading condition and sliding velocity.

Figure 4.5 (a) shows variation of friction coefficient of uncoated or base plate and chrome plating in dry and flooded condition at 50 N load and sliding velocity 1 m/s and 319 rpm was found to be 0.4044, 0.3874 and 0.01288 it can be observed that highest coefficient of friction for the uncoated sample and reduces after coating and shows a rapid downfall in flooded condition. At the same rpm of 319 and sliding velocity 1 m/s applied load was 80 N and behaviour was shown in Figure 4.5 (d), friction coefficient of uncoated sample and coated in dry and flooded condition was 0.3359, 0.3140 and 0.0332. It is showing that in flooded condition when the load is increased at same rpm, friction coefficient is increasing and for the chrome plated in dry condition it is decreasing by increasing the load. Binshi Xu. et. al. also reported that friction coefficient of aluminium alloy decreases with increase in load [80]. Friction coefficient was decreased with

increasing load condition may be due to reason that at increase load ,the wear rate will be more, that's why the direct rubbing will be less and it shows less friction of coefficient.

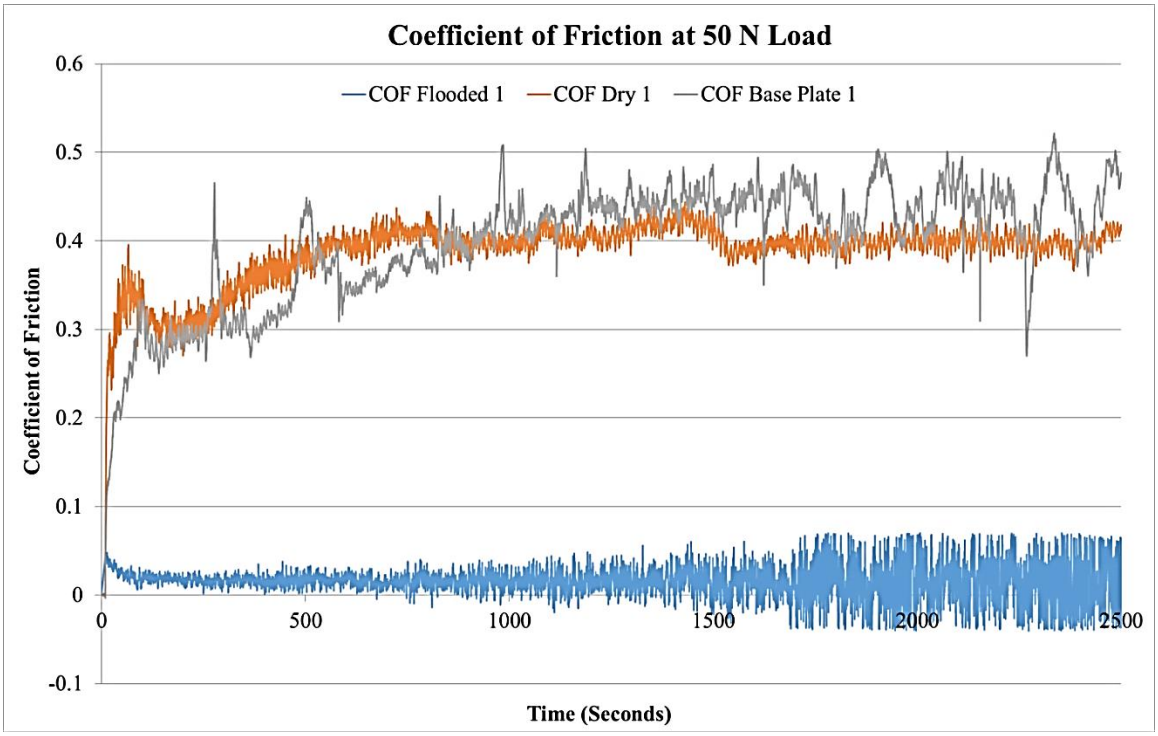

Figure 4.5 (a): Coefficient of Friction at 50 N Load and Sliding Velocity of 1 m/s

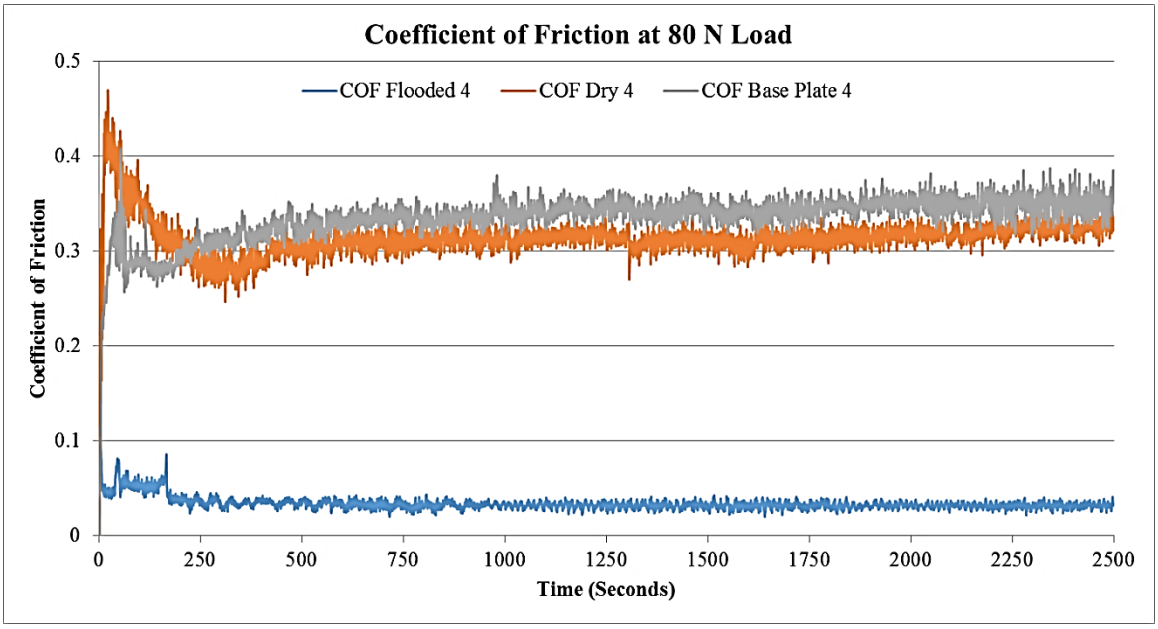

Figure 4.5 (d): Coefficient of Friction at 80 N Load and Sliding Velocity of 1 m/s

Figure 4.5 (b) shows the variation of coefficient of friction at 60 N load and sliding velocity of 2 m/s and 764 rpm. It is observed that friction coefficient of base plate was 0.4736 and chrome plated sample in dry and flooded condition was 0.3831 and 0.0131 which is showing that with the increase in load and sliding velocity from 50 to 60 N and sliding velocity 1 m/s to 2 m/s and 319 to 764 rpm there is increase in friction coefficient of uncoated and coated sample in dry condition. At the same sliding velocity of 2 m/s, when the load is increased to 90 N at same 764 rpm (Figure 4.5 (e)), the friction coefficient of uncoated and coated in dry and flooded condition was 0.3931, 0.3452 and 0.01651 respectively. It is observed that with increase in load friction coefficient in flooded condition increases.

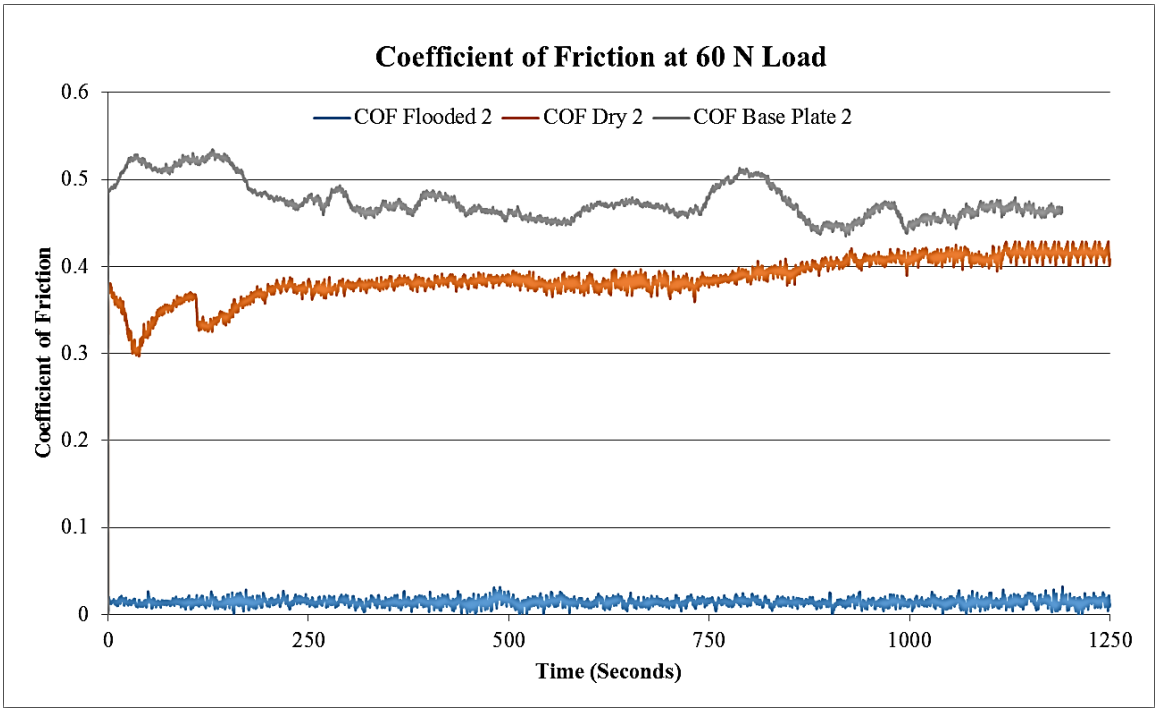

Figure 4.5 (b): Coefficient of Friction at 60 N Load and Sliding Velocity of 2 m/s

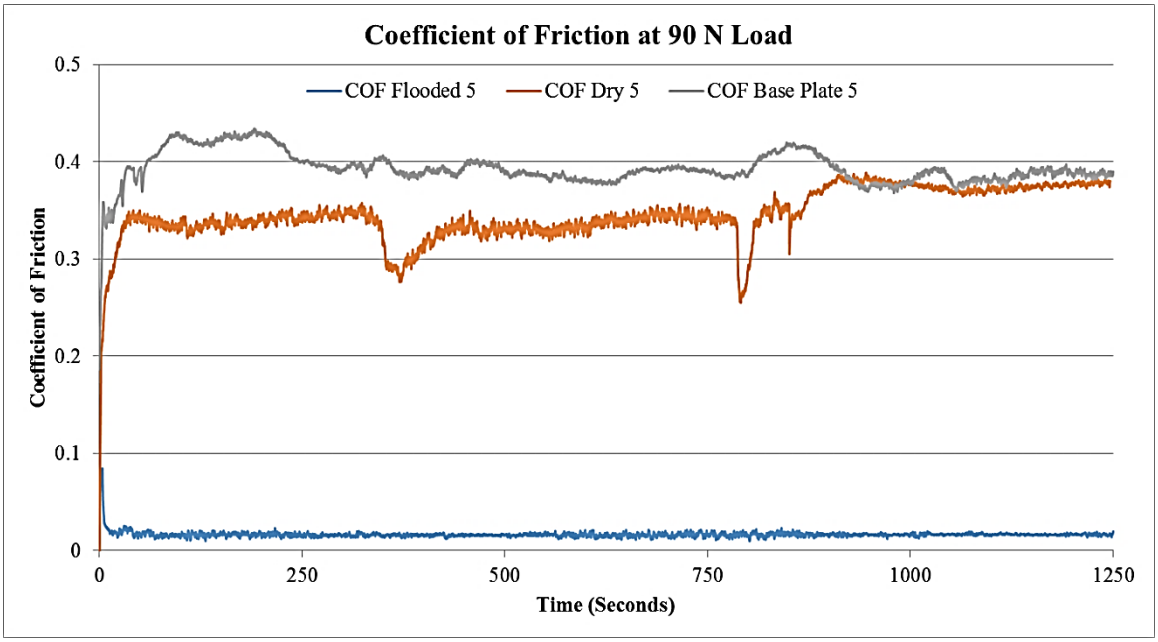

Figure 4.5 (e): Coefficient of Friction at 90 N Load and Sliding Velocity of 2 m/s

Figure 4.5 (c) shows the behaviour of friction coefficient at 70 N load and sliding velocity 3 m/s and 1433 rpm. Result shows the coefficient of friction of uncoated specimen was 0.3919 and chrome plating was 0.3411 and chrome plating in flooded condition was 0.0206 which is showing that after plating friction is reducing and in flooded condition it shows rapid downfall. While in second run at 70 N load and 764 rpm friction coefficient were higher than these but at higher speed of 1433 rpm value is decreasing significantly. At the same rpm of 1433 when applying the load of 100 N the behaviour of coefficient of friction is shown in Figure 4.5 (f). Result shows that friction coefficient of uncoated sample was 0.3458 and chrome plating in dry and flooded condition was 0.2859 and 0.02574. H. S. Arora et. al. (2013) also reported that that friction coefficient decreases with the increase in sliding velocity [81].

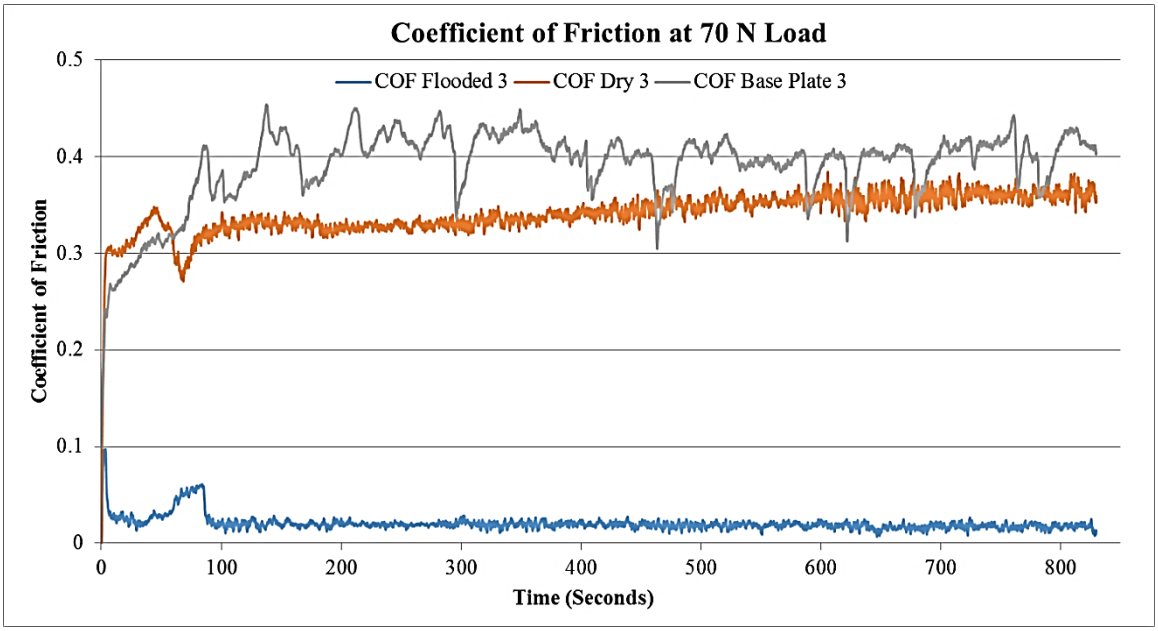

Figure 4.5 (c): Coefficient of Friction at 70 N Load and Sliding Velocity of 3 m/s

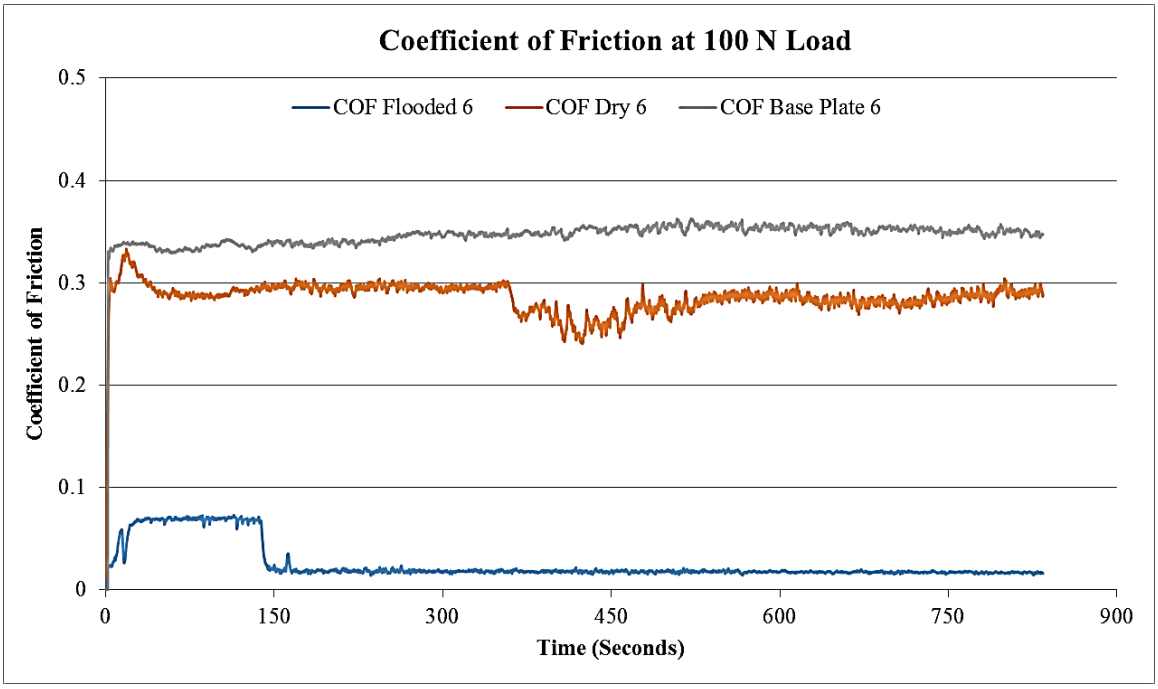

Figure 4.5 (f): Coefficient of Friction at 100 N Load and Sliding Velocity of 3 m/s

4.3 WEIGHT LOSS

During test, weight loss in the coated plate and counter body is measured by electronic weighing machine in the laboratory after each run in dry and flooded condition.

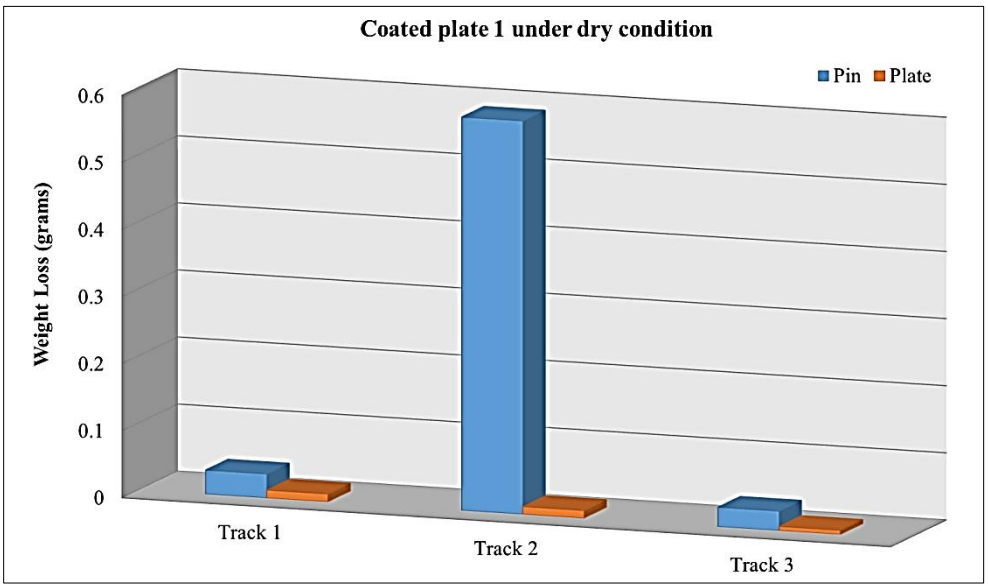

Figure 4.6 (a): Weight Loss of coated plate under dry condition

Weight loss is varying with the load and sliding velocity at each run in Figure 4.6 (a). In track 1, load was 50 N and sliding velocity 1 m/s at 319 rpm for a constant run of 2500 m throughout all the runs. Weight loss of coated sample and counter body in first run at dry condition was 0.0117 and 0.0358 gram. Second run was performed at 60N load and sliding velocity 2 m/s and 764 rpm, weight loss of coated plate and counter body was 0.0114 gram and 0.586 gram. In the third run or track operating condition was 70 N load and sliding velocity 3 m/s at 1433rpm.The weight loss in this run at coated plate and counter body was 0.0062 gram and 0.029 gram. As shown in above graph that chrome coating is showing a large mass reduction in comparison to uncoated sample. At moderate sliding velocity pin is showing a large mass reduction it may be due to some

impurity or presence of some hard material and weight loss of coating is decreasing with increase in sliding velocity and load.

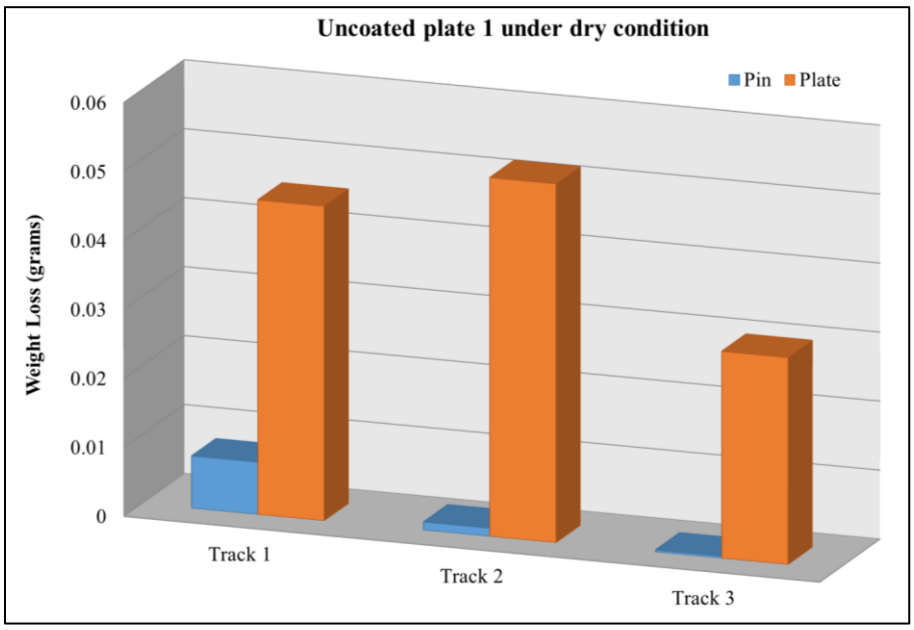

Figure 4.6 (b): Weight Loss of uncoated plate under dry condition

Wear analysis of cast iron plate against the pin of cylinder liner material is analysed. As shown in Figure 4.6 (b): weight loss of the plate is 0.0456 gram and in counter body is 0.0076 gram at track diameter 60mm, load 50 N and sliding velocity 1 m/s. This run takes 2500 seconds at 319 rpm. Successively, at increasing the loads; result shows that at 60 N, sliding velocity 2 m/s and track diameter 50 mm the weight loss of the plate and pin 0.052 gram, 0.0012 gram, means when the load and sliding velocity are increased, the weight loss of plate is increasing and that of pin is decreasing. In the third track of plate the operating condition was 70 N load and sliding velocity 3 m/s for a fixed sliding distance of 2500 meter. In this case also, weight loss of the plate and pin is observed that is 0.03 gram and 0.0003 gram. In the third track, the rpm was 1434 which is more high in comparison to track1 was 319 rpm.

4.4 WEAR MECHANISM IN DRY CONDITIONS

In order to identify wear mechanism of chromium coating at cast iron as base plate by ion plating in presence of nitrogen during wear testing at Pin-On-Disc Tribometer, the worn surfaces was analyzed by Scanning Electron Microscopy (SEM) and Energy dispersive spectroscopy (EDS). The scanning electron microscope gives the 3D surface morphology of the wear track which helps in the interpretation of the wear mechanism. It was observed that wear rate of uncoated and coated sample in dry and flooded condition were different. Therefore wear mechanism described here at various load and sliding velocity.

At 50 N and 80 N load: SEM image of chrome plating subjected to wear test at 50 N load and 80 N load at constant sliding velocity of 1 m/s for a run of 2500 m. Figure 4.7 (a) is showing the wear surface is by the presence of long continuous grooves, fractured surface and feature of micro-cutting and ploughing, these are all indicative of abrasion. Another simultaneously occurring wear mechanism under these conditions is oxidation wear as evident from presence of oxide layer, which is also verified by EDS analysis.

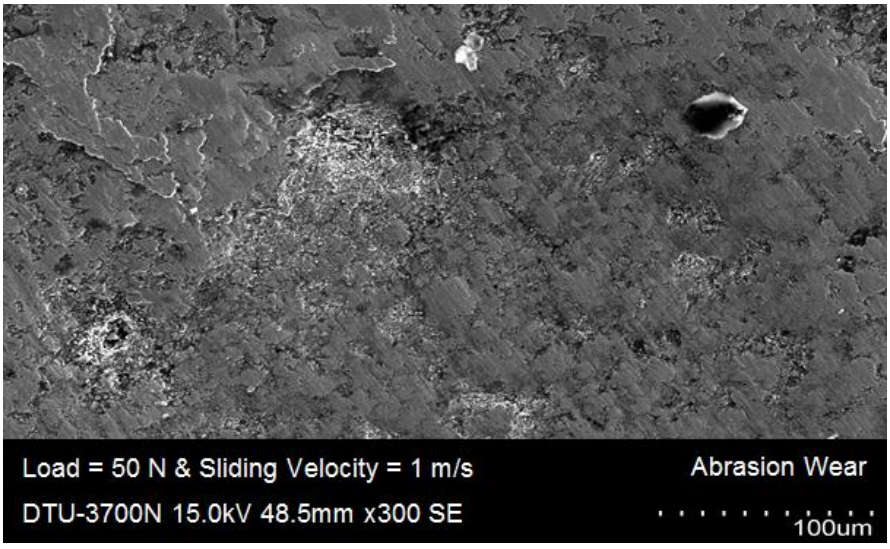

Figure 4.7 (a): SEM Image of wear track at 50 N Load and Sliding Velocity of 1 m/s

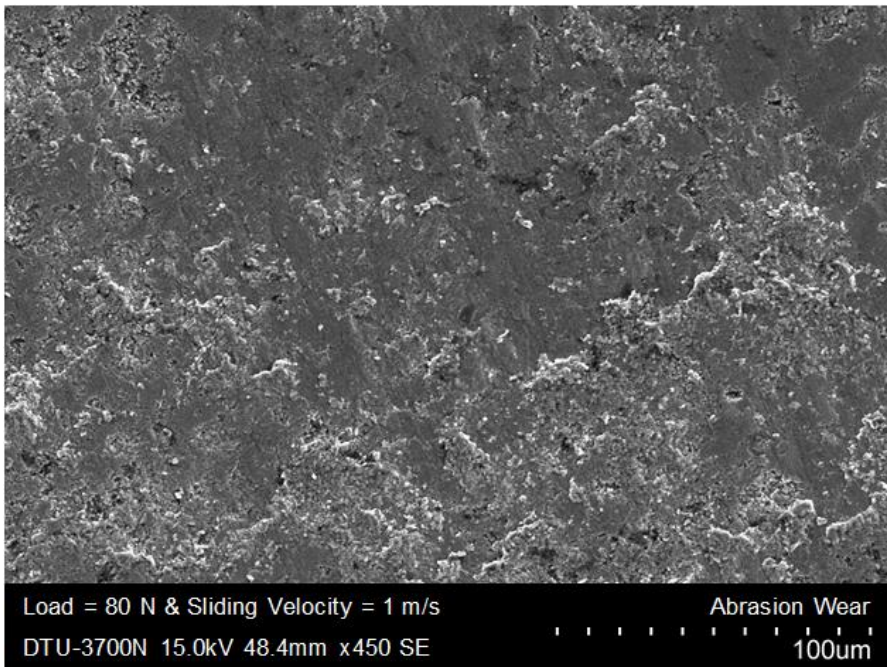

Figure 4.7 (d): SEM Image of wear track at 80 N Load and Sliding Velocity of 1 m/s

At 60 N and 90 N load: Figure 4.7 (b) is showing the fatigue wear of chrome plated sample at 60 N load and sliding velocity 2 m/s for a run of 2500 m. Test was carried out at dry condition in tribometer. Fatigue wear during sliding is the cause of crack development in deformed layer which depends upon the coating thickness and particle size of the coated powder. N. Soda et. al quoted that fatigue wear resistance is also affected by the atmospheric oxygen which also cause to oxidation and confirmed by elemental analysis [82]. Figure 4.7 (e) showing that grooves is long and noticeable and EDS analysis of the worn surface reveals significant weight % of oxygen which indicates surface oxidation and oxidation wear at surface.

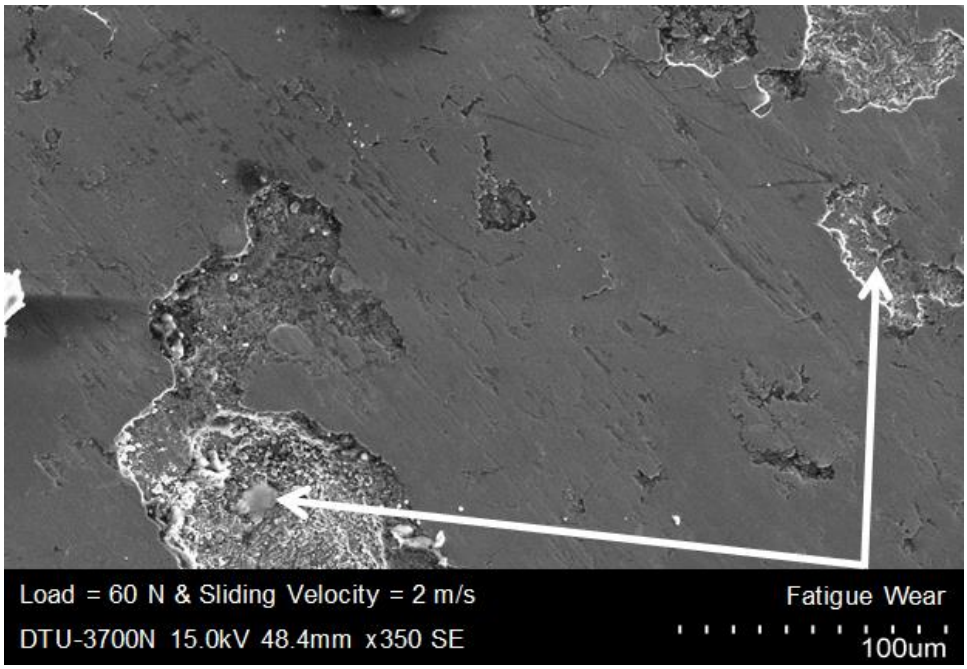

Figure 4.7 (b): SEM Image of wear track at 60 N Load and Sliding Velocity of 2 m/s

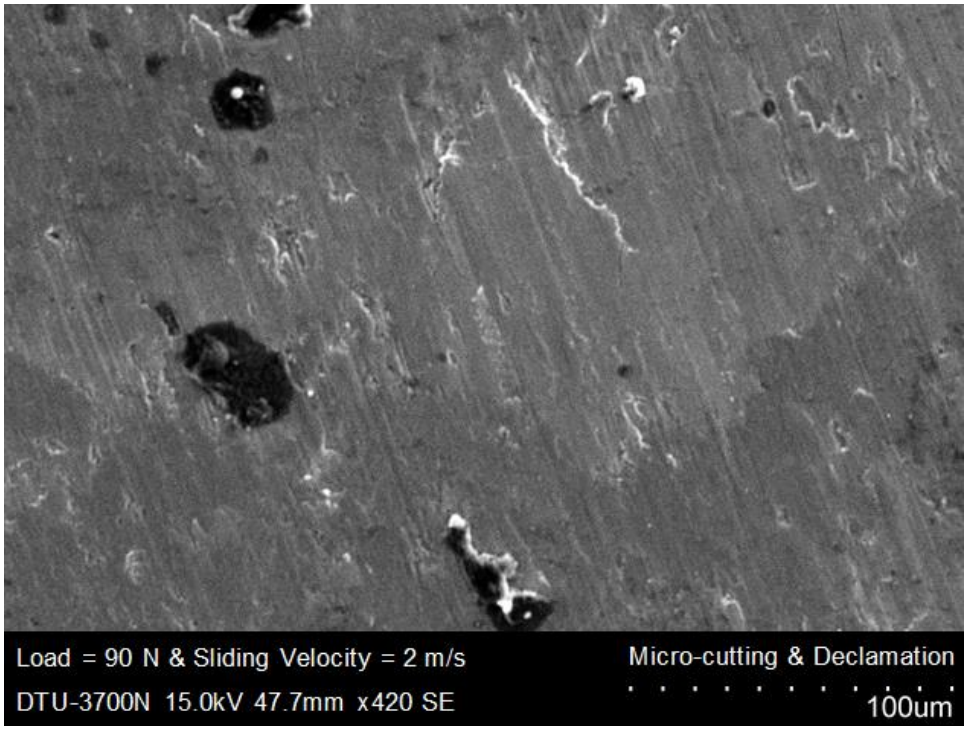

Figure 4.7 (e): SEM Image of wear track at 90 N Load and Sliding Velocity of 2 m/s

At 70 N and 100 N load: SEM image of worn surface at 70 N load and sliding velocity 3 m/s is shown in Figure 4.7 (c). It is evident from the image that the surface appearance relatively clean and shiny without much trace of abrasion. It is also observed at high sliding velocity the specimen surface was subjected to declamation and plastic deformation. Surface oxidation is evident in the form of oxide layer.

Figure 4.7 (f) shows the worn surface after the wear test of chrome plating at 100 N load and sliding velocity 3 m/s for a constant run of 2500 m in dry condition. Sliding velocity plays a major role in erosive wear when speed is high then generated stress will be insufficient for plastic deformation to occur and wear by fatigue. J. E. Goodwin et. al. quoted that problem of erosive wear associated with the particle size 5-500 µm and chromium which is a hard particle showing the higher wear rate comparable to soft coating [83].

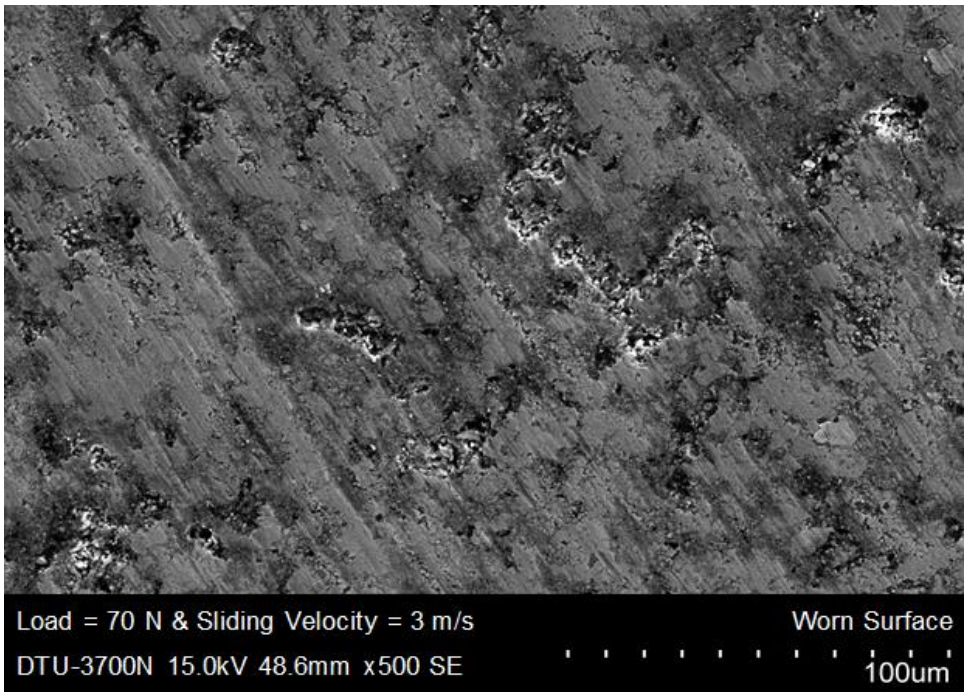

Figure 4.7 (c): SEM Image of wear track at 70 N Load and Sliding Velocity of 3 m/s

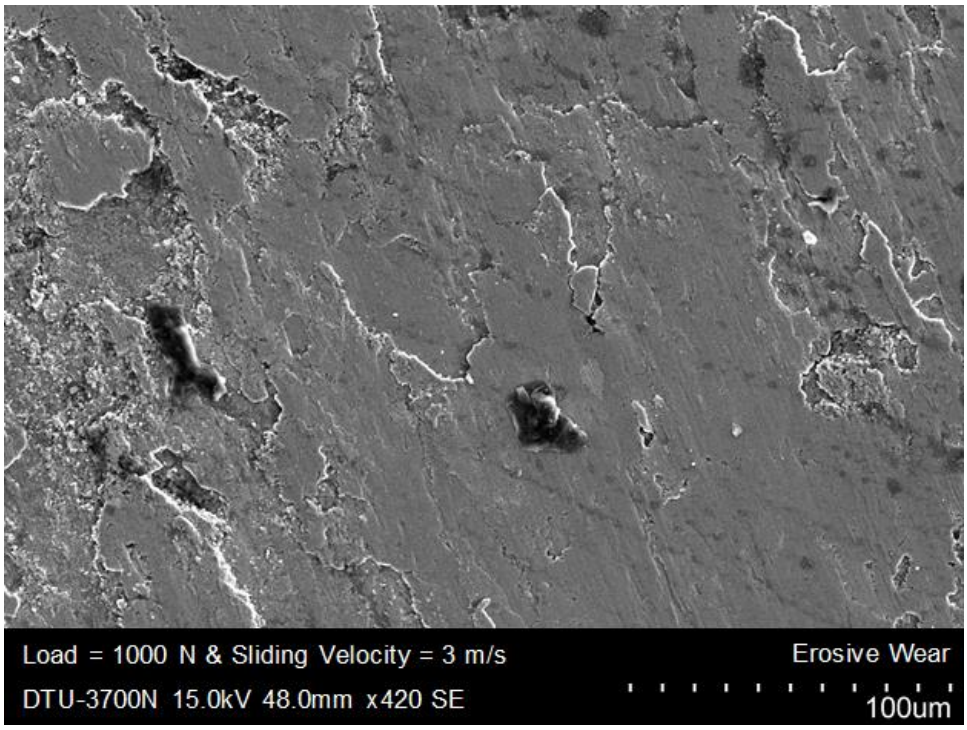

Figure 4.7 (f): SEM Image of wear track at 100 N Load and Sliding Velocity of 3 m/s

4.5 WEAR MECHANISM IN FLOODED CONDITION

SEM morphology of chrome plating in flooded condition is carried out with Castrol-GT 20W50 engine oil in wear test at tribometer. Figure 4.8 (a) and (b) is showing image at 70 N load and sliding velocity 1 m/s probably covered with a film composed of chromium oxide as indicated by elemental analysis tribological mechanism occur by the reaction of oxygen in the oil with chrome coating. Some sticking is also observed at lower load and micro-cutting is observed at 100 N load as shown in figure 4.8 (b).

To prevent the large amount of mass loss, the cast iron is coated by hard chromium. Chrome plated sample in dry condition is also showing considerable mass loss. Further mass reduction, 20W50 engine oil was used for lubrication which shows large reduction in mass loss because of some chemicals which react with the material and forms a layer to protect the material from wear by M. A. Nicholls [84]. Chrome plated sample at 70 N load and sliding velocity 3 m/s showing the sliding wear as shown in figure 4.8 (a), at the same velocity with increasing load of 100 N showing the plastic deformation in the Scanning Electron microscopy (SEM). Some declamation and sticking action is also analysed in the image. R. Bosman et. al. also reported Mild wear in lubrication at low sliding velocity and coefficient of friction 0.15 whereas in this test COF is 0.25 at sliding velocity 3 m/s [54].

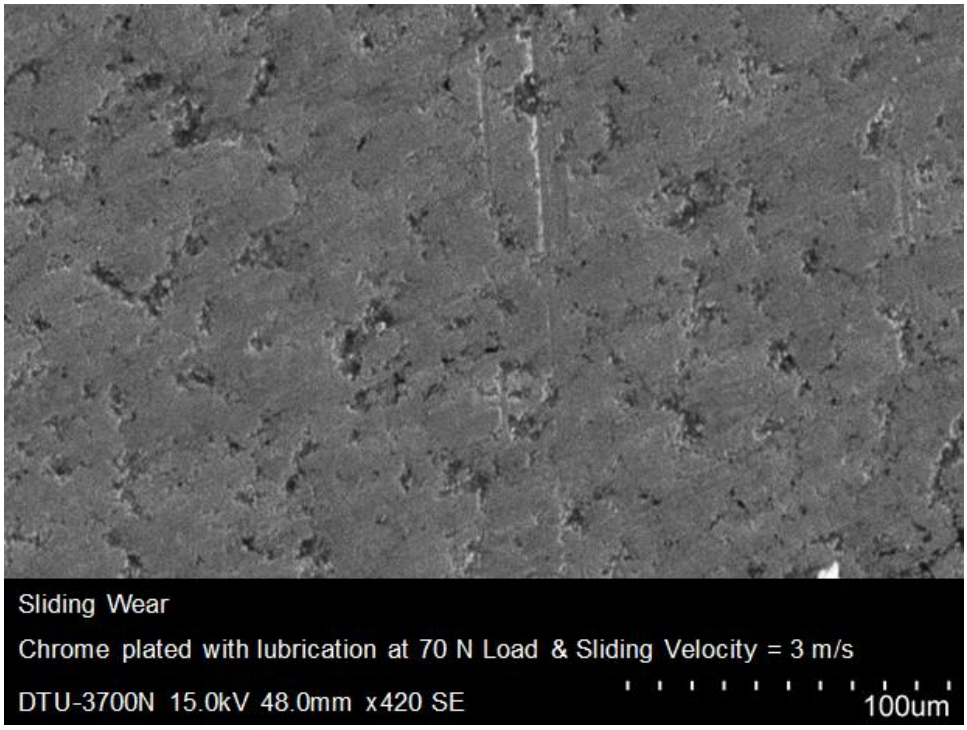

Figure 4.8 (a): SEM Image of wear track at 70 N Load and Sliding Velocity of 3 m/s in flooded condition

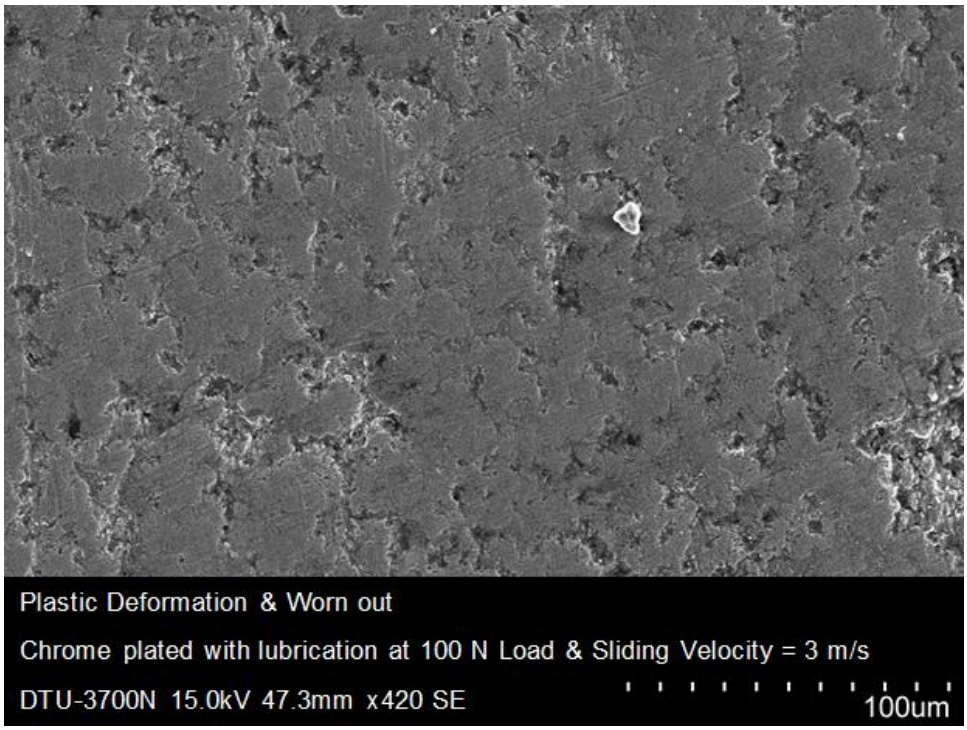

Figure 4.8 (b): SEM Image of wear track at 100 N Load and Sliding Velocity of 3 m/s in flooded condition

4.6 ELEMENTAL ANALYSIS OF WEAR TRACK

It is done by Energy dispersive spectroscopy (EDS) which is showing that oxygen content is in considerable amount of 14.29 % by weight that is enough to form an oxide layer at surface and cause to occur oxidation wear. Some impurity of silicon and, molybdenum also is observed through table but that is negligible. If silicon is present in considerable amount it worked as a lubrication as seen in the literature reported by some authors. Elemental analysis of the wear track under flooded condition is illustrated in figure 4.9 and table 4.2 shows the composition breakdown.

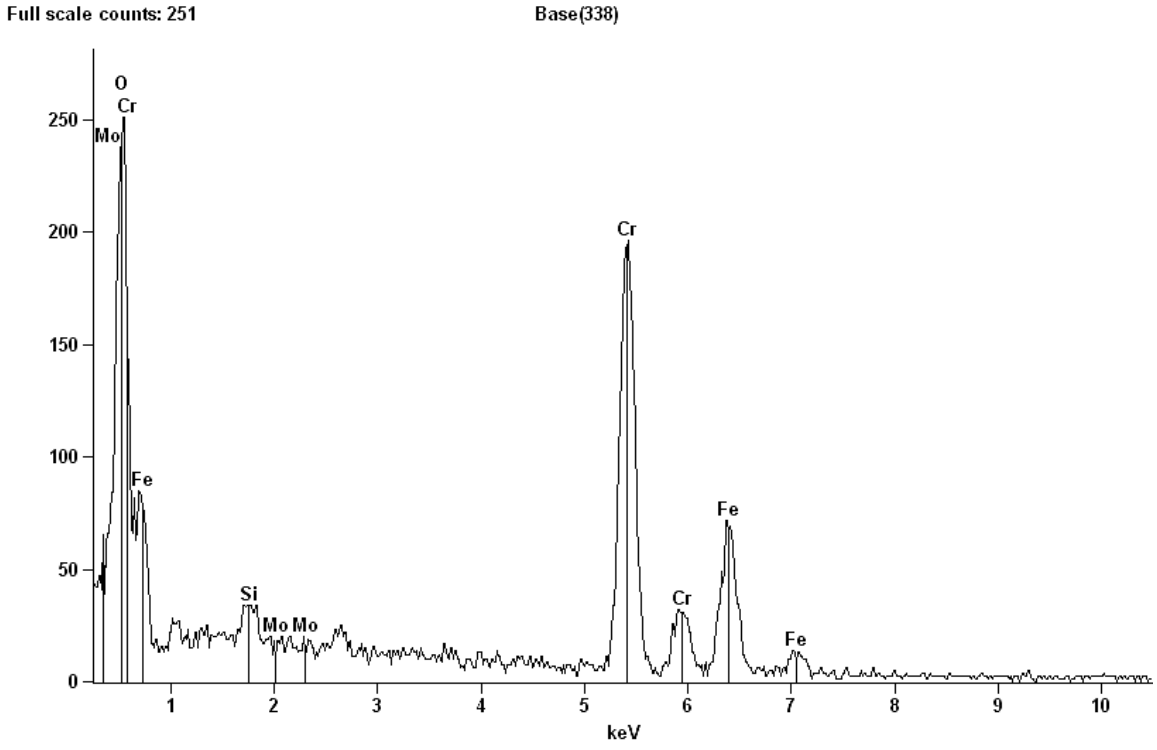

Figure 4.9: EDS analysis of Wear Track

Table 4.2: Elemental Analysis of Wear Track

Element	Net Counts	Weight %	Weight % Error	Atom %	Atom % Error
Oxygen	2384	14.29	± 0.55	35.55	± 1.36
Silicon	141	0.69	± 0.13	0.98	± 0.19
Chromium	3467	54.88	± 1.58	42.02	± 1.21
Iron	1194	30.05	± 1.36	21.42	± 0.97
Molybdenum	12	0.09	± 0.32	0.04	± 0.13
Total		100.00		100.00	

4.7 EFFECT OF TEMPERATURE

Experimental investigation of friction and wear behavior and is devoted to analyse the behavior of hard chrome plating and roll of temperature in mechanical properties and wear also discussed by recording the track temperature in starting and end of each run out of three runs in dry and flooded condition.

In the first run of the experiment, at 50 N load, sliding velocity 1 m/s and 319 rpm for a run of 2500 m which takes time of 2500 seconds. Temperatures are reported in starting and end of experiment in Figure 4.10 (a) & (b). Maximum and minimum in starting are 50.1°C, 37.6°C and in end of experiment were 56.1°C, 41.7°C.While the average temperature in starting was 42.1°C and in end was 48.2°C. In second run of chrome plating the operating parameter was 60 N load and 764 rpm for a constant run of 2500 m throughout the each run. This run takes time of 1250 second and temperatures were recorded after every five minute but reporting was done only starting and end conditions.

During second run i.e. at 60 N and sliding velocity 2 m/s, Figure 4.10 (c) & (d) shows the image of track and the linear variation of temperature at the plate. Minimum temperature in starting was 42.6°C and Maximum was 72.1°C.While after 2500 second minimum temperature was 54.4°C and maximum was 85.9°C whereas average temperature in starting and end were 57.7°C and 71.9°C.

Third run of the experiment were carried out at 70 N load and 1433 rpm which is very high speed comparable to first and second run. Temperature variation in third run of starting experiment and end of experiment is shown in Figure 4.10 (e) & (f), respectively. Maximum and minimum temperatures in starting are 106.5°C and 64.3°C while in end

128.9°C and 57.7°C. It is observed that when load is increased from 50 to 70 N and rpm from 319°C to 1433°C temperature was increasing in starting from 50.1°C to 106.5°C while at end of experiment it varies from 37.6°C to 128.9°C. High temperature causes to high wear and irregular asperities at surface. K.V. Arun et. al. (2008) also reported the failure of hard chrome plating has been started from the internal residual stress and voids which induced by higher temperature [85]. Thermal stresses directly affect the fracture toughness of chrome plating. It also affected by coating thickness beyond 30µm of coating thickness fracture toughness decreases drastically.

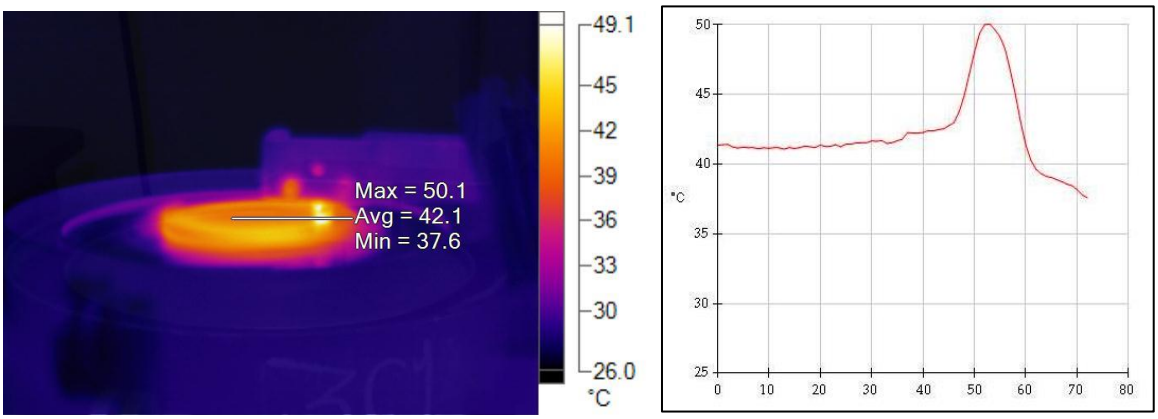

Figure 4.10 (a): Temperature Distribution of wear track at 50 N and 1 m/s (Initial Stage)

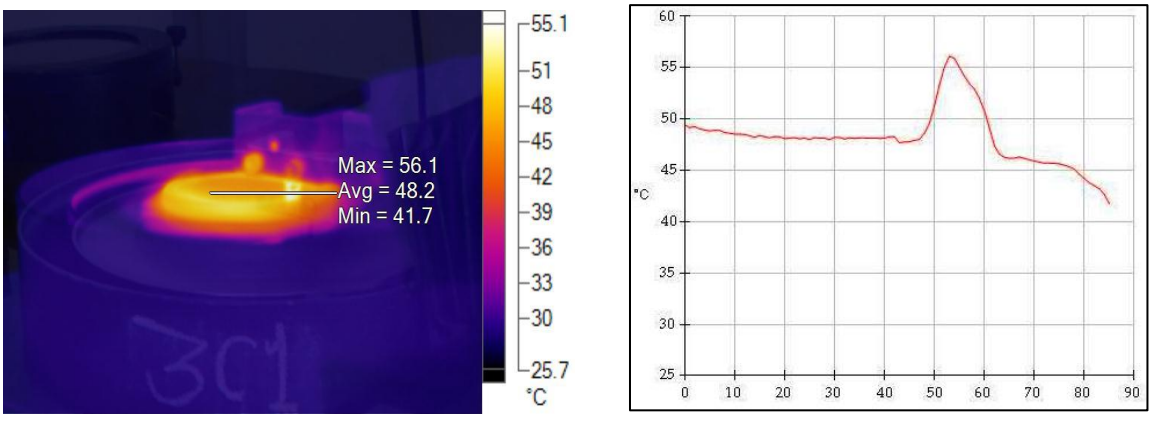

Figure 4.10 (b): Temperature Distribution of wear track at 50 N and 1 m/s (Final Stage)

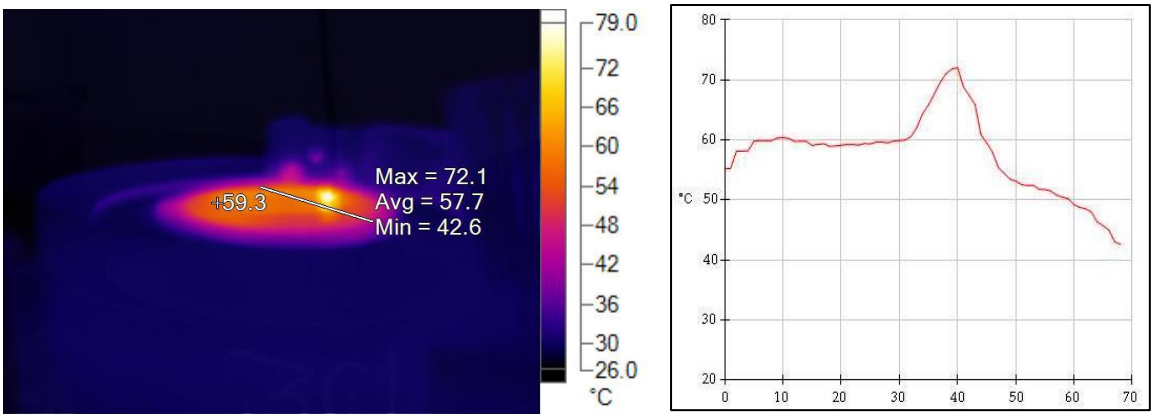

Figure 4.10 (c): Temperature Distribution of wear track at 60 N and 2 m/s (Initial Stage)

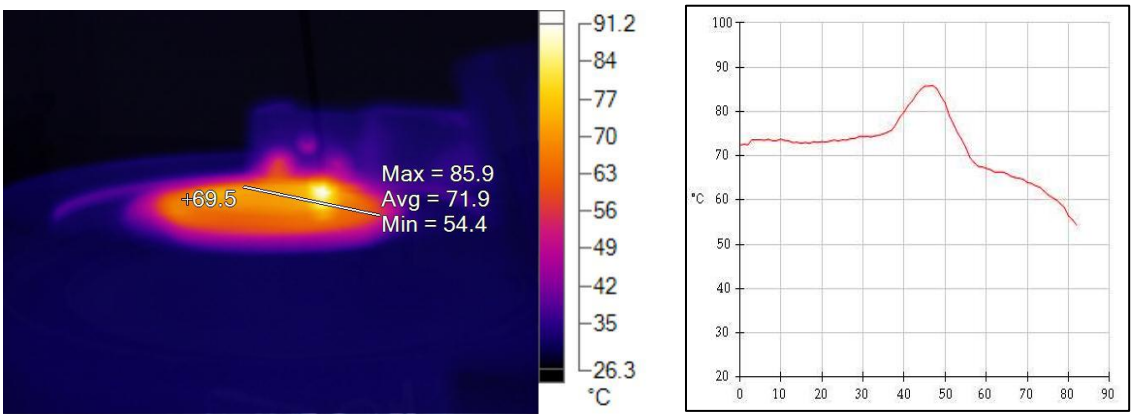

Figure 4.10 (d): Temperature Distribution of wear track at 60 N and 2 m/s (Final Stage)

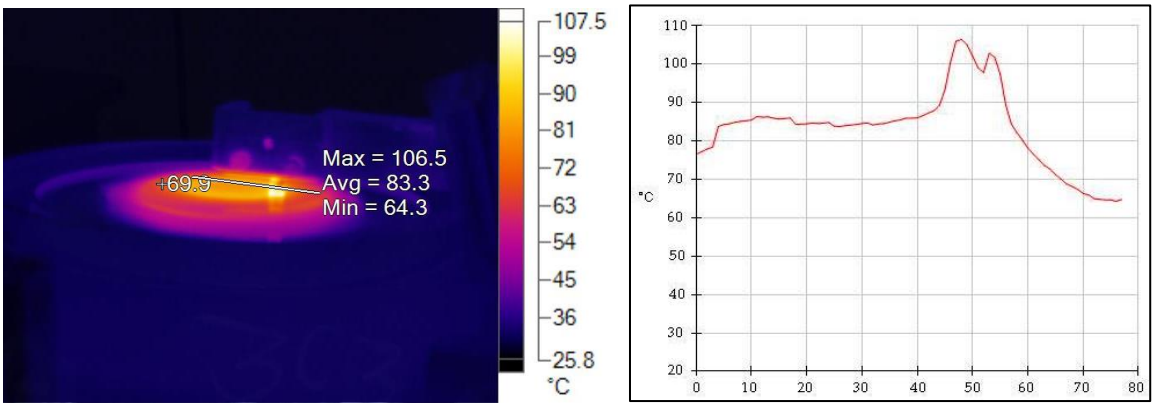

Figure 4.10 (e): Temperature Distribution of wear track at 70 N and 3 m/s (Initial Stage)

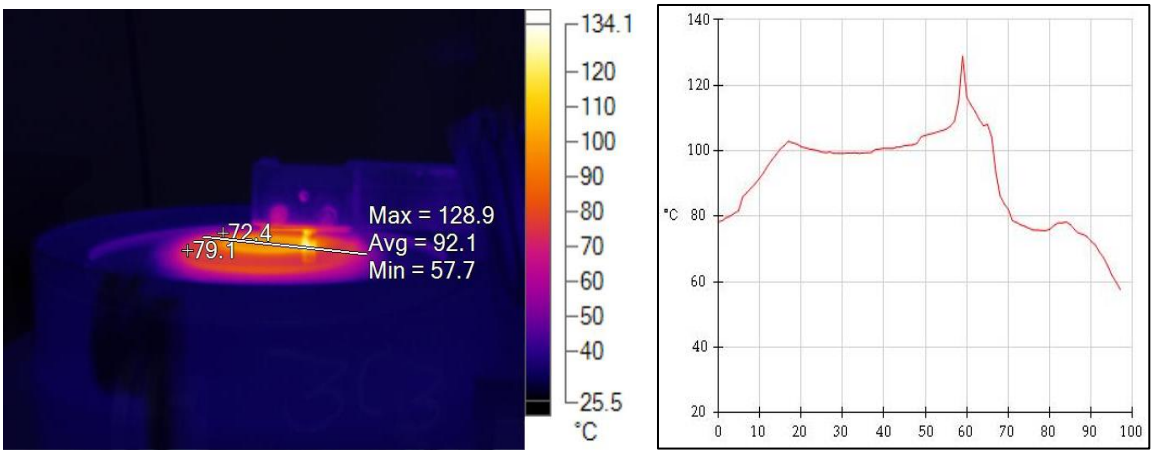

Figure 4.10 (f): Temperature Distribution of wear track at 70 N and 3 m/s (Final Stage)

Figure 4.11 (a) is showing the temperature distribution of hard chrome plating in flooded condition at load of 50 N, sliding velocity 1 m/s and 319 rpm minimum and maximum temperatures were 28.8°C and 30.2°C while the average temperature was 29.4°C which is very less than in dry condition at same operating parameter average temperature in starting was 42.1°C. In the end of this run temperature distribution is shown in Figure 4.11 (b). Maximum, minimum and average temperatures are 34.1°C, 33.3°C and 33.7°C while average in dry at the end of first run with the same load and velocity was 48.2°C. Figure 4.11 (c) & (d) shows the temperature distribution in second run with continuous flow of 20W50 engine oil at 60 N load and 764 rpm for a run of 2500 meter. Maximum, minimum and average temperature was in starting 33.1°C, 32.5°C and 32.8°C; while at end of run it was 35.1°C, 34.4°C and 34.8°C whereas in dry condition at same operating parameter average temperature in starting and end were 57.7°C and 71.9°C. Figure 4.11 (e) & (f) shows the temperature distribution with flooded condition at 70N load and 1433 rpm. It can be observed that minimum, maximum and average temperatures in starting were 32.6^0C, 34.0^0C and 33.4^0C. While at the end of experiment maximum, minimum and average temperatures were 36.0°C, 34.8°C and 35.5°C.

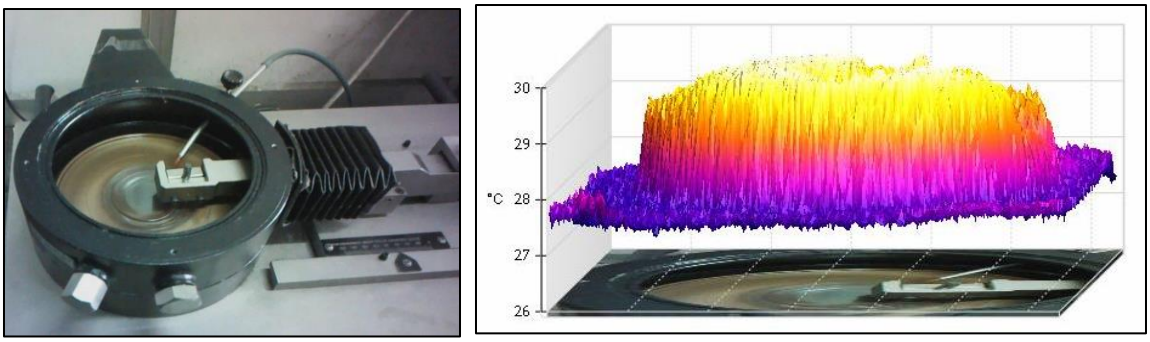

Figure 4.11 (a): 3 – D Temperature distribution of hard chrome plating in flooded condition at load of 50 N and sliding velocity 1 m/s (Initial Stage)

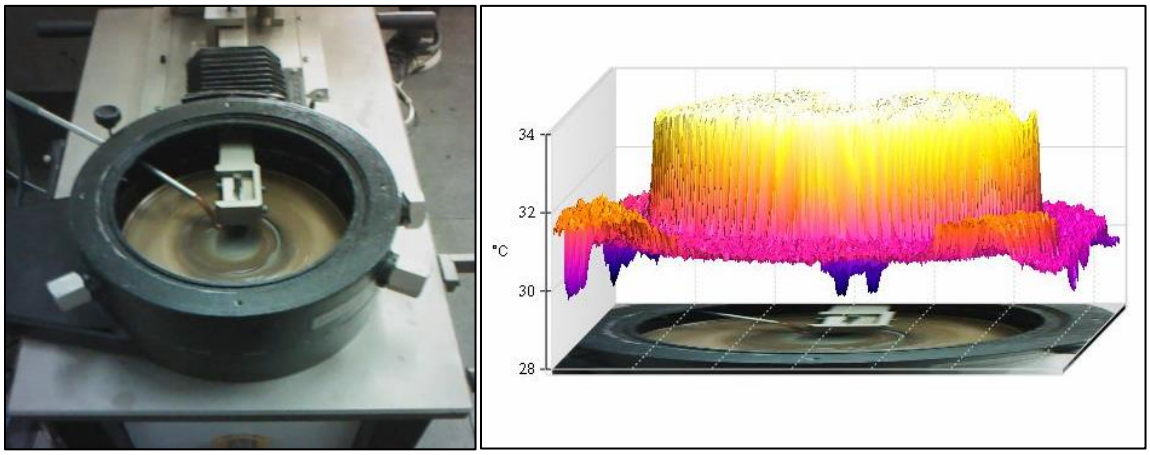

Figure 4.11 (b): 3 – D Temperature distribution of hard chrome plating in flooded condition at load of 50 N and sliding velocity 1 m/s (Final Stage)

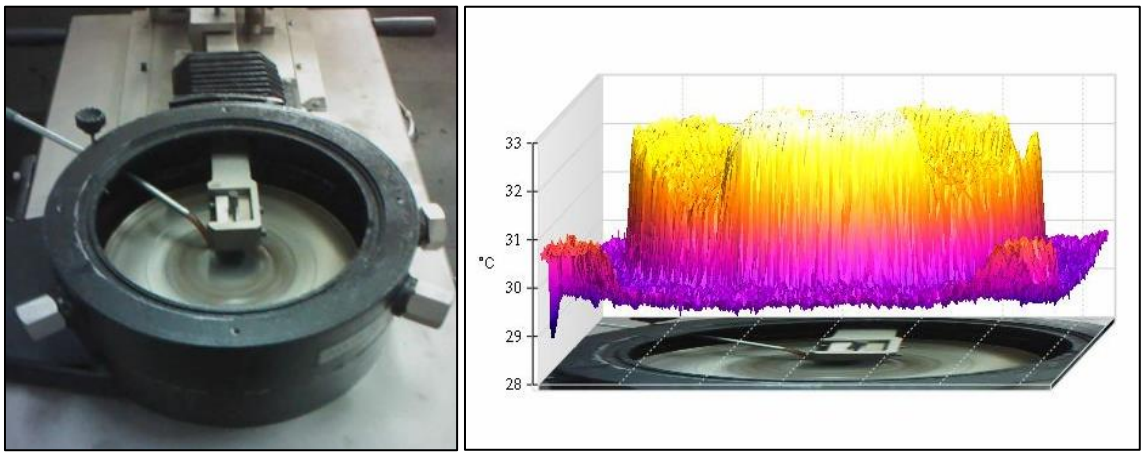

Figure 4.11 (c): 3 – D Temperature distribution of hard chrome plating in flooded condition at load of 60 N and sliding velocity 2 m/s (Initial Stage)

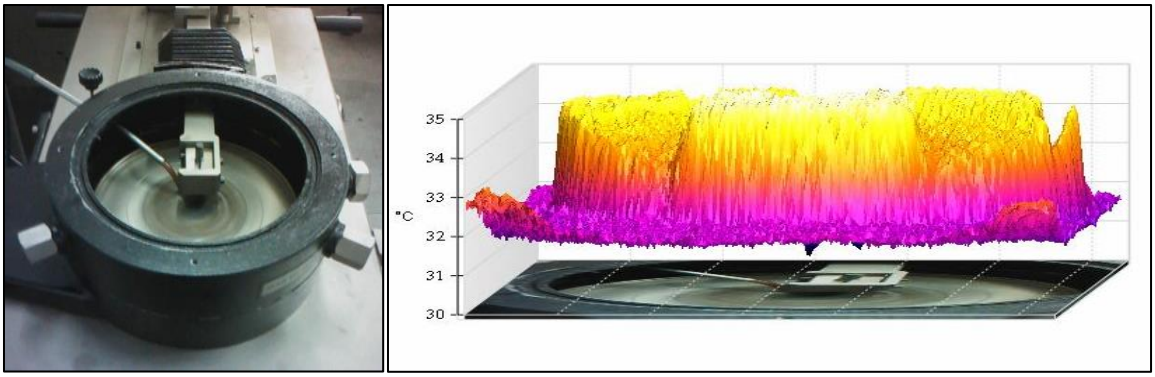

Figure 4.11 (d): 3 – D Temperature distribution of hard chrome plating in flooded condition at load of 60 N and sliding velocity 2 m/s (Final Stage)

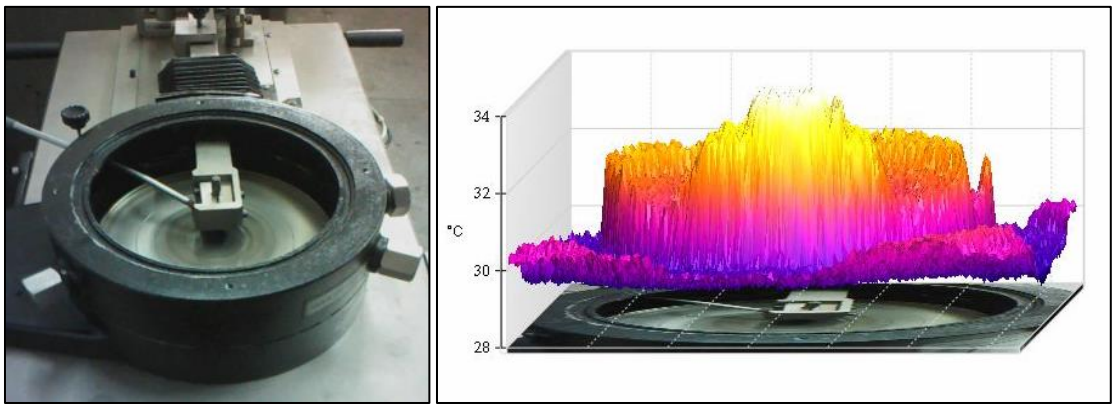

Figure 4.11 (e): 3 – D Temperature distribution of hard chrome plating in flooded condition at load of 70 N and sliding velocity 3 m/s (Initial Stage)

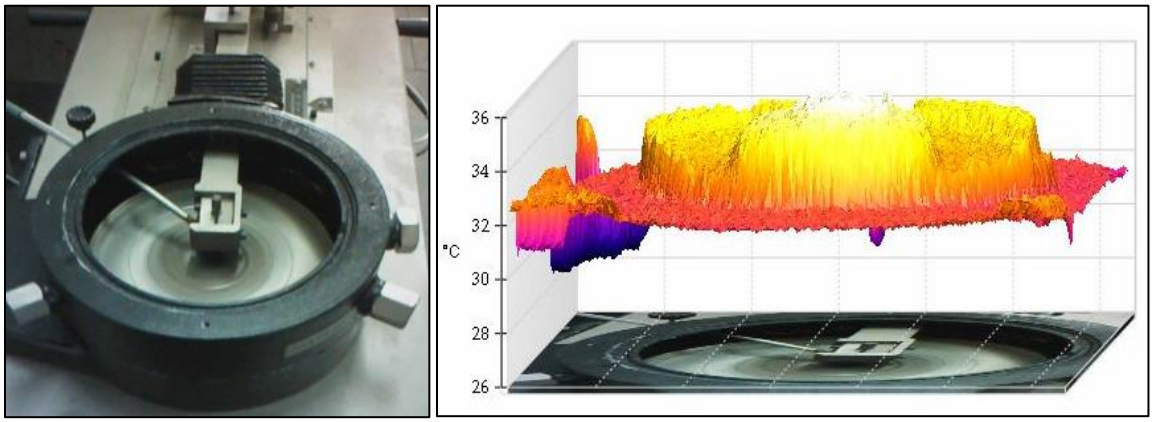

Figure 4.11 (f): 3 – D Temperature distribution of hard chrome plating in flooded condition at load of 70 N and sliding velocity 3 m/s (Final Stage)

CHAPTER 5

CONCLUSION AND SCOPE FOR FUTURE STUDY

5.0 CONCLUSION

Specific wear rate of the chrome coatings is calculated by Holmberg equation while using a pin-on-disc tribometer test setup under dry and flooded conditions. The effect of varying loads (50, 60, 70, 80, 90 & 100 N) and sliding speeds (1, 2, & 3m/s) for a constant sliding distance of 2500 meter is studied. The following conclusions could be drawn from a series of exhaustive trials –

1. Specific wear rate of chrome plating is increasing with the increase of load from 50 to 70 N and a simultaneous increase in sliding velocity 1 to 3 m/s in dry condition and flooded condition. The rate of increase of specific wear rate is is decreasing with an increase in load at same speed. Also, there is a huge reduction in the specific wear rate of coated sample when compared to uncoated sample at dry conditions.
2. Co-efficient of friction was found to be low at higher sliding velocity and load. It is observed that at 50 N load, COF is 0.3874 while at 80 N, it is 0.3140 in dry condition and same speed. In flooded condition and 50 N load, friction coefficient was 0.01288 which is very low comparable to dry condition.
3. The SEM micrographs showed that the wear mechanism of the coating was accompanied by the presence of long continuous grooves, fractured surface and feature of microcutting and ploughing which are all indications of abrasion,

adhesion and erosion. Another, simultaneously occurring wear mechanism under these conditions are oxidation wear as evident from presence of oxide layer, which is also verified by EDS analysis.

4. Temperature at the point of contact in pin-on-disc test is important to consider because a sudden or progressive temperature rise may cause to develop stress followed by failure. At 50, 60, 70 N load average temperatures in initial and final stage were 42.1°C and 48.2°C; 57.7°C and 71.9°C; 78.3°C and 84.2°C, respectively, while the maximum temperature in the experiment was 128.6°C. At same parameters, in flooded condition average temperature in initial and final stage were 29.4°C and 31.2°C; 32.8°C and 34.8°C; 33°C and 35.5°C, respectively. Above discussed temperature during wear was low due to high heat conduction capacity of coating.
5. The coatings can be used for piston rings and cylinder liner or for light weight and high strength application such as bonnet and bumper of cars.

5.1 SCOPE FOR FUTURE STUDY

- There is a lot of gap in the bonding mechanism of coating and substrate. Researchers can predict a model to elaborate the bonding mechanism properly according to substrate.
- Coating characterization and different type of constituent in the coating powder such as effect of the Molybdenum on the coating characteristic can be studied.
- Effect of various Nano-powders with the mixing of Castrol 20W50 engine oil used for lubrication at wear can be studied. Some solid lubrication and doping technique can also be studied in wear and friction analysis of coating.
- Similarly, a cladding of carbon fiber can be applied on the coating so that it becomes stiffer as compared to the coating alone. It is expected that the cladding of carbon fiber would increase the tensile strength and stiffness of the coating.
- The coatings can be further subjected to scratch test so that it can be used as scratch resistance coating on vehicles bonnet and bumper. Erosion test of the coating can be performed to find erosion properties, for potential marine applications.
- Wear map can be plotted by analyzing the wear mechanism according to load and sliding velocity.

REFERENCES

1. Donald M. Mattox; Handbook of Physical Vapor Deposition (PVD) Processing (Second Edition), William Andrew Publishing, Boston, 2010, ISBN 9780815520375.
2. Stachowiak, G. W, and A. W Batchelor; Engineering Tribology, Butterworth-Heinemann, Boston, 2014, ISBN 9780123970473.
3. K.O. Legg, M. Graham, P. Chang, F. Rastagar, A. Gonzales, B. Sartwell, The replacement of electroplating, Surface and Coatings Technology, Volume 81, Issue 1, May 1996, Pages 99-105, ISSN 0257-8972, http://dx.doi.org/10.1016/0257-8972(95)02653-3.
4. Sadao Asanabe, Applications of ceramics for tribological components, Materials & Design, Volume 9, Issue 5, September–October 1988, Pages 253-262, ISSN 0261-3069, http://dx.doi.org/10.1016/0261-3069(88)90002-7.
5. Davi Neves, Anselmo Eduardo Diniz, Milton Sérgio Fernandes Lima, Microstructural analyses and wear behavior of the cemented carbide tools after laser surface treatment and PVD coating, Applied Surface Science, Volume 282, Issue 1 October 2013, Pages 680-688, ISSN 0169-4332, http://dx.doi.org/10.1016/j.apsusc.2013.06.033.
6. Bach, Friedrich-Wilhelm: The Coatings in Manufacturing Engineering, Stafa-Zuerich: Trans Tech, 2010. ISBN 9780878492725.
7. Bhushan, Bharat, and B. K Gupta. Handbook of Tribology: Materials, Coatings, and Surface Treatments. New York: McGraw-Hill, 1991. ISBN 97815752405035.

8. Martin, Peter M. Handbook of Deposition Technologies for Films and Coatings. Amsterdam: Elsevier, 2010. ISBN 9780815520313.
9. F. Rastegar, D.E. Richardson, Alternative to chrome: HVOF cermet coatings for high horse power diesel engines, Surface and Coatings Technology, Volume 90, Issues 1–2, 15 March 1997, Pages 156-163, ISSN 0257-8972, http://dx.doi.org/10.1016/S0257-8972 (96)03112-X.
10. Fischer, Alfons, and Kirsten Bobzin. Friction, Wear and Wear Protection. Weinheim: Wiley, 2011. ISBN 9783527628520, http://dx.doi.org/10.1002/9783527628513.
11. J.F. Archard, Single Contacts and Multiple Encounters, Journal of Applied Physics, Volume 90, Issues 1–2, 15 March 1997, Pages 156-163, ISSN 0257-8972, http://dx.doi.org/10.1016/S0257-8972 (96)03112-X
12. Archard, J. F. 'Contact And Rubbing Of Flat Surfaces'. Journal of Applied Physics. Volume 24. Issue 8 (1953): 981-988. http://dx.doi.org/10.1063/1.1721448.
13. Kerridge, M., and J. K. Lancaster. 'The Stages In A Process Of Severe Metallic Wear'. Proceedings of the Royal Society A: Mathematical, Physical and Engineering Sciences 236.1205 (1956): 250-264. http://dx.doi.org/10.1098/rspa.1956.0133.
14. Cocks, M. 'Interaction Of Sliding Metal Surfaces'. Journal of Applied Physics. Volume 33. Issue 7 (1962): 2152-2161. http://dx.doi.org/10.1063/1.1728920.

15. Morton Antler, Processes of metal transfer and wear, Wear, Volume 7, Issue 2, March–April 1964, Pages 181-203, ISSN 0043-1648, http://dx.doi.org/10.1016/0043-1648(64)90053-5.
16. Sasada T, Norose S, Mishina H. 'The Behavior Of Adhered Fragments Interposed Between Sliding Surfaces And The Formation Process Of Wear Particles'. ASME Journal of Tribology Volume 103. Issue 2 (1981): 195-202. http://dx.doi.org/10.1115/1.3251627.
17. D.A. Rigney, J.P. Hirth, Plastic deformation and sliding friction of metals, Wear, Volume 53, Issue 2, April 1979, Pages 345-370, ISSN 0043-1648, http://dx.doi.org/10.1016/0043-1648(79)90087-5.
18. J. Sato, M. Shima, T. Sugawara, A. Tahara, Effect of lubricants on fretting wear of steel, Wear, Volume 125, Issues 1–2, July 1988, Pages 83-95, ISSN 0043-1648, http://dx.doi.org/10.1016/0043-1648(88)90195-0.
19. W.-Y. Li, C. Zhang, X.P. Guo, G. Zhang, H.L. Liao, C.-J. Li, C. Coddet, Effect of standoff distance on coating deposition characteristics in cold spraying, Materials & Design, Volume 29, Issue 2, 2008, Pages 297-304, ISSN 0261-3069, http://dx.doi.org/10.1016/j.matdes.2007.02.005.
20. R.L. Deuis, C. Subramanian, J.M. Yellup, Dry sliding wear of aluminium composites—A review, Composites Science and Technology, Volume 57, Issue 4, 1997, Pages 415-435, ISSN 0266-3538, http://dx.doi.org/10.1016/S0266-3538(96)00167-4.

21. P.L. Hurricks, The fretting wear of mild steel from 200° to 500°C, Wear, Volume 30, Issue 2, November 1974, Pages 189-212, ISSN 0043-1648, http://dx.doi.org/10.1016/0043-1648(74)90175-6.
22. T. Kayaba, A. Iwabuchi, The fretting wear of 0.45% C steel and austenitic stainless steel from 20 to 650 °C in air, Wear, Volume 74, Issue 2, 22 December 1981, Pages 229-245, ISSN 0043-1648, http://dx.doi.org/10.1016/0043-1648(81)90165-4.
23. R.B. Waterhouse, A. Iwabuchi, High temperature fretting wear of four titanium alloys, Wear, Volume 106, Issues 1–3, November 1985, Pages 303-313, ISSN 0043-1648, http://dx.doi.org/10.1016/0043-1648(85)90114-0.
24. M.M. Hamdy, R.B. Waterhouse, The fretting wear of Ti-6Al-4v and aged inconel 718 at elevated temperatures, Wear, Volume 71, Issue 2, September 1981, Pages 237-248, ISSN 0043-1648, http://dx.doi.org/10.1016/0043-1648(81)90342-2.
25. Oduoza, Chike F., Enam Khan, and Tarsem Sihra. 'Chromium Electroplating Of Aluminium Alloys Using Electroless Nickel As Underlayer'. Journal of Materials Science and Chemical Engineering, Volume 02, Issue 07, 2014, Pages 59-74, ISSN 2327-6045,. http://dx.doi.org/10.4236/msce.2014.27007.
26. Trent, E. M, and Paul Kenneth Wright. Metal Cutting. Boston: Butterworth-Heinemann, 2000. ISBN 9780750670692.
27. Glaeser, William A., Brundle C. R., Evans C., Characterization Of Tribological Materials. [New York, N.Y.] (222 East 46th Street, New York, NY 10017): Momentum Press, 2013. ISBN 9781606502570, http://dx.doi.org/10.5643/9781606502594.

28. P.A. Engel, Percussive impact wear: A study of repetitively impacting solid components in engineering, Tribology International, Volume 11, Issue 3, June 1978, Pages 169-176, ISSN 0301-679X, http://dx.doi.org/10.1016/0301-679X(78)90002-6.
29. François, Dominique, A Pineau, and A Zaoui. Mechanical Behaviour of Materials. Dordrecht: Springer Science + Business Media, 2013. ISBN 9789400725454, http://dx.doi.org/10.1007/9789400725461.
30. Stephen L. Rice, The role of microstructure in the impact wear of two aluminum alloys, Wear, Volume 54, Issue 2, June 1979, Pages 291-301, ISSN 0043-1648, http://dx.doi.org/10.1016/0043-1648(79)90121-2.
31. A. Karimi, F. Avellan, Comparison of erosion mechanisms in different types of cavitation, Wear, Volume 113, Issue 3, 31 December 1986, Pages 305-322, ISSN 0043-1648, http://dx.doi.org/10.1016/0043-1648(86)90031-1.
32. Trethewey, K. R., T. J. Haley, and C. C. Clark. 'Effect Of Ultrasonically Induced Cavitation On Corrosion Behaviour Of A Copper – Manganese – Aluminium Alloy'. British Corrosion Journal, Volume 23, Issue 1, January 1988, Pages 55-60. http://dx.doi.org/10.1179/000705988798271090.
33. R.C.D. Richardson, The maximum hardness of strained surfaces and the abrasive wear of metals and alloys, Wear, Volume 10, Issue 5, October 1967, Pages 353-382, ISSN 0043-1648, http://dx.doi.org/10.1016/0043-1648(67)90276-1.
34. M.V. Swain, Microscopic observations of abrasive wear of polycrystalline alumina, Wear, Volume 35, Issue 1, November 1975, Pages 185-189, ISSN 0043-1648, http://dx.doi.org/10.1016/0043-1648(75)90152-0.

35. C Friedrich, G Berg, E Broszeit, F Rick, J Holland, PVD CrxN coatings for tribological application on piston rings, Surface and Coatings Technology, Volume 97, Issues 1–3, December 1997, Pages 661-668, ISSN 0257-8972, http://dx.doi.org/10.1016/S0257-8972(97)00335-6.
36. E Broszeit, C Friedrich, G Berg, Deposition, properties and applications of PVD CrxN coatings, Surface and Coatings Technology, Volume 115, Issue 1, June 1999, Pages 9-16, ISSN 0257-8972, http://dx.doi.org/10.1016/S0257-8972(99)00021-3.
37. M.Y.P. Costa, M.O.H. Cioffi, H.J.C. Voorwald, V.A. Guimarães, An investigation on sliding wear behavior of PVD coatings, Tribology International, Volume 43, Issue 11, November 2010, Pages 2196-2202, ISSN 0301-679X, http://dx.doi.org/10.1016/j.triboint.2010.07.002.
38. B Navinšek, P Panjan, I Milošev, Industrial applications of CrN (PVD) coatings, deposited at high and low temperatures, Surface and Coatings Technology, Volume 97, Issues 1–3, December 1997, Pages 182-191, ISSN 0257-8972, http://dx.doi.org/10.1016/S0257-8972(97)00393-9.
39. Simon C. Tung, Hong Gao, Tribological characteristics and surface interaction between piston ring coatings and a blend of energy-conserving oils and ethanol fuels, Wear, Volume 255, Issues 7–12, August–September 2003, Pages 1276-1285, ISSN 0043-1648, http://dx.doi.org/10.1016/S0043-1648(03)00240-0.
40. I. Etsion, G. Halperin, E. Becker, The effect of various surface treatments on piston pin scuffing resistance, Wear, Volume 261, Issues 7–8, 20 October 2006, Pages 785-791, ISSN 0043-1648, http://dx.doi.org/10.1016/j.wear.2006.01.032.

41. J. Lanigan, H. Zhao, A. Morina, A. Neville, Tribochemistry of silicon and oxygen doped, hydrogenated Diamond-like Carbon in fully-formulated oil against low additive oil, Tribology International, Volume 82, Part B, February 2015, Pages 431-442, ISSN 0301-679X, http://dx.doi.org/10.1016/j.triboint.2014.03.019.
42. M.B. dos Santos, H.L. Costa, J.D.B. De Mello, Potentiality of triboscopy to monitor friction and wear, Wear, Volumes 332–333, May–June 2015, Pages 1134-1144, ISSN 0043-1648, http://dx.doi.org/10.1016/j.wear.2014.10.017.
43. Rohollah Ghasemi, Lennart Elmquist, The relationship between flake graphite orientation, smearing effect, and closing tendency under abrasive wear conditions, Wear, Volume 317, Issues 1–2, 15 September 2014, Pages 153-162, ISSN 0043-1648, http://dx.doi.org/10.1016/j.wear.2014.05.015.
44. Giovanni Bolelli, Valeria Cannillo, Luca Lusvarghi, Sara Riccò, Mechanical and tribological properties of electrolytic hard chrome and HVOF-sprayed coatings, Surface and Coatings Technology, Volume 200, Issue 9, 8 February 2006, Pages 2995-3009, ISSN 0257-8972, http://dx.doi.org/10.1016/j.surfcoat.2005.04.057.
45. K. Yamamoto, Hirotaka Ito, S. Kujime, Nano-multilayered CrN/BCN coating for anti-wear and low friction applications, Surface and Coatings Technology, Volume 201, Issues 9–11, 26 February 2007, Pages 5244-5248, ISSN 0257-8972, http://dx.doi.org/10.1016/j.surfcoat.2006.07.165.
46. Cengiz Öner, Hanbey Hazar, Mustafa Nursoy, Surface properties of CrN coated engine cylinders, Materials & Design, Volume 30, Issue 3, March 2009, Pages 914-920, ISSN 0261-3069, http://dx.doi.org/10.1016/j.matdes.2008.05.018.

47. Hetal N. Shah, R. Jayaganthan, Avinash C. Pandey, Nanoindentation study of magnetron-sputtered CrN and CrSiN coatings, Materials & Design, Volume 32, Issue 5, May 2011, Pages 2628-2634, ISSN 0261-3069, http://dx.doi.org/10.1016/j.matdes.2011.01.031.
48. P.Z. Shi, J. Wang, C.X. Tian, Z.G. Li, G.D. Zhang, D.J. Fu, B. Yang, Structure, mechanical and tribological properties of CrN thick coatings deposited by circular combined tubular arc ion plating, Surface and Coatings Technology, Volume 228, Supplement 1, 15 August 2013, Pages S534-S537, ISSN 0257-8972, http://dx.doi.org/10.1016/j.surfcoat.2012.04.041.
49. C. Lorenzo-Martin, O. Ajayi, A. Erdemir, G.R. Fenske, R. Wei, Effect of microstructure and thickness on the friction and wear behavior of CrN coatings, Wear, Volume 302, Issues 1–2, April–May 2013, Pages 963-971, ISSN 0043-1648, http://dx.doi.org/10.1016/j.wear.2013.02.005.
50. Chang-Ming Shi, Tie-Gang Wang, Zhi-Liang Pei, Jun Gong, Chao Sun, Effects of the Thickness Ratio of CrN vs Cr2O3 Layer on the Properties of Double-layered CrN/Cr2O3 Coatings Deposited by Arc Ion Plating, Journal of Materials Science & Technology, Volume 30, Issue 5, May 2014, Pages 473-479, ISSN 1005-0302, http://dx.doi.org/10.1016/j.jmst.2014.01.007.
51. Hao-Jie Song, Zhao-Zhu Zhang, Xue-hu Men, Effect of nano-Al2O3 surface treatment on the tribological performance of phenolic composite coating, Surface and Coatings Technology, Volume 201, Issue 6, 4 December 2006, Pages 3767-3774, ISSN 0257-8972, http://dx.doi.org/10.1016/j.surfcoat.2006.09.084.

52. Hejun Li, Zishan Chen, Kezhi Li, Qingliang Shen, Yanhui Chu, Qiangang Fu, Wear behavior of SiC nanowire-reinforced SiC coating for C/C composites at elevated temperatures, Journal of the European Ceramic Society, Volume 33, Issues 15–16, December 2013, Pages 2961-2969, ISSN 0955-2219, http://dx.doi.org/10.1016/j.jeurceramsoc.2013.06.018.
53. R.N. Rao, S. Das, D.P. Mondal, G. Dixit, S.L. Tulasi Devi, Dry sliding wear maps for AA7010 (Al–Zn–Mg–Cu) aluminium matrix composite, Tribology International, Volume 60, April 2013, Pages 77-82, ISSN 0301-679X, http://dx.doi.org/10.1016/j.triboint.2012.10.007.
54. R. Bosman, D.J. Schipper, Mild wear maps for boundary lubricated contacts, Wear, Volumes 280–281, 20 March 2012, Pages 54-62, ISSN 0043-1648, http://dx.doi.org/10.1016/j.wear.2012.01.019.
55. A.R. Riahi, A.T. Alpas, Wear map for grey cast iron, Wear, Volume 255, Issues 1–6, August–September 2003, Pages 401-409, ISSN 0043-1648, http://dx.doi.org/10.1016/S0043-1648(03)00100-5.
56. S.R. Pearson, P.H. Shipway, J.O. Abere, R.A.A. Hewitt, The effect of temperature on wear and friction of a high strength steel in fretting, Wear, Volume 303, Issues 1–2, 15 June 2013, Pages 622-631, ISSN 0043-1648, http://dx.doi.org/10.1016/j.wear.2013.03.048.
57. Zhiqiang Liu, Meng Hua, Wear transitions and mechanisms in lubricated sliding of a molybdenum coating, Tribology International, Volume 32, Issue 9, September 1999, Pages 499-506, ISSN 0301-679X, http://dx.doi.org/10.1016/S0301-679X(99)00079-1.

58. M.B Karamış, K Yıldızlı, H Çakırer, An evaluation of surface properties and frictional forces generated from Al–Mo–Ni coating on piston ring, Applied Surface Science, Volume 230, Issues 1–4, 31 May 2004, Pages 191-200, ISSN 0169-4332, http://dx.doi.org/10.1016/j.apsusc.2004.02.053.
59. Shunyan Tao, Zhijian Yin, Xiaming Zhou, Chuanxian Ding, Sliding wear characteristics of plasma-sprayed Al2O3 and Cr2O3 coatings against copper alloy under severe conditions, Tribology International, Volume 43, Issues 1–2, January–February 2010, Pages 69-75, ISSN 0301-679X, http://dx.doi.org/10.1016/j.triboint.2009.04.037.
60. S. Johansson, C. Frennfelt, A. Killinger, P.H. Nilsson, R. Ohlsson, B.G. Rosén, Frictional evaluation of thermally sprayed coatings applied on the cylinder liner of a heavy duty diesel engine: Pilot tribometer analysis and full scale engine test, Wear, Volume 273, Issue 1, 1 November 2011, Pages 82-92, ISSN 0043-1648, http://dx.doi.org/10.1016/j.wear.2011.06.021.
61. Ulf Helmersson, Martina Lattemann, Johan Bohlmark, Arutiun P. Ehiasarian, Jon Tomas Gudmundsson, Ionized physical vapor deposition (IPVD): A review of technology and applications, Thin Solid Films, Volume 513, Issues 1–2, 14 August 2006, Pages 1-24, ISSN 0040-6090, http://dx.doi.org/10.1016/j.tsf.2006.03.033.
62. Colligon, John S. 'Energetic Condensation: Processes, Properties, And Products'. Journal of Vacuum Science & Technology A: Vacuum, Surfaces, and Films Volume 13. Issue 3, 1995: Pages 1649-1657. http://dx.doi.org/10.1116/1.579746.

63. Donald M. Mattox, Technical Report ‘Film Deposition Using Accelerated Ions’. Sandia National Laboratories, Albuquerque, New Mexico, 1963. http://www.osti.gov/scitech/biblio/4038817; Accessed on 20th May 2015.
64. Donald M. Mattox, 'Fundamentals of Ion Plating'. Journal of Vacuum Science & Technology. Volume 10. Issue 1, 1973, Page 47. http://dx.doi.org/10.1116/1.1318041.
65. S. Aisenberg, R.W. Chabot, Physics of Ion Plating and Ion Beam Deposition, Journal of Vacuum Science & Technology, Volume 10, Issue 1, 1973, Page 104, http://dx.doi.org/10.1116/1.1317915.
66. S. Aisenberg, The role of ion-assisted deposition in the formation of diamond-like-carbon films, Journal of Vacuum Science & Technology A: Vacuum, Surfaces, and Films Volume 8, Issue 3, 1990, Page 2150, http://dx.doi.org/10.1116/1.577031.
67. C. Weissmantel, G. Reisse, H.-J. Erler, F. Henny, K. Bewilogua, U. Ebersbach, C. Schürer, Preparation of hard coatings by ion beam methods, Thin Solid Films, Volume 63, Issue 2, 1 November 1979, Pages 315-325, ISSN 0040-6090, http://dx.doi.org/10.1016/0040-6090(79)90035-X.
68. Donald M. Mattox, Surface effects in reactive ion plating, Applied Surface Science, Volumes 48–49, 1991, Pages 540-547, ISSN 0169-4332, http://dx.doi.org/10.1016/0169-4332(91)90388-Z.
69. K. S. Fancey, C. A. Porter, A. A. Matthews, Relative importance of bombardment energy and intensity in ion plating, Journal of Vacuum Science & Technology A: Volume 13, Issue 2, 1995, Page 428, http://dx.doi.org/10.1116/1.579375.

70. Petrov, F. Adibi, J.E. Greene, W.D. Sproul, W.-D. Münz, Use of an externally applied axial magnetic field to control ion/neutral flux ratios incident at the substrate during magnetron sputter deposition, Journal of Vacuum Science & Technology A: Vacuum, Surfaces, and Films Volume 10, Issue 5, 1992, Page 3283, http://dx.doi.org/10.1116/1.577812.
71. Tadahiro Ohmi, Tadashi Shibata, Advanced scientific semiconductor processing based on high-precision controlled low-energy ion bombardment, Thin Solid Films, Volume 241, Issues 1–2, 1 April 1994, Pages 159-166, ISSN 0040-6090, http://dx.doi.org/10.1016/0040-6090(94)90418-9.
72. A. Bessaudou, J. Machet, C. Weissmantel, Transport of evaporated material through support gas in conjunction with ion plating: I, Thin Solid Films, Volume 149, Issue 2, 25 May 1987, Pages 225-235, ISSN 0040-6090, http://dx.doi.org/10.1016/0040-6090(87)90299-9.
73. Suzuki, E. 'High-Resolution Scanning Electron Microscopy of Immunogold-Labelled Cells By The Use Of Thin Plasma Coating Of Osmium'. Journal of Microscopy, Volume 208, Issue 3, 2002, Pages 153-157, http://dx.doi.org/10.1046/j.1365-2818.2002.01082.x.
74. R.W. Horne, Principles and techniques of electron microscopy: Edited by M. A. Hayat The Macmillan Press Limited, Basingstoke, Electron Microscopy Reviews, Volume 3, Issue 2, 1990, Pages i-iii, ISSN 0892-0354, http://dx.doi.org/10.1016/0892-0354(90)90008-G.

75. Reimer, L. 'Scanning Electron Microscopy-Present State and Trends'. Scanning, Volume 1, Issue 1, October 2011, Pages 3–16, http://dx.doi.org/10.1002/sca.4950010102.
76. R. Chattopadhyay; Surface Wear: Analysis, Treatment, and Prevention, ASM International, 2001, ISBN 9781615030606.
77. A.L. Bandeira, R. Trentin, C. Aguzzoli, M.E.H. Maia da Costa, A.F. Michels, I.J.R. Baumvol, M.C.M. Farias, C.A. Figueroa, Sliding wear and friction behavior of CrN-coating in ethanol and oil–ethanol mixture, Wear, Volume 301, Issues 1–2, April–May 2013, Pages 786-794, ISSN 0043-1648, http://dx.doi.org/10.1016/j.wear.2013.01.111.
78. Giovanni Bolelli, Valeria Cannillo, Luca Lusvarghi, Tiziano Manfredini, Wear behaviour of thermally sprayed ceramic oxide coatings, Wear, Volume 261, Issues 11–12, 20 December 2006, Pages 1298-1315, ISSN 0043-1648, http://dx.doi.org/10.1016/j.wear.2006.03.023.
79. M Singh, D.P Mondal, O.P Modi, A.K Jha, Two-body abrasive wear behaviour of aluminium alloy–sillimanite particle reinforced composite, Wear, Volume 253, Issues 3–4, August 2002, Pages 357-368, ISSN 0043-1648, http://dx.doi.org/10.1016/S0043-1648(02)00153-9.
80. Binshi Xu, Zixin Zhu, Shining Ma, Wei Zhang, Weimin Liu, Sliding wear behavior of Fe–Al and Fe–Al/WC coatings prepared by high velocity arc spraying, Wear, Volume 257, Issue 11, December 2004, Pages 1089-1095, ISSN 0043-1648, http://dx.doi.org/10.1016/j.wear.2004.05.012.

81. H.S. Arora, H. Singh, B.K. Dhindaw, Wear behaviour of a Mg alloy subjected to friction stir processing, Wear, Volume 303, Issues 1–2, 15 June 2013, Pages 65-77, ISSN 0043-1648, http://dx.doi.org/10.1016/j.wear.2013.02.023.
82. N. Soda, Y. Kimura, A. Tanaka, Wear of some F.C.C. metals during unlubricated sliding part IV: Effects of atmospheric pressure on wear, Wear, Volume 43, Issue 2, June 1977, Pages 165-174, ISSN 0043-1648, http://dx.doi.org/10.1016/0043-1648(77)90111-9.
83. J.E. Goodwin, W. Sage and G.P. Tilly, Study of Erosion by Solid Particles, Proceedings of the Institution of Mechanical Engineers, Volume 184, Number 1, June 1969, Pages 279-292, http://dx.doi.org/10.1243/pime_proc_1969_184_024_02.
84. Mark A. Nicholls, Than Do, Peter R. Norton, Masoud Kasrai, G.Michael Bancroft, Review of the lubrication of metallic surfaces by zinc dialkyl-dithiophosphates, Tribology International, Volume 38, Issue 1, January 2005, Pages 15-39, ISSN 0301-679X, http://dx.doi.org/10.1016/j.triboint.2004.05.009.
85. Arun Kumar, Patrick L. Gurian, Robin H. Bucciarelli-Tieger And Jade Mitchell-Blackwood, Iron oxide-coated fibrous sorbents for arsenic removal, Journal - American Water Works Association, Volume 100, Issue 4, April 2008, Pages 151-164, ISSN 0003-150X, http://www.jstor.org/stable/41314608.